U.S. DEPARTMENT OF COMMERCE
National Technical Information Service

PB-277 377

Quality Control for Environmental Measurements Using Gamma-Ray Spectrometry

Environmental Monitoring and Support Lab, Las Vegas, Nev

Dec 77

PB 277 377

EPA

nited States
nvironmental Protection
gency

Office of
Reseach and
Development

Environmental Monitoring
and Support Laboratory
Las Vegas Nevada 89114

EPA-600/7-77-144

December 1977

QUALITY CONTROL FOR ENVIRONMENTAL MEASUREMENTS USING GAMMA-RAY SPECTROMETRY

Interagency
Energy-Environment
Research and Development
Program Report

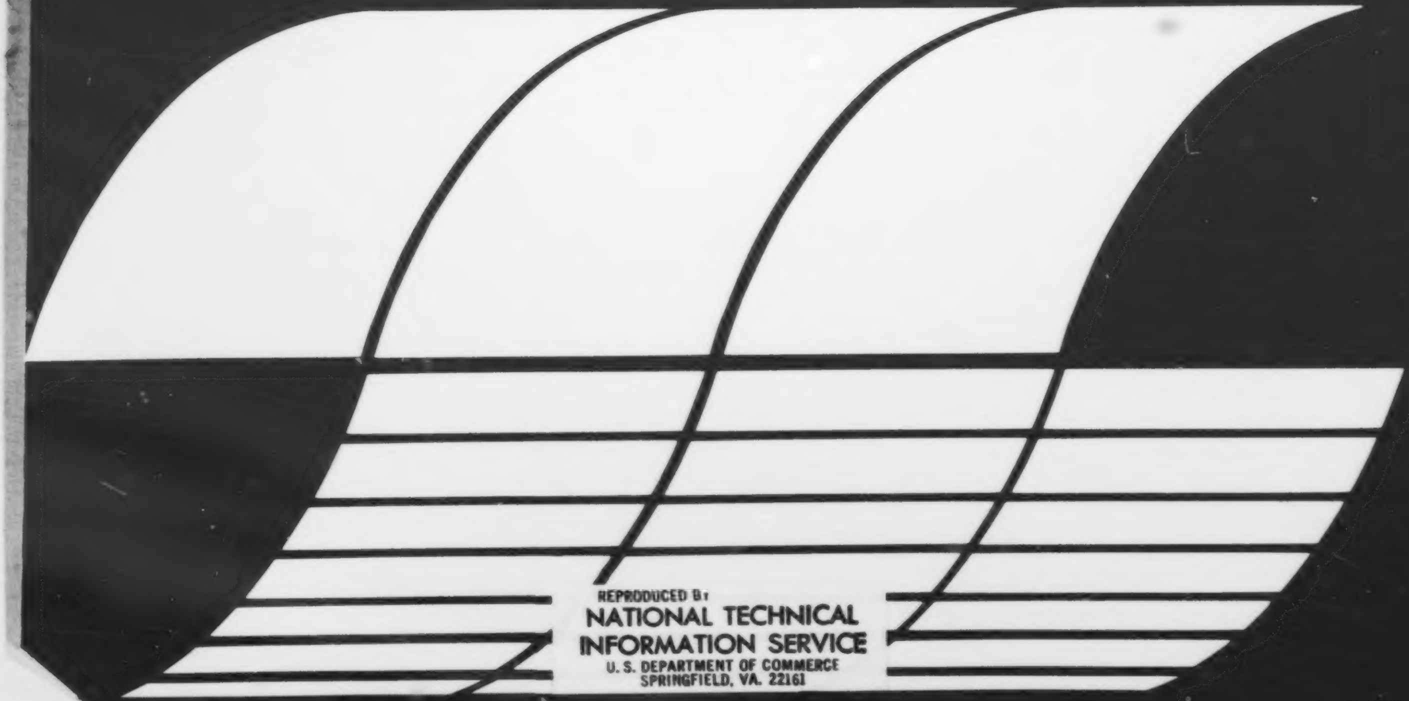

REPRODUCED BY
NATIONAL TECHNICAL
INFORMATION SERVICE
U. S. DEPARTMENT OF COMMERCE
SPRINGFIELD, VA. 22161

RESEARCH REPORTING SERIES

Research reports of the Office of Research and Development, U.S. Environmental Protection Agency, have been grouped into nine series. These nine broad categories were established to facilitate further development and application of environmental technology. Elimination of traditional grouping was consciously planned to foster technology transfer and a maximum interface in related fields. The nine series are:

1. Environmental Health Effects Research
2. Environmental Protection Technology
3. Ecological Research
4. Environmental Monitoring
5. Socioeconomic Environmental Studies
6. Scientific and Technical Assessment Reports (STAR)
7. Interagency Energy-Environment Research and Development
8. "Special" Reports
9. Miscellaneous Reports

This report has been assigned to the INTERAGENCY ENERGY—ENVIRONMENT RESEARCH AND DEVELOPMENT series. Reports in this series result from the effort funded under the 17-agency Federal Energy/Environment Research and Development Program. These studies relate to EPA'S mission to protect the public health and welfare from adverse effects of pollutants associated with energy systems. The goal of the Program is to assure the rapid development of domestic energy supplies in an environmentally-compatible manner by providing the necessary environmental data and control technology. Investigations include analyses of the transport of energy-related pollutants and their health and ecological effects; assessments of, and development of, control technologies for energy systems; and integrated assessments of a wide range of energy-related environmental issues.

This document is available to the public through the National Technical Information Service, Springfield, Virginia 22161

TECHNICAL REPORT DATA
(Please read Instructions on the reverse before completing)

1. REPORT NO. EPA-600/7-77-144	2.	3. RECIPIENT'S ACCESSION NO. PB277377
4. TITLE AND SUBTITLE QUALITY CONTROL FOR ENVIRONMENTAL MEASUREMENTS USING GAMMA-RAY SPECTROMETRY		5. REPORT DATE December 1977
		6. PERFORMING ORGANIZATION CODE
7. AUTHOR(S) Lee H. Ziegler and Hiram M. Hunt		8. PERFORMING ORGANIZATION REPORT NO.
9. PERFORMING ORGANIZATION NAME AND ADDRESS Environmental Monitoring and Support Laboratory Office of Research and Development U.S. Environmental Protection Agency Las Vegas, Nevada 89114		10. PROGRAM ELEMENT NO. 1NE625
		11. CONTRACT/GRANT NO.
12. SPONSORING AGENCY NAME AND ADDRESS U.S. Environmental Protection Agency-Las Vegas, NV Office of Research and Development Environmental Monitoring and Support Laboratory Las Vegas, Nevada 89114		13. TYPE OF REPORT AND PERIOD COVERED Final FY-77
		14. SPONSORING AGENCY CODE EPA/600/07

15. SUPPLEMENTARY NOTES

16. ABSTRACT

This report describes the quality control procedures, calibration, collection, analysis, and interpretation of data in measuring the activity of gamma ray-emitting radionuclides in environmental samples. Included in the appendices are basic data for selected gamma ray-emitting radionuclides, the uranium-235 series, the uranium-238 series, and the thorium-232 series. Typical pulse height spectra of selected gamma ray-emitting radionuclides measured with a NaI(Tl) detector are included in an appendix.

17. KEY WORDS AND DOCUMENT ANALYSIS

a. DESCRIPTORS	b. IDENTIFIERS/OPEN ENDED TERMS	c. COSATI Field/Group
Quality Control Gamma-Ray Spectroscopy		14D 07B 18D 20F

18. DISTRIBUTION STATEMENT RELEASE TO PUBLIC	19. SECURITY CLASS *(This Report)* UNCLASSIFIED	21. NO. OF PAGES 159
	20. SECURITY CLASS *(This page)* UNCLASSIFIED	22. PRICE A08, A01

EPA Form 2220-1 (9-73)

EPA-600/7-77-144
December 1977

QUALITY CONTROL FOR ENVIRONMENTAL MEASUREMENTS USING GAMMA-RAY SPECTROMETRY

by
Lee H. Ziegler
Monitoring Systems Research and Development Division
Environmental Monitoring and Support Laboratory
Las Vegas, Nevada 89114

and

Hiram M. Hunt, Ed.D
Professor, Radiation Technology
University of Nevada, Las Vegas
Las Vegas, Nevada 89154

U.S. ENVIRONMENTAL PROTECTION AGENCY
OFFICE OF RESEARCH AND DEVELOPMENT
ENVIRONMENTAL MONITORING AND SUPPORT LABORATORY
LAS VEGAS, NEVADA 89114

DISCLAIMER

This report has been reviewed by the Environmental Monitoring and Support Laboratory, U.S. Environmental Protection Agency, and approved for publication. Mention of trade names or commercial products does not constitute endorsement or recommendation for use.

FOREWORD

Protection of the environment requires effective regulatory actions which are based on sound technical and scientific information. This information must include the quantitative description and linking of pollutant sources, transport mechanisms, interactions, and resulting effects on man and his environment. Because of the complexities involved, assessment of specific pollutants in the environment requires a total systems approach which transcends the media of air, water, and land. The Environmental Monitoring and Support Laboratory-Las Vegas contributes to the formation and enhancement of a sound integrated monitoring data base through multidisciplinary, multimedia programs designed to:

- develop and optimize systems and strategies for monitoring pollutants and their impact on the environment

- demonstrate new monitoring systems and technologies by applying them to fulfill special monitoring needs of the Agency's operating programs.

This report describes the quality control procedures, the calibration, collection, analysis, and interpretation of data in measuring the activity of gamma ray-emitting radionuclides in environmental samples. The data from these measurements are used for a wide variety of purposes including assessment of health effects, establishment of standards and guides, and enforcement activities. This report is intended to introduce the techniques of gamma ray spectroscopy to those persons who are initiating a radioactivity monitoring program. The Quality Assurance Branch at the U.S. Environmental Protection Agency's Environmental Monitoring and Support Laboratory in Las Vegas encourages the development and implementation of quality control procedures at all levels of sample collection, analysis, data handling and reporting of environmental radiation measurements and can provide further assistance upon request.

George B. Morgan

George B. Morgan
Director
Environmental Monitoring and Support Laboratory
Las Vegas

TABLE OF CONTENTS

	Page
FOREWORD	iii
LIST OF FIGURES	vi
LIST OF TABLES	viii
INTRODUCTION	1
BASIC PRINCIPLES	3
GAMMA RAY INTERACTIONS WITH MATTER	11
TERMINOLOGY OF GAMMA RAY SPECTROSCOPY	15
EQUIPMENT	21
INITIAL SETUP	27
CONTROL CHARTS	32
DATA ANALYSES	34
CALIBRATION OF THE SYSTEM	40
STATISTICS AND UNCERTAINTIES IN MEASUREMENTS	45
INEFFICIENT STATISTICS	56
SUPERPOSITION OF SEVERAL INDEPENDENT RANDOM PROCESSES	61
STATISTICAL TESTING FOR NORMAL AND NON-NORMAL DATA	66
LOWER LIMIT OF DETECTION	79
REFERENCES	85
BIBLIOGRAPHY	88
APPENDIX A. BASIC DATA FOR SELECTED GAMMA RAY-EMITTING RADIONUCLIDES	89
APPENDIX B. THORIUM-232 SERIES DECAY DATA	95
APPENDIX C. URANIUM-238 SERIES DECAY DATA	97
APPENDIX D. URANIUM-235 SERIES DECAY DATA	99
APPENDIX E. PULSE HEIGHT SPECTRA OF SELECTED RADIONUCLIDES	101

Preceding page blank

LIST OF FIGURES

Number Page

1 Cesium-137 decay scheme. 6

2 Decay scheme for iron-59 (Fe). 7

3 Decay scheme for cobalt-60 (Co). 7

4 Spectrum of Fe-59 at 10 keV per channel. 8

5 Spectrum of Co-60 at 20 keV per channel. 9

6 "Ideal" spectrum of Compton interactions. 12

7 Mass attenuation coefficient of sodium iodide. 14a

8 Spectrum of CS-137 at 10 keV per channel. 16

9 Typical block diagram of gamma ray spectrometer. 23

10 Gamma-ray spectrometer at the Environmental Monitoring and Support Laboratory-Las Vegas, Nevada. 24

11 Schematic representation of a typical pulse from a preamplifier coupled to a NaI(Tl) detector. 25

12 Schematic representation of typical pulses from a linear amplifier in a NaI(Tl) spectrometer. 25

13 400-minute background spectrum measured with a 10.2-cm by 10.2-cm NaI(Tl) detector. 30

14 Idealized spectra illustrating interference factors and summation of gamma rays in a gamma-ray spectrometer. 36

15 Common sample holders. 41

16 Comparison of analytical results from several participants when systematic results are not estimated correctly. 46

17 Comparison of analytical results from several participants with correct estimation of systematic errors. 46

18 Normal distribution with a mean value, m, of 100 and a standard deviation, σ, of 10. 48

LIST OF FIGURES (continued)

Number		Page
19	Poisson distribution with a mean value, m, of 100.	50
20	Control chart for low energy (0.57 MeV) peak from bismuth-207.	51
21	Control chart for high energy (1.063 MeV) peak from Bi-207.	69
22	Probability plot for low energy (0.57 MeV) peak from Bi-207.	74
23	Probability plot for high energy (1.063 MeV) peak from Bi-207.	75
24	Probability plot for 10-minute background counts measured with a 10.2-cm by 10.2-cm NaI(Tl) detector.	76

LIST OF TABLES

Number Page

1 Compton Edge Energy as a Function of Incident Radiation Energy 13

2 Limiting Values of r at Probabilities of 95% and 99% for the Mean Square of the Successive Differences Statistical Test 67

3 MSSD Test Applied to Counts of a Bi-207 Sample Obtained with a Multichannel Gamma-Ray Spectrometer 68

4 MSSD Test for Background Measurements of a 10.2-cm by 10.2-cm NaI(Tl) Detector 70

5 Kolmogorov-Smirnov Test on Low Energy (0.57 Mev) Gamma Rays from Bi-207 71

6 Kolomogorov-Smirnov Test on High Energy (1.063 Mev) Gamma Rays from Bi-207 72

7 Kolmogorov-Smirnov Test on Background Measurements of a 10.2-cm by 10.2-cm NaI(Tl) detector 73

8 Limiting Values for D_α in the Kolmogorov-Smirnov Test 78

9 Risk and Confidence Values 80

INTRODUCTION

This monograph is intended to introduce the field of gamma-ray spectroscopy to analysts engaged in environmental radiation monitoring. The emphasis of this document is on quality control procedures that assist the analyst engaged in measuring and interpreting gamma-ray spectra in producing accurate and valid data. Because of this emphasis, many interesting aspects of the field have been neglected here. However, the references in the bibliography do cover much omitted material of relevance and should be consulted by those who have interest in further aspects of the field of spectroscopy.

Gamma-ray spectroscopy is a valuable tool for identifying radionuclides in environmental media. Usually requiring a minimum of sample preparation, gamma-ray analysis provides a means for the specific identification and quantification of radionuclides in any material. Typically, a sample which has been shown to contain alpha or beta activity through routine screening is assayed for gamma activity by the use of a suitable detector and multichannel analyzer.

There are many types of detectors capable of detecting gamma rays, but those suitable for environmental monitoring are limited in number. The ideal detector for gamma-ray analysis will discriminate against other types of radiation and will produce signals proportional to the energy and intensity* of the gamma rays received. Factors leading to the choice of a particular detector are cost, resolution, and sensitivity. One of the more commonly used detectors for gamma-ray analysis is the thallium-activated sodium iodide [NaI(Tl)] crystal optically coupled to a photomultiplier which is, in turn, electrically connected to a multichannel analyzer. The NaI(Tl) detector is moderate in cost, has a moderately good resolution, and has good sensitivity. The use of solid state detectors is increasing, but they are still more expensive and have less sensitivity than NaI(Tl) detectors. The resolution of solid state detectors is superior to NaI(Tl) detectors, and in some cases, they are easier to use for identifying individual radionuclides in complex mixtures of radioactive substances. Although many of the principles of gamma-ray spectroscopy are the same whether a lithium-drifted germanium [Ge(Li)] detector or a NaI(Tl) detector is used, this monograph applies only to gamma-ray spectroscopy using a NaI(Tl) detector.

There is a substantial quantity of literature available describing the principles and applications of NaI(Tl) detectors for gamma-ray spectroscopy. The accompanying list of references, though brief, is informative and to the point. The publications by Crouch (1) Heath et al., (2) and Heath (3, 4) are particularly helpful to persons who have not been introduced to gamma-ray spectroscopy. The catalog of gamma-ray spectra by Heath (4) is very helpful in identifying radionuclides from the results of gamma-ray measurements and for calibrating gamma-ray detection equipment for pulse height versus energy. A good introduction to radioactive analysis of environmental media is the EPA publication "Radioassay Procedures for Environmental Samples" edited by Douglas (5). Reference works by Crouthamel (6) and Siegbahn (7) are also available. Other EPA publications (8, 9) describe services available to laboratories engaged in environmental monitoring.

---

*Intensity is the number of gamma rays contained in a beam, emitted from a source, or incident on a detector per unit time.

BASIC PRINCIPLES

Radioactivity is the outward manifestation of the spontaneous transformations of radioactive nuclei. The quantity of radioactivity can be expressed in a number of ways. For example, one may specify the activity, at any given time, in terms of disintegrations per second. The radioactivity has the dimension second^{-1} and is often expressed in curies. The curie is defined by international agreement as the quantity of radioactivity equal to 3.7×10^{10} disintegrations per second.

Several assumptions are made in defining the fundamental law of radioactive decay. Among these assumptions are:

1. The probability of decay is the same for all atoms of a single radioactive species.

2. The probability of decay is independent of the age of the particular atom.

3. All atoms of a single radioactive species are identical in their nuclear properties.

4. The intensity of the radiation originating in the sample is due to the nuclear properties of the species present.

5. Each radioactive event is defined as the disintegration of one atom of the radioactive species and the formation of one new atom of a new species. (The new species may or may not be radioactive depending on the original species.)

6. The intensity of the radiation emerging from a sample of radioactive material can be measured with high precision and with known, or at least reproducible, efficiency.

7. The amount of radiation originating in a sample is directly proportional to the amount of radioactive material present (although the constant of proportionality varies from species to species). For a single species, if N is the number of atoms present at time t, the radioactivity in disintegrations per unit time is given by the rate at which the active species is disappearing, so that the rate of radioactive decay is

$$-\frac{dN}{dt} = +\lambda N \qquad \text{(Eq. 1)}$$

where λ is the constant of proportionality characteristic of the species. λ is referred to as the decay constant of the species. The above equation can be integrated to give

$$N = N_o e^{-\lambda(t-t_o)} \qquad \text{(Eq. 2)}$$

where N has the value N_o at the arbitrarily chosen time t_o. If we measure the radiation from the sample with an instrument having an efficiency η for the characteristic radiations of the species, the observed "counting rate" is $\lambda\eta N$. Therefore, N, and consequently, $\lambda\eta N$ decrease exponentially with time.

The half-life, $T_{\frac{1}{2}}$, i.e., the time it takes for the activity of the radionuclide to decrease to one-half the value of activity at any given time, t, is related to the decay constant, λ, as follows:

$$\frac{N_{(t=T_{\frac{1}{2}})}}{N_o} \equiv \tfrac{1}{2} = e^{-\lambda T_{\frac{1}{2}}}$$

$$\ln(\tfrac{1}{2}) = -\ln 2 = \ln e^{-\lambda T_{\frac{1}{2}}} = -\lambda T_{\frac{1}{2}}$$

$$T_{\frac{1}{2}} = \frac{\ln 2}{\lambda}$$

$$= \frac{0.693}{\lambda} \qquad \text{(Eq. 3)}$$

$T_{\frac{1}{2}}$ is expressed in time units and λ in units of reciprocal time. $T_{\frac{1}{2}}$ and λ must be expressed in the same time unit to balance the half-life formula, but any unit of convenient size may be used.

Generally, one is interested in finding the activity, $A(A = \lambda N)$, at a time, t, based upon an original activity, A_o, at time t_o. The following formula is convenient for the reason that half-life values are usually more readily available than radioactive constants.

$$A = A_o e^{-\frac{\ln 2\,(t-t_o)}{T_{\frac{1}{2}}}} \qquad \text{(Eq. 4)}$$

Conversely, if the activity, A, is determined, then the activity, A_o, for any arbitrarily chosen time, t_o, can be found using the relation

$$A_o = Ae^{\frac{\ln 2\,(t-t_o)}{T_{\frac{1}{2}}}} \qquad \text{(Eq. 5)}$$

The disintegration law applies universally to all radionuclides, but the constant λ is different for each nuclide. The known radioactive nuclides have decay constants between $\lambda = 2.3 \times 10^6$ second^{-1} (for $^{212}_{84}$Po) to $\lambda = 1.51 \times 10^{-18}$ second^{-1} (for $^{232}_{90}$Th), a range of over 10^{24}.

Gamma-ray emission is a common way for an excited nucleus to lose energy. A gamma transition can be defined as any deexcitation of an excited nuclear state to a state of lower energy without changing the charge, Z, or the mass, A, of the nucleus with the emission of a gamma ray. Excited states appear as the result of alpha or beta decay processes, nuclear reactions, direct excitation from the ground state, and gamma transitions from higher excited states. For each radioactive nuclide the possible ways of deexcitation are summarized in the decay scheme. A complete decay scheme includes all the modes of decay of the nuclide, the energies of the radiations, their abundances, the sequence in which the radiations are emitted, and the measured half-lives of any intermediate states. There exist several useful compilations of the decay schemes of the nuclides (10, 11, 12, 13).

The various nuclear transitions indicated in the decay schemes represent only the primary processes. The complete degradation of the energy of the nuclear transition will usually include a sequence of secondary events. Some of these events are the emission of bremsstrahlung radiation, emission of characteristic x-rays, emission of Auger electrons, pair formation, and emission of annihilation photons. These secondary events can also involve the external atoms in the environment of the disintegrating nucleus, in the detector, or with other matter in the vicinity of the disintegrating nucleus and the detector, e.g. source holders or a shield.

An example of a simplified decay scheme is presented in Figure 1. This decay scheme indicates most of the pertinent information known about the decay of cesium-137. The ground state of cesium-137 is indicated by the heavy horizontal line at the top of the figure. The half-life of cesium-137, indicated as 30.0 years, is shown just to the right of the ground state line. Two arrows extending to the right from the ground state line to lower horizontal lines indicate respectively a beta transition to a metastable state of barium (barium-137m) and a beta transition to the ground state of barium-137. The fraction that each transition is of the total beta emission is expressed as a percent. In this example 94.7 percent of all beta transitions are to the barium-137 metastable state and 5.3 percent to the barium-137 ground state (14). Also indicated with the transition probabilities (in percent) are the transition energies. Only the transitions from the metastable state of barium-137 will produce gamma rays. Other than decaying with a gamma emission, the transition can be made by ejecting a conversion electron and associated x-rays and Auger electrons. The total internal conversion coefficient is defined as the number of electrons ejected by the nucleus divided by the number of gamma rays emitted for a given transition. The total internal conversion coefficient, α, accounts for all of the "conversion" electrons ejected so that the fraction of gamma rays emitted, I_λ, from the intermediate level is

$$I_\lambda = \frac{1}{1 + \alpha} \qquad \text{(Eq. 6)}$$

The compilations will either list the number of gamma rays per disintegration of the parent nuclide, or the number of disintegrations going to an intermediate state, and values for the internal conversion coefficient. The internal conversion coefficient for the 0.6616 MeV to ground state is 0.11. Therefore, the fraction of gamma rays emitted is

$$\begin{aligned} I_\lambda &= \frac{1}{1 + 0.11} \\ &= 0.90 \qquad \text{(Eq. 7)} \end{aligned}$$

The fraction of gamma rays emitted per decay of cesium-137 is therefore 0.947 × 0.90 = 0.85.

A cesium-137 ($^{137}_{55}Cs$) spectrum produced by the interaction of gamma rays with a sodium iodide (NaI(Tl) detector is presented in Figure 8 on page 16.

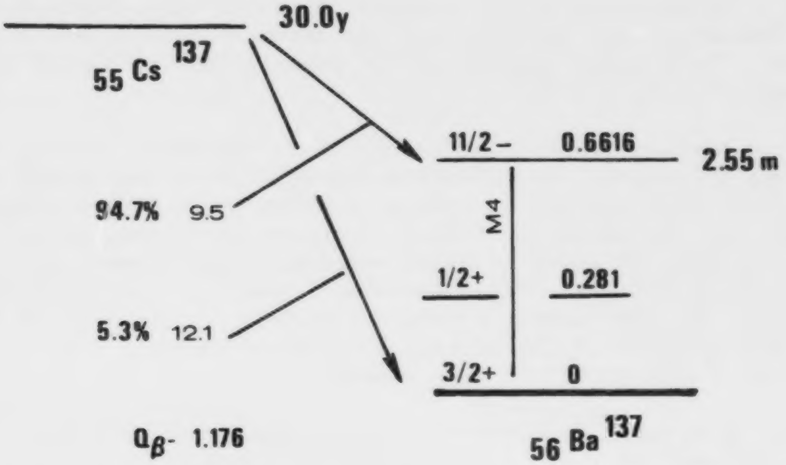

Figure 1. Cesium-137 Decay scheme.

The spectrum was obtained by feeding the signal from a sodium iodide detector into a multichannel analyzer calibrated at 10 keV per channel. The prominent peak in channel 66 represents the characteristic 0.6616-MeV cesium-137 gamma ray. The spectrum is complex for the reason that there are other interactions including partial exchanges of energy, characteristic rays emitted by the detector, and those rays emitted by daughter nuclides.

Figures 2 and 3 illustrate the decay schemes of $^{59}_{26}$Fe (iron-59) and $^{60}_{27}$Co (cobalt-60) respectively. The spectra of $^{59}_{26}$Fe and $^{60}_{27}$Co produced by the interaction of gamma rays with a sodium iodide detector are presented in Figures 4 and 5. These spectra were obtained from the same system which was used to obtain the cesium-137 spectrum mentioned previously, but was calibrated at 20 keV per channel for these figures. These spectra are very similar; the most significant differences are the shape and structure of the $^{60}_{27}$Co spectrum above channel 70 (1.4 MeV) (20 keV per channel) compared to the shape and structure of the $^{59}_{26}$Fe spectrum above channel 140 (1.4 MeV) (10 keV per channel.)

$^{59}_{26}$Fe decays principally by 0.46 MeV maximum beta emission to the 1.095 MeV level of ^{59}Co (53 percent) and by 0.26 MeV maximum beta emission to the 1.292 MeV level of ^{59}Co (45 percent). 1.1 percent of the beta emissions from $^{59}_{26}$Fe decay to an energy level of 1.435 MeV of ^{59}Co. By inspection of the $^{59}_{26}$Fe decay scheme one may see that the 70 percent portion of the deexcitation of the 1.435 MeV level results in a 0.1430 MeV gamma ray and the 30 percent portion results in a 0.34 MeV gamma ray. Subsequently, 95 percent of the deexcitation of the 1.292 MeV energy level is to ground state producing a 1.292 MeV gamma ray and the remaining 5 percent decays to the 1.095 MeV level producing a 0.193 MeV gamma ray. The deexcitation of the 1.095 MeV energy level is strictly to the ground state of $^{59}_{27}$Co thus producing a 1.095 MeV gamma ray 100 percent of the time.

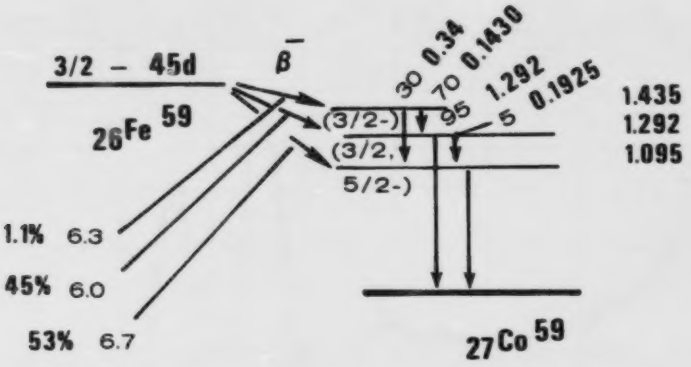
3/2 − 45d
$\bar{\beta}$
$_{26}Fe^{59}$
1.1% 6.3
45% 6.0
53% 6.7
(3/2-)
(3/2,
5/2-)
30 0.34
70 0.1430
95 1.292
5 0.1925
1.435
1.292
1.095
$_{27}Co^{59}$

Figure 2. Decay scheme for iron-59 (Fe).

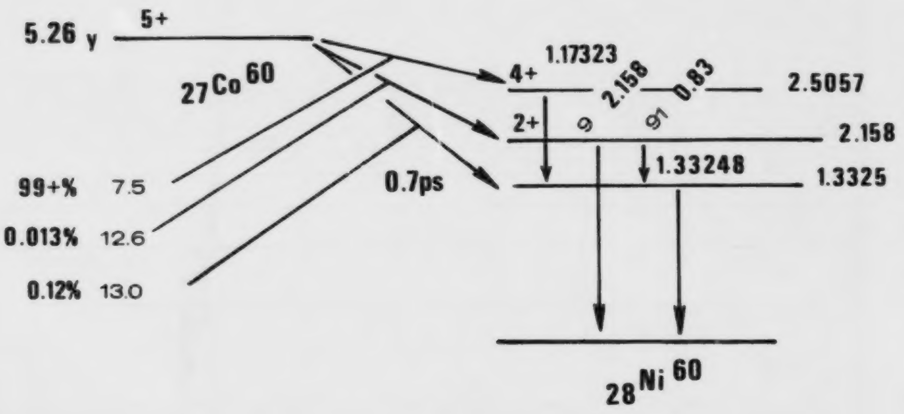
5.26 y
5+
$_{27}Co^{60}$
99+% 7.5
0.013% 12.6
0.12% 13.0
0.7ps
4+
1.17323
9 2.158
91 0.83
2+
1.33248
2.5057
2.158
1.3325
$_{28}Ni^{60}$

Figure 3. Decay scheme for cobalt-60 (Co).

The following calculations to determine the number of gamma rays emitted per decay are based upon the preceding data and internal conversion coefficients. (10, p. 190). The number of 1.292 MeV gamma rays emitted per decay of $^{59}_{26}$Fe is:

$$\left\{(0.70 \times 0.011 + 0.45) \times 0.95\right\} \frac{1}{1 + 0.00011} = 0.43 \qquad \text{(Eq. 8)}$$

from the γ transition 1.435 MeV level to the 1.292 MeV level

from the β decay to the 1.292 MeV level

internal conversion correction

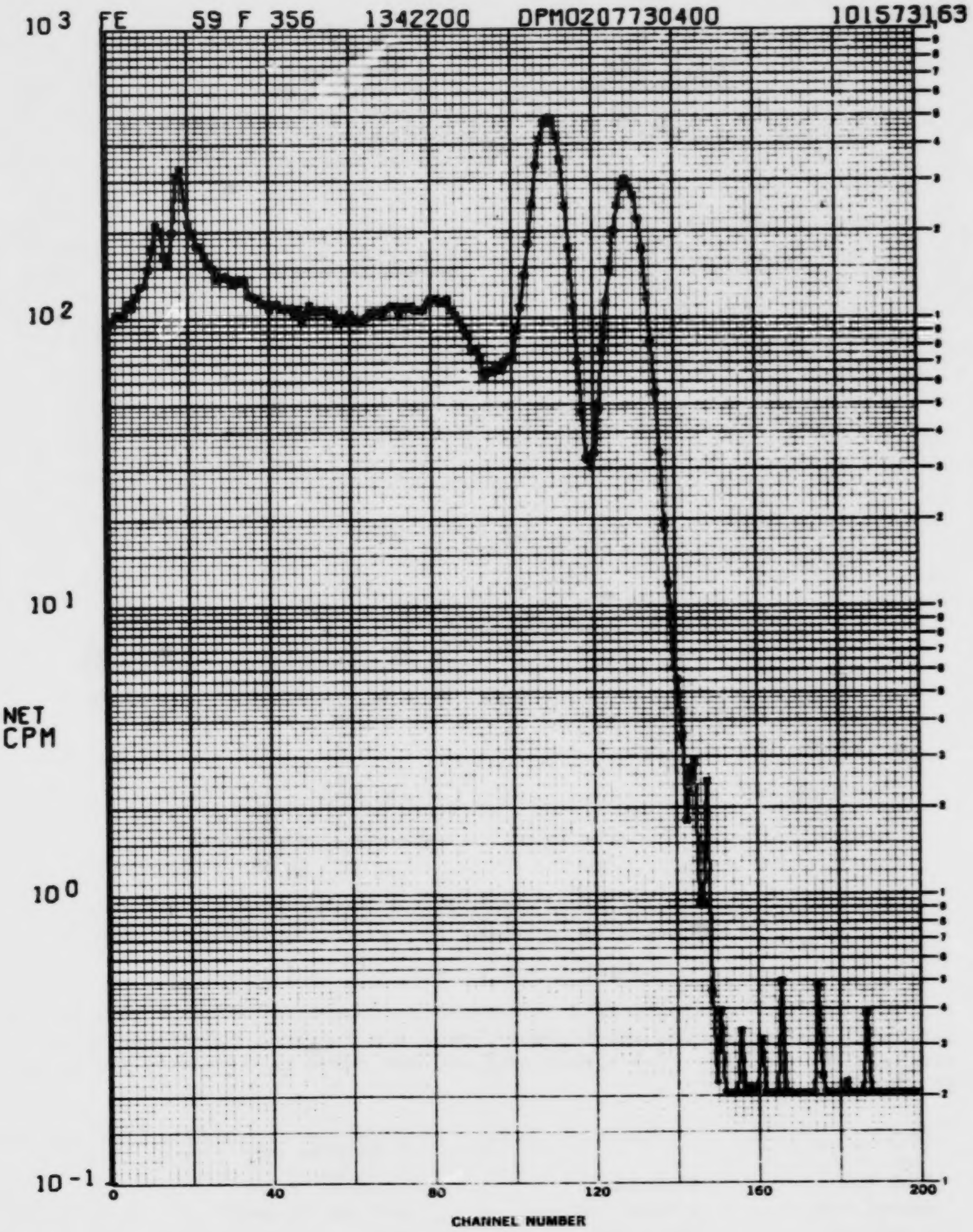

Figure 4. Spectrum of Fe-59 at 10 keV per channel.

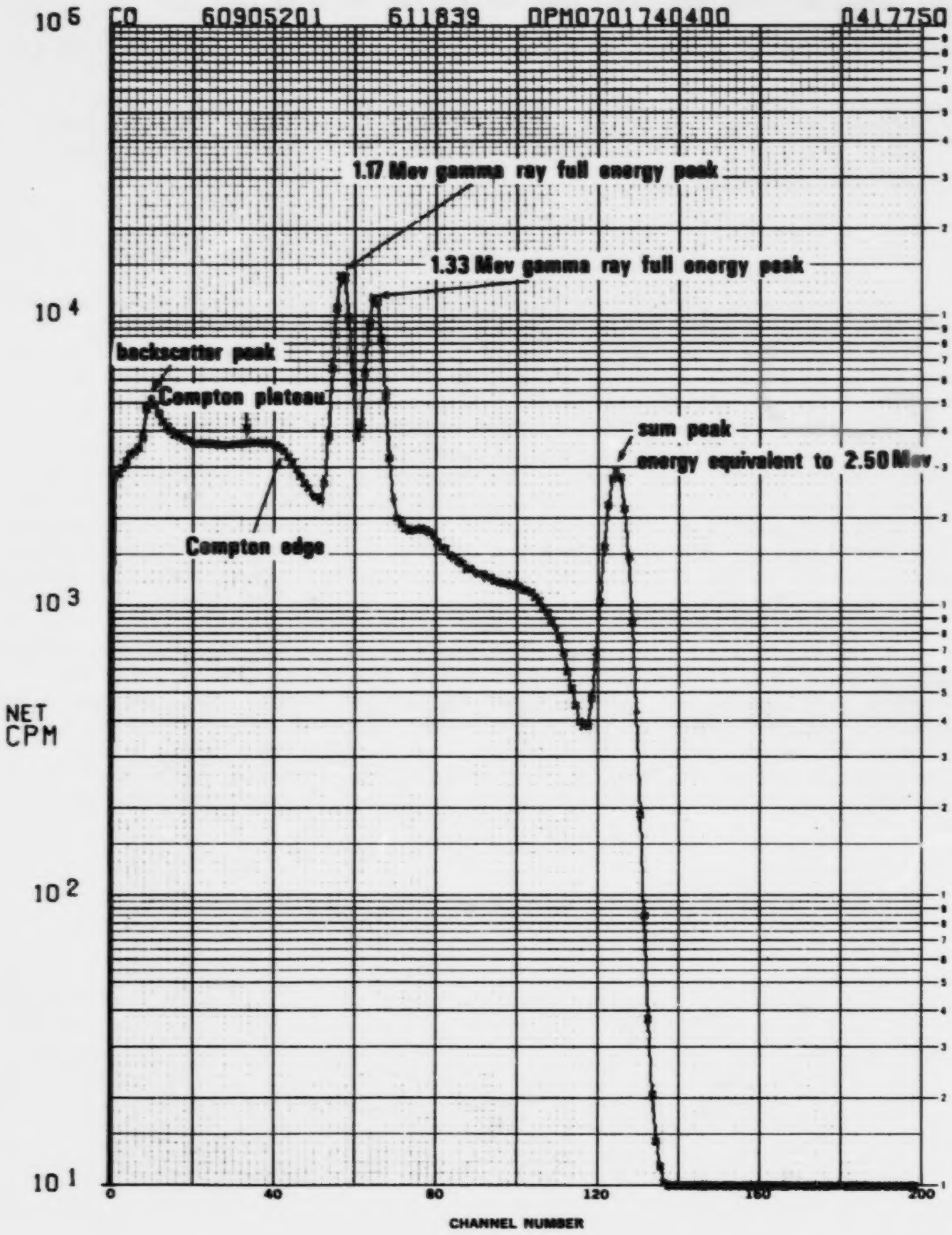

Figure 5. Spectrum of Co-60 at 20 keV per channel.

The number of 1.095 MeV gamma rays emitted per decay of $^{59}_{26}\text{Fe}$ is:

$$\left\{(0.30 \times 0.011) + (0.05)(0.70 \times 0.011 + 0.45) + 0.53\right\} \frac{1}{1 + 0.00014} = 0.56 \quad \text{(Eq. 9)}$$

from the γ transition 1.435 MeV level to the 1.095 MeV level	number of transitions from from the 1.292 MeV level to the 1.095 MeV level	from the β transitions to the 1.095 MeV level of $^{60}_{27}\text{Co}$	internal conversion correction

The beta decay $^{59}_{26}\text{Fe}$ to the 1.292 MeV level of $^{59}_{27}\text{Co}$ is not time related to the beta decay of $^{59}_{26}\text{Fe}$ to the 1.095 MeV level of $^{59}_{27}\text{Co}$. Experimentally the 1.292 MeV and the 1.095 MeV gamma rays are detected independently. $^{60}_{27}\text{Co}$, on the other hand, decays primarily through one beta branch to a 2.5057 MeV level of $^{60}_{28}\text{Ni}$. $^{60}_{28}\text{Ni}$ decays by emitting a 1.17 MeV gamma ray followed by a 1.33 MeV gamma ray to reach ground state. These two gamma rays are emitted in cascade and occur within a few picoseconds of each other for a given nuclear decay and also exhibit angular dependence. The internal conversion coefficients are small (approximately 0.00017), consequently the intensities of the 1.17 MeV and 1.33 MeV gamma rays are very nearly equal. There is one 1.17 MeV and one 1.33 MeV gamma ray per disintegration of $^{60}_{27}\text{Co}$. The summing of the two gamma-ray responses in the NaI(Tl) crystal account for the pulses above the singles peak in the ^{60}Co spectra which does not occur in the ^{59}Fe spectra.

Lederer, et al., (10), has tabulations of the types, approximate energies and intensitities of the major radiations of all the radionuclides. The *Nuclear Data Sheets* (11) are compilations of recent data, give complete decay schemes, but don't always present the number of gamma rays emitted per disintegration of the parent radionuclide. The *Nuclear Data Sheets* however list the internal conversion coefficients by which the number of gamma rays emitted per disintegration can be calculated as indicated in preceding paragraphs.

GAMMA-RAY INTERACTIONS WITH MATTER

A knowledge of the basic processes by which a photon interacts with matter is essential to an understanding of the gamma-ray response of a scintillation detector. Photons interact with the scintillator (crystal or phosphor) of a gamma-sensitive scintillation detector producing a tiny quantity of light called a scintilla. When all of the energy of a gamma ray is absorbed by the scintillator of a scintillation detector, the quantity of light that is produced is very nearly proportional to the energy of the absorbed gamma photon. The quantity of light produced in the scintillator falls on a photocathode causing the ejection of electrons. The electrons ejected from the photocathode are multiplied in number by a photomultiplier tube. A good scintillation detector will deliver to its associated recording instrument a measureable current pulse or a measureable electric charge that is proportional to the energy deposited in the scintillator by the gamma ray.

Matter absorbs energy from gamma rays principally by (a) the photoelectric effect, (b) Compton scattering, and (c) pair production. These effects are described briefly in the following paragraphs. It must be kept in mind, however, that the information produced by (or response from) a scintillation detector results from the energy deposited in the scintillator.

Photoelectric effect:

The photoelectric effect is the process by which a photon is annihilate through the total transfer of its energy to an electron in the vicinity of an atomic nucleus. The photoelectron leaves the neighborhood of the atomic nucleus with a kinetic energy of the interacting photon minus the binding energy (energy to remove the electron from its orbit about the atomic nucleus). Gamma-ray absorption by means of the photoelectron effect is possible only when the photon has more energy than the binding energy of the electron. Electrons have much smaller ranges in matter than gamma rays. Consequently, the probability that an electron might escape from a scintillator when emitted near its surface is much smaller than the probability that a photon might escape under similar circumstances. Therefore, almost all photoelectric events result in complete absorption of the photoelectron energy.

The nucleus of an atom in the scintillator from which a photoelectron has been ejected is left in an excited state. When the ejected electron is replaced, there is an emission of a characteristic x-ray photon. The x-ray photon may escape from the scintillator, thus producing what is called an "escape peak." More commonly, the x-ray photon will also be absorbed in the scintillator which results in the recording of an event in a "full energy peak." The probability that an x-ray will escape from the scintillator is generally small so that the peak resulting from a photoelectric event without the x-ray being detected is much smaller than the full energy peak. When a 7.6-cm by 7.6-cm NaI(Tl) detector is used, the escape peak is 6 percent of the full energy peak for 100 keV photons, but only 1.2 percent of the full energy peak for 200-keV photons. The spectra of cerium-141 and cerium-144 in Appendix E are illustrative of full energy peaks accompanied with escape peaks recorded by NaI(Tl) detectors. The iodine escape peak is 29 keV below the full energy peak.

Compton scattering:

Incoherent or Compton scattering results when a photon collides with an electron giving up part of its energy to the ejected electron, with the scattered photon retaining the remaining energy. The ejected electron loses its energy in the scintillator. These high energy photons have a high probability of escape. The maximum energy that can be deposited by Compton events in scintillators represents the maximum quantity of light that can be produced by the incident gamma photons if the scattered photon does not interact with the scintillator. The broad region of lower energy and less height in the Compton spectrum is principally representative of the Compton electron energies that are converted to quantities of light in the scintillator when their corresponding Compton photons escape. Figure 6 is a pictorial representation of a scintillation spectrum for Compton events.

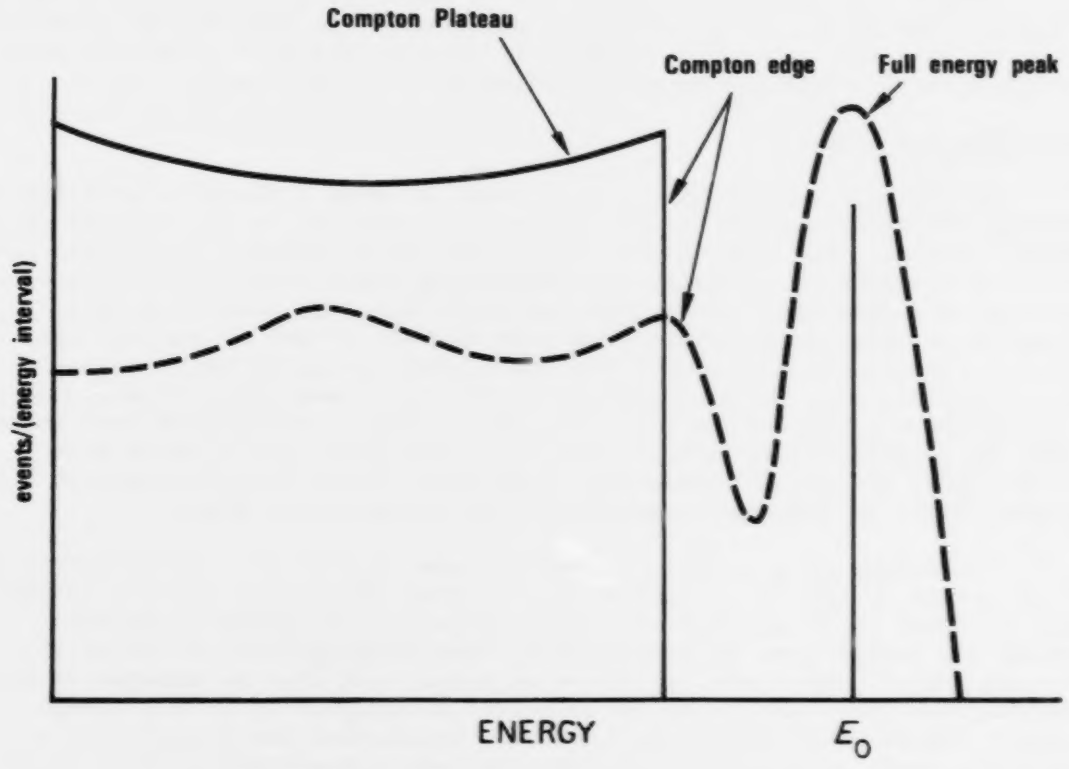

Figure 6. "Ideal" spectrum of Compton interactions.

In the Compton process the energies of the scattered photon and electron have the following relationships:

$$E'_{\gamma} = \frac{E\gamma}{1 + \frac{E\gamma}{0.511}(1 - \cos\theta)} \qquad \text{(Eq. 10)}$$

$$E_{e} = E_{\gamma} - \frac{E\gamma}{1 + \frac{E\gamma}{0.511}(1 - \cos\theta)} \qquad \text{(Eq. 11)}$$

where E_{γ} is the incident gamma ray energy in MeV, E_{e} is the scattered electron energy in MeV, 0.511 is the rest mass energy of an electron and θ is the angle between the direction of the incident photon and the scattered photon. The energy of an electron at the Compton edge, E_{ce}, is related to the energy of the incident photon as follows:

$$E_{ce} = E_{\gamma} - \frac{E\gamma}{1 + \frac{2\,E\gamma}{0.511}} \qquad \text{(Eq. 12)}$$

where E_{γ} is in MeV. Table 1 lists the energy of the Compton edge as a function of the incident photon energy.

TABLE 1. COMPTON EDGE ENERGY AS A FUNCTION OF INCIDENT RADIATION ENERGY

E_{γ} (MeV)	E_{ce} (MeV)	E_{γ} (MeV)	E_{ce} (MeV)
0.1	0.03	1.1	0.90
0.2	0.09	1.2	0.99
0.3	0.16	1.3	1.09
0.4	0.25	1.4	1.19
0.5	0.33	1.5	1.29
0.6	0.42	1.6	1.38
0.7	0.52	1.7	1.48
0.8	0.61	1.8	1.58
0.9	0.70	1.9	1.68
1.0	0.80	2.0	1.78

Pair production:

Pair production is possible when the incident photon has an energy in excess of 1.02 MeV (the rest mass energy of an electron-positron pair). Pair production occurs in the presence of the coulomb field of an atomic nucleus. The incident photon disappears and an electron-positron pair is created. The total energy of the electron-positron pair will be equal to the total energy of the incident photon and their kinetic energy will be equal to the total energy minus 1.02 MeV. An unstable condition occurs when a positron comes to rest in the field of an electron. The positron and electron are annihilated and two photons of 0.511 MeV are emitted. All of the energy of an incident photon may be absorbed by the scintillator or one or both of the 0.511 MeV electrons may escape detection. Consequently, the following transfers of energy to the scintillator are possible:

1. All of the energy of the incident photon.

2. The energy of the incident photon minus 0.511 MeV (single escape annihilation peak).

3. The energy of the incident photon minus 1.02 MeV (double escape annihilation peak).

An incident photon will interact with a scintillator by one of the three processes described in the preceding paragraphs. The fraction of photons that interact by any one process is related to the mass attenuation coefficient for that process at the energy of the incident photon. The total mass attenuation coefficient, μ/ρ (cm/g), is the linear sum of the individual mass attenuation coefficients:

$$(\mu/\rho)_{\text{total}} = (\mu/\rho)_{\text{photoelectric}} + (\mu/\rho)_{\text{Compton}} + (\mu/\rho)_{\text{pair production}} \qquad \text{(Eq. 13)}$$

The total probability, P, of photon interaction with a scintillator is a function of the size of the scintillator and the total mass attenuation coefficients. The following formula may be used:

$$P \approx 1 - e^{-\left[(\mu/\rho)_{\text{total}}\right]x} \qquad \text{(Eq. 14)}$$

where x is the thickness of the scintillator in grams per square centimeter (gm/cm^2) seen by the incident photon. The total mass attenuation coefficient for NaI(Tl) is shown in Figure 7. (15).

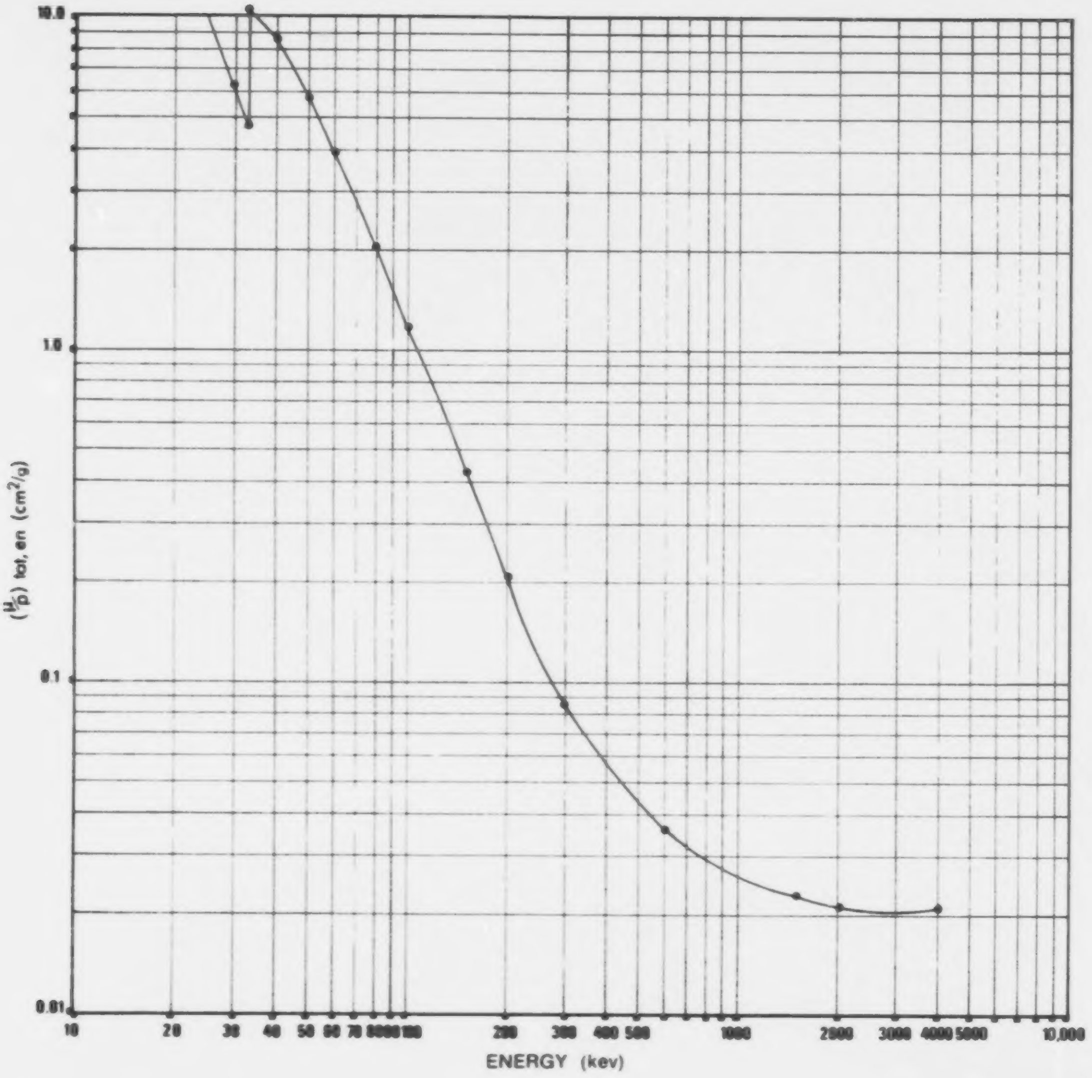

Figure 7. Mass attenuation coefficient of sodium iodide.

TERMINOLOGY OF GAMMA-RAY SPECTROSCOPY

Several terms are commonly used in describing prominent portions of the spectrum obtained from a spectrometer. Figures 5 and 8 illustrate these terms.

1. Efficiency -- the term that relates some predefined (by predetermined convention) observed count rate to the true disintegration rate of the specific radionuclide in the sample which is being counted. Although several definitions of efficiency are used, the basic concept is:

$$\text{efficiency} = \frac{\text{counts per unit time}}{\text{disintegrations per unit time}} \qquad \text{(Eq. 15)}$$

With experience, one can choose the conventions best suited for a particular analysis. Whichever convention is chosen, it should be used consistently. One should avoid choosing conventions which are based upon the edges of regions that lie in rapidly varying parts of a spectrum.

2. Full energy peak -- a peak which represents complete transfer to the detector of the energy of a monoenergetic incident photon. The peak is prominent in Figure 8 with its center located at channel 66. Full energy peaks in Figure 5 are located in channels 57 and 64.

3. Peak energy -- the energy of the center of a spectral peak. This energy can be obtained from tables concerning the disintegration schemes of radionuclides when the radionuclide is identified, or from a previously determined calibration when using calibration standards with known gamma-ray energies.

4. Peak area -- the area under a spectral peak. Several conventions (16, pp. 245-251) are used in determining peak areas. Any one of the conventions will be satisfactory, but only one should be used to assure consistency in analyzing data and calibrating the spectrometer.

5. Compton edge -- the termination of the Compton plateau below the full energy peak which represents the high-energy boundary of the Compton distribution. The energy of the Compton edge is related to the energy of the full energy peak by:

$$E_{ce} = E_{\text{full energy peak}} - \frac{E_{\text{full energy peak}}}{1 + 3.91E_{\text{full energy peak}}} \qquad \text{(Eq. 16)}$$

where E is expressed in MeV.

For the 0.661 keV gamma ray in Figure 8, the Compton edge falls at 0.48 MeV.

6. Compton area -- the area under the portion of the spectrum which is

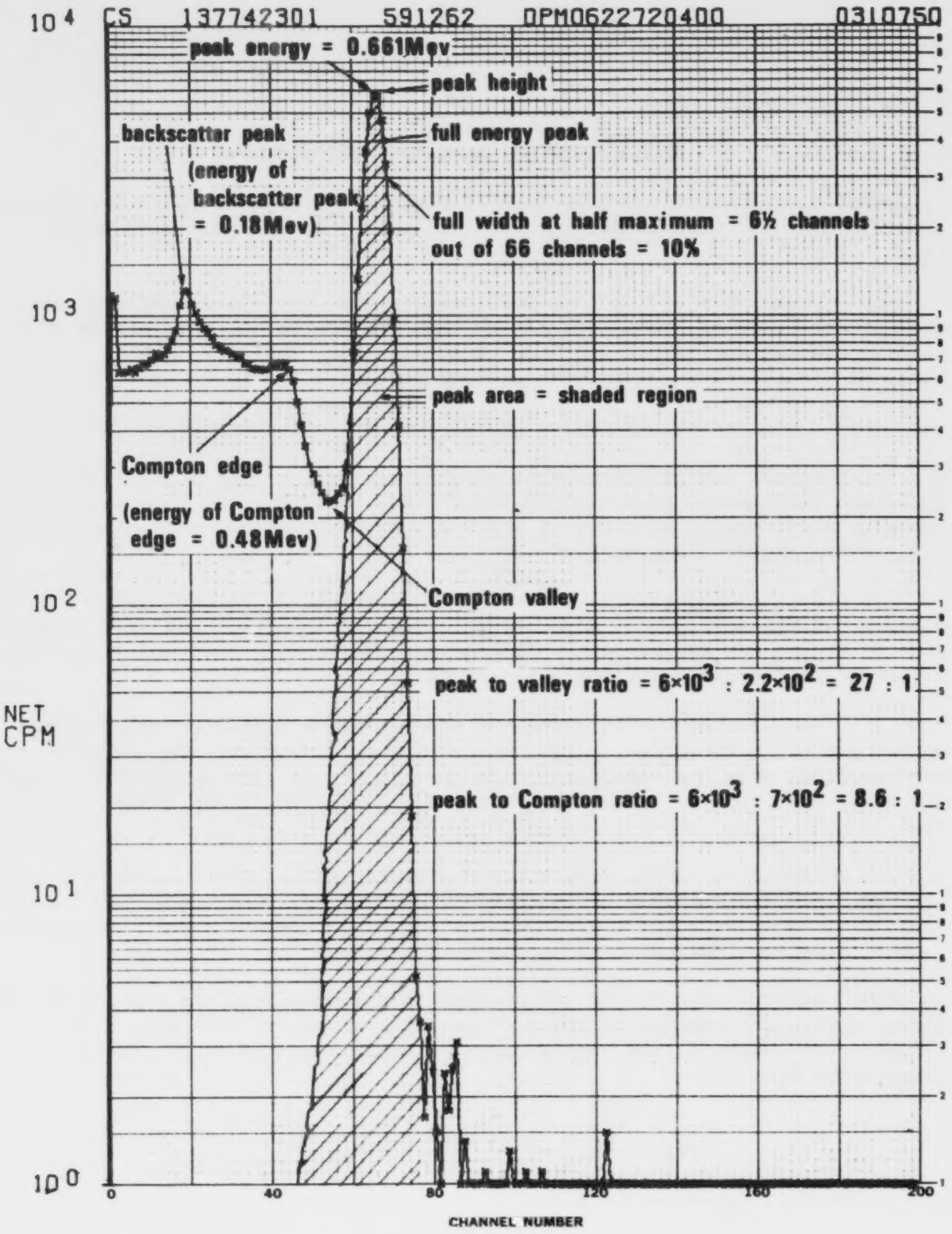

Figure 8. Spectrum of Cs-137 at 10 keV per channel.

due to partial energy transfer by Compton interaction (e.g., the area under the Compton plateau). This should not include counts due to the other effects, such as the backscatter peak, but can be used for each geometry when systematic care is used.

7. Compton valley -- the low portion of the spectrum immediately preceeding the full energy peak.

8. Backscatter peak -- Another characteristic of the Compton area is the backscatter peak. When photons emitted from the sample interact (by Compton effect) with surrounding materials such as the background shield, the photons that are scattered through an angle of approximately 180° have a possibility of interacting with the crystal detector. Quite often these "backscattered" photons result in a peak which is superimposed on the Compton continuum. The energy of the "backscatter peak" is equal to the energy of the incident gamma ray minus the energy of the ejected electron. This backscatter peak energy can be calculated by the equation:

$$\text{Energy backscatter peak} = \frac{E_\gamma}{1 + 3.91\,E_\gamma} \qquad \text{(Eq. 17)}$$

where E_γ is the incident photon energy.

The backscatter peak becomes less noticeable as the incident gamma energy increases. This is due to the fact that with increasing energy the total Compton cross section decreases, and the angular distribution of the scattered photons from Compton interaction becomes more predominant in the forward direction; therefore, the backscattering becomes less. Unlike the Compton edge, the backscatter peak has a maximum energy of 0.256 MeV.

The backscatter peak may also be affected by the geometry relationship between the sample and crystal. This effect is especially observed when comparing a well crystal with a flat crystal. The flat crystal will have a more prominent backscatter peak, due to the greater probability of the photons interacting with other substances before they interact with the crystal. Examples of backscatter peaks are shown in Figures 5 and 8.

9. Escape peaks -- Escape peaks are denoted as spectrum peaks at some energy less than the photopeak energy. These result when discrete amounts of energy escape from the crystal. Using a similar nomenclature, the so-called Compton continuum might well be called a Compton escape continuum.

The most predominant type of escape peak is due to pair-production interaction and its subsequent annihilation radiation. When the pair-production positron interacts with an electron, they both disappear and two 0.51-MeV photons are given off at 180° from each other. If this annihilation takes place near the surface of the crystal, one of the two photons may escape the crystal while the other is absorbed. By repetitions of this occurrence, a second peak occurs in the spectrum which is at an energy 0.51 MeV less than the photopeak. Of course, this type of escape peak will only be seen for incident gamma rays of over 1.02 MeV as pair production will not occur below this energy. There is also the possibility that both annihilation photons will escape, causing a second escape peak to occur at 1.02 MeV less than the photopeak energy. The occurrence of two such escape peaks, at 0.51 and 1.02 MeV less than the photopeak, is sometimes referred to as pair peaks.

A second type of escape peak is due to the fact that the photoelectric absorption in sodium iodide scintillation crystals occurs mainly in the iodine K-shells. This requires a minimum of 33.2 keV energy in the incident radiation in order to eject a K-shell electron from the iodine atom. The binding energies of the K- and L-shell electrons are 33.2 and 5.2 keV respectively. A characteristic x-ray equal to the differences between these binding energies, 33.2-5.2 = 28 keV, is emitted when the K-shell vacancy is filled. If this X-ray is emitted near the boundaries of the detector, there is an appreciable probability of its escape. This results in another peak in the spectrum 28 keV less than the photopeak and is referred to as the iodine X-ray escape peak. Iodine escape peaks are significant features of spectra of gamma rays with energies between 33 and 200 keV. The energy of the escape peak may be too low to appear in the spectrum, or at higher incident gamma energies (approximately above 200 keV) it may be incompletely resolved from the photopeak. Further, the probability of generating an iodine X-ray escape peak declines with increasing energy of the incident radiation. For the most part, this is a result of greater penetration of the more energetic radiation into the crystal before the photoelectric interaction takes place, with the resulting smaller probability for escape of characteristic X-rays originating deeper in the crystal. Figures E-36 and E-37, Appendix E, illustrate iodine X-ray escape peaks.

10. Sum peaks -- "sum peaks" is the general terminology for portions of gamma-ray spectra that are the result of more than one photon interacting with the crystal within a sufficiently short period of time so that the combined light emissions of the crystal are seen as one single light pulse by the photomultiplier tube.

One common type of sum peak is associated with positron annihilation radiation when a positron-emitting source is counted in a well crystal. In this case, the two back-to-back 0.51 MeV gamma photons may both interact, resulting in a spectrum peak at 1.02 MeV.

Some of the 0.51 MeV photons may escape, resulting in both a 0.51 and a 1.02 MeV peak from positron emitters. With a flat crystal there is little probability that a 1.02 MeV peak will occur, and the 0.51 MeV peak will be the only indication of a positron emitter.

Coincidence sum peaks result when two or more gamma rays are emitted from a nucleus in cascade, and are absorbed by the detector. Coincidence sum peaks have been discussed previously in describing the spectra of $^{60}_{27}$Co. Figure 5 illustrates this type of sum peak.

Accidental sum peaks occur when gamma rays from two or more nuclei, or origins, are detected simultaneously. The intensity of an accidental sum peak varies as the product of the intensities of the peaks being summed. At low count rates, they will be weak. As the count rate increases, the intensity of the accidental sum peak will increase faster than the intensity of the full energy peaks being summed. Figure E-2, Appendix E, shows an accidental sum peak resulting from the coincidence of a 1.274 MeV gamma ray and a gamma ray from a positron annihilation.

The intensity of coincident full-energy peaks is linearly related to the efficiency and geometry of the source-detector combination. The intensity of a sum peak is proportional to the product of two efficiency terms and is proportional to the square of the geometrical efficiency. Thus, to tell if a peak is a full-energy peak or a sum peak one can either change the geometry of the counting system or otherwise vary the efficiency of gamma detection of the gamma rays. For example, suppose the intensity of one gamma ray is related to the activity of the sample by:

$$I_1 = E_1 A_o \qquad \text{(Eq. 18)}$$

where E_1 is the probability of detecting the peak, A_o is the activity of the sample, and I_1 is the measured intensity of the gamma ray. The intensity of the second gamma ray is related to the activity of the sample by:

$$I_2 = E_2 A_o \qquad \text{(Eq. 19)}$$

and that the gamma rays are emitted in coincidence; then the intensity of the sum peak is:

$$I_{sum} = E_1 E_2 A_o \qquad \text{(Eq. 20)}$$

If the efficiencies of detection are reduced by two, and a second measurement is made, the recorded intensities designated with asterisks will be:

$$I^*_1 = \frac{E_1}{2} A_o = \frac{I_1}{2}$$

$$I^*_2 = \frac{E_2}{2} A_o = \frac{I_2}{2}$$

$$I^*_{sum} = \frac{E_1}{2} \frac{E_2}{2} A_o = \frac{I_{sum}}{4} \qquad \text{(Eq. 21)}$$

Thus, by changing the efficiencies by a factor of 2, the ratio of I_1/I_2 remains the same, but the ratio of either full energy peak to the sum peak (I_1/I_{sum} or I_2/I_{sum}) increases by 2.

11. Resolution -- the resolution of a spectrometer is a measure of its ability to resolve two peaks that are fairly close together in energy. The resolution of a full energy peak is defined as follows:

$$R = \frac{\Delta E}{E} \times 100 \qquad \text{(Eq. 22)}$$

where R = the resolution in percent

ΔE = the full width of the full energy peak at half of the maximum count level [full width half maximum (FWHM)], measured in energy units (channels times the energy per channel)

E = energy of the photopeak (energy represented by the centroid of the photopeak)

In Figure 8 the full energy peak is in channel 66 and the FWHM is 5.5 channels. With a calibration of 10 keV/channel, the resolution is calculated to be 8.3%.

Using Figure 8 for reference, one could choose channels 52 thru 55 to determine the low energy boundary of the full energy peak. It is recommended that channels 59 through 66 not be used for this selection since instrumental drift and small changes in resolution can lead to selecting a different efficiency. Channels 77 through 85 would provide a satisfactory boundary on the high energy side. If computer analysis is not available, one should take as much leeway as possible in defining regions to determine count rates.

The convention for activity is not as simple as it first seems. Activity *per se* is defined as the number of nuclear disintegrations per unit time. Some conventions choose to relate this to the parent activity of a nuclide which has radioactive daughters. Other definitions relate efficiency only to the number of gamma rays of a particular energy. When suitable samples, e.g. those that only emit one gamma ray, or those that emit two gamma rays not in coincidence, are available, it is recommended that one determine:

$$\text{total efficiency} = \frac{\text{sum of all the counts per unit time}}{\text{activity of the sample}} \qquad \text{(Eq. 23)}$$

$$\text{gamma efficiency} = \frac{\begin{array}{c}\text{sum of the counts in full energy}\\ \text{peak per unit time}\end{array}}{\begin{array}{c}\text{number of gamma rays emitted from}\\ \text{the sample per unit time}\end{array}} \qquad \text{(Eq. 24)}$$

$$\text{sample efficiency} = \frac{\text{counts in a defined area}}{\text{activity of the parent radionuclide}} \qquad \text{(Eq. 25)}$$

where the number of gamma rays is determined from the activity by $N_{\gamma g}$, which is the gamma branching ratio times the activity.

When measuring sample efficiency, one must know that the sample is in equilibrium, or make a curve relating efficiency to the time of purification of the sample.

EQUIPMENT

Gamma ray scintillation detectors are usually obtained from commercial suppliers as an integral unit consisting of a NaI(Tl) crystal optically coupled to a photomultiplier. The detector unit is constructed light-tight and hermetically sealed because of the hygroscopic nature of the NaI(Tl) crystal. Some detector units are furnished without a bias network or tube base, which must then be ordered separately from any of the vendors.

A NaI(Tl) crystal fluoresces with a blue light when exposed to ionizing radiation. The light emitted from the crystal is proportional except for low values due to the energy deposited in the crystal by the ionizing radiation. Photomultipliers are able to detect the light pulse and produce a corresponding charge pulse. The amount of charge produced by the photomultiplier is proportional to the amount of light incident on the photocathode of the photomultiplier which in turn is proportional to the light produced by the interaction of the gamma rays with the NaI(Tl) crystal. The optical efficiency of the gamma ray scintillation detector is enhanced by:

1. Optically coupling the NaI(Tl) crystal to the photomultiplier tube by the use of ophthalmological petroleum jelly or a silicone oil to reduce light losses through total internal reflection.

2. Rough grinding the surfaces not in contact with the photomultiplier tube to improve the transmission of light to the exit surface.

3. Placing a reflective material, e.g., magnesium oxide or alpha aluminum oxide (Linde 'A'® abrasive), in contact with the exposed surfaces of the NaI(Tl) crystal.

Gamma rays have well-defined and unique energies. When a gamma ray is totally absorbed in the NaI(Tl) crystal, the resulting light pulse and the subsequent current pulse from the photomultiplier will be quantified and the amplitude will be proportional to the energy of the gamma ray. This electrical pulse (charge), as measured by a multichannel analyzer, is called the full energy peak or, sometimes, the photopeak. If the gamma ray is not totally absorbed in the NaI(Tl) crystal, the resulting pulse will be of a lesser magnitude than the full energy peak and constitutes a pulse in the Compton continuum. The Compton continuum extends from essentially zero to a maximum energy value called the Compton edge.

The number of gamma rays that are totally absorbed versus the number of gamma rays partially absorbed is a function of (a) the energy of the gamma rays, (b) a combination of the source geometry and detection geometry, (c) the

---

®Registered trade name.

material surrounding the source and the detector. Although it is possible to calculate the portion of gamma rays that will be totally absorbed, it is easier and usually more accurate to measure this portion by using calibrated radionuclide sources for each radionuclide and geometry of interest.

NaI(Tl) crystal sizes suitable for environmental analysis range from 5.1-cm diameter (2-inch) by 5.1-cm thick (2-inch) to 22.9-cm diameter (9-inch) by 10.2-cm thick (4-inch). The more commonly used sizes are the 7.6-cm (3-inch) by 7.6-cm (3-inch) and the 10.2-cm (4-inch) by 10.2-cm (4-inch). Detection efficiency is a function of volume; thus the larger NaI(Tl) detectors are more desirable, but they are also more easily damaged and more expensive. Furthermore, the larger the detector, the more poorly it measures low-energy gamma rays. Large detectors require a thicker shield to protect the NaI(Tl) crystal, resulting in the absorption of many photons. Also, those photons which do enter the crystal tend to interact the farthest from the light exit, resulting in a lower efficiency through excessive light loss. Small samples may be analyzed efficiently and with high resolution by the use of well detectors. The well detector NaI(Tl) crystal is metal-sheathed and has a cavity or well into which radioactive samples are placed for counting. The geometrical factor for samples in a well counter is as much as twice that possible for a cylindrical detector, resulting in a proportionally higher sample count rate.

Components of gamma spectroscopy systems have been largely standardized following the advent of the U.S. Energy Research and Development Administration (formerly U.S. AEC) "NIM" (nuclear instrumentation module) specifications.(17) Amplifiers, single channel analyzers and other components supplied by one manufacturer can be used with the components supplied by other manufacturers. Unfortunately, the NIM standards are not complete and there are, therefore, some units that are not interchangeable. The most notable exceptions to compatibility between modules are found in printing units such as printing timers and printing scalers. If any part of a data readout system is different from the other parts of the data system, one must ascertain the compatibility of the units. The other area of possible noncompatibility is between amplifiers and preamplifiers. If a separate power supply and signal cable are used for the preamplifier, the noncompatibility does not matter. However, if the power and signal for the preamplifier are connected directly to the amplifier, care must be used to make sure the units are compatible. In most cases, a small wiring change will be necessary, but this is easily accomplished by any electronics technician.

The NIM bin and power supply is the mainstay of modern electronics. All other modules go into this one unit. Amplifiers, single channel analyzers, power supplies, timers, scalers, etc., are compatible with these units. A fully-wired NIM bin gives the user all the versatility available.

There are many configurations and electronic options available for gamma spectroscopy. The following basic gamma spectroscopy system is adequate for routine environmental analysis, but other combinations of components are also used. The necessary components are:

1. A NaI(Tl) detector, 7.6-cm by 7.6-cm or 10.2-cm by 10.2-cm, optically coupled to a photomultiplier tube.

2. A tube base or stand to support the detector and to support the detector and samples.

3. A preamplifier.

4. NIM bin.

5. A linear amplifier.

6. A high voltage supply.

7. A multichannel analyzer having a minimum of 200 channels.

8. Signal and power cables.

9. A readout unit.

10. A radiation shield

Figure 9 is a typical block diagram and Figure 10 is a photograph of a gamma spectroscopy system in use at the Environmental Monitoring and Support Laboratory in Las Vegas, Nevada.

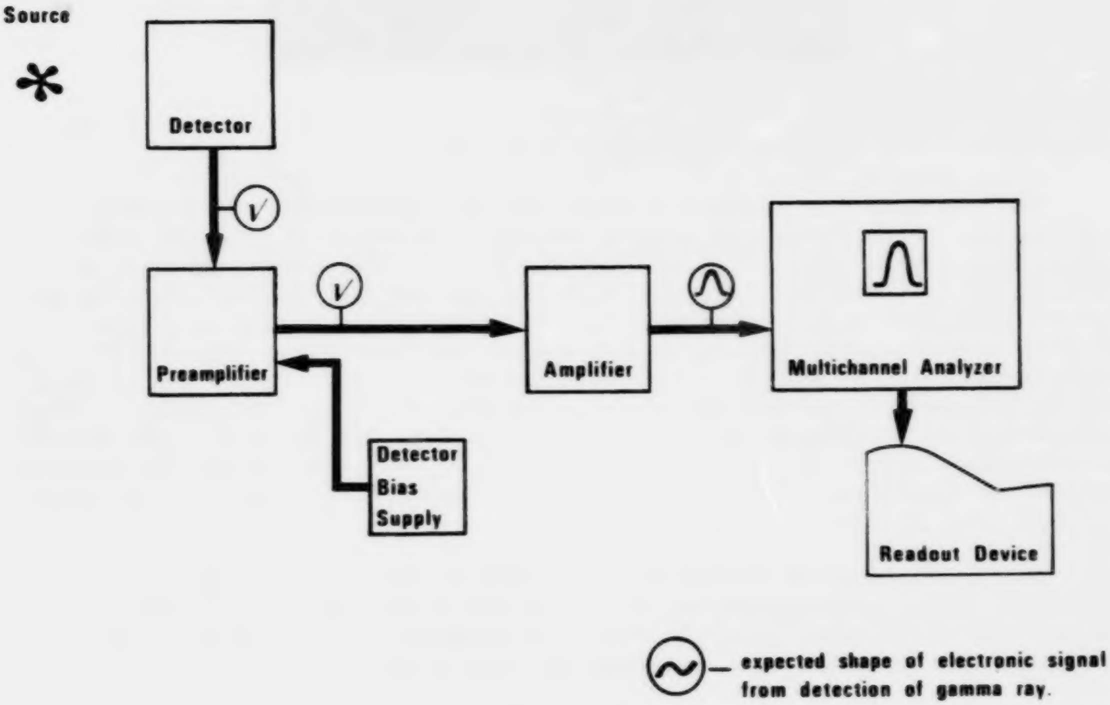
Source
Detector
Preamplifier
Amplifier
Multichannel Analyzer
Detector Bias Supply
Readout Device
expected shape of electronic signal from detection of gamma ray.

Figure 9. Typical block diagram of gamma ray spectrometer.

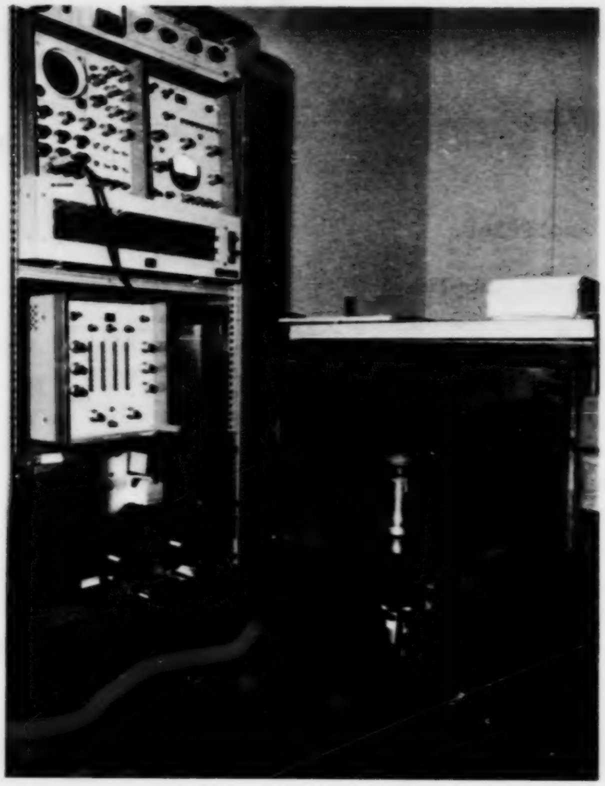

Figure 10. Gamma-ray spectrometer at the Environmental Monitoring and Support Laboratory, Las Vegas, Nevada.

The tube base is connected directly to the detector-photomultiplier tube combination. High voltage is usually connected directly to the tube base although it can be fed through the preamplifier in some cases. The preamplifier should be coupled to the tube base with as short a cable as possible to reduce electronic noise. The detector and preamplifier should be suitably mounted in a shield of iron or lead to reduce the background from radiation as much as possible. Mounting of the detector-photomultiplier tube for environmental measurements is very important. The mounting should be stable so that samples can be positioned reproducibly and close to the detector. The shield must be large enough to hold the detector and any sample that will be counted. The shield should be at least large enough to accommodate a 4-liter Marinelli beaker. (See Figure 15.)

The signal from the photomultiplier tube is fed to the preamplifier and the signal from the preamplifier is fed to the linear amplifier. The final signal from the linear amplifier should be between 1 and 10 volts for most analyzers, though some older analyzers require other signal levels.

A typical signal from a preamplifier is shown in Figure 11. The signal has an amplitude of approximately 5 millivolts, a rise time of 100 nanoseconds and a 50-microsecond decay. This pulse is amplified and shaped by the linear amplifier resulting in a pulse similar to that sketched in Figure 12.

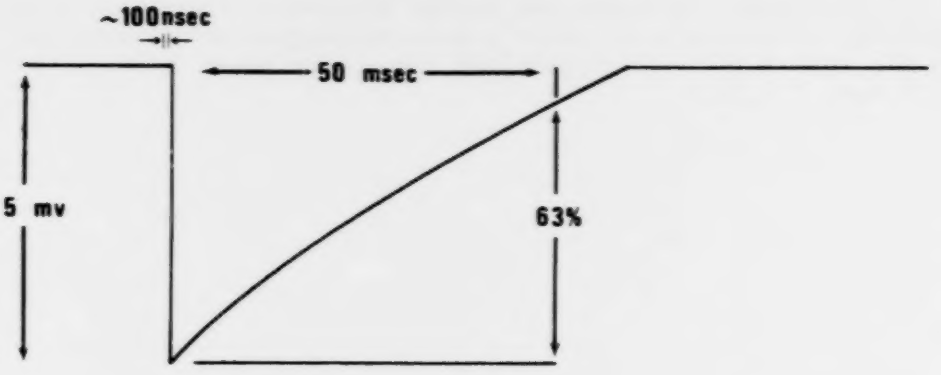
~100nsec
50 msec
5 mv
63%

Figure 11. Schematic representation of a typical pulse from a preamplifier coupled to a NaI(Tl) detector.

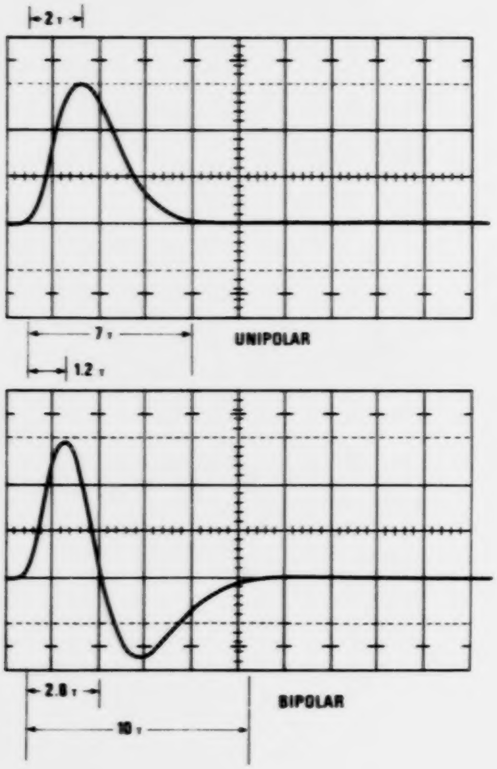
2τ
7τ
UNIPOLAR
1.2τ
2.8τ
BIPOLAR
10τ

Figure 12. Schematic representation of typical pulses from a linear amplifier in a NaI(Tl) spectrometer.

The signals from the linear amplifier are analyzed by the use of a multichannel analyzer. This instrument sorts the electrical pulses from the linear amplifier according to their magnitude and records each in its appropriate "channel." Multichannel analyzers for NaI(Tl) detectors should have a minimum of 200 channels, a display unit, usually an oscilloscope, and a means for recording the data, e.g., a teletypewriter, paper tape punch, parallel printer, or magnetic tape.

INITIAL SETUP

The counting room should be specifically set up for counting source preparations. Laboratory work should not be performed in the same room, or at least not in the same work area, as the detector shield. The counting room should be well ventilated to eliminate the possibility of radon buildup. The temperature should be regulated to within 2 degrees Celsius. Although it is not mandatory for some applications, the counting area should be free of vibration when high resolution or high precision experiments are being performed. The electric power supply for counting instruments should be well regulated and isolated from motors, air conditioners, electric adding machines and typewriters, etc. An electrical interference filter placed in the electric power supply of the offending appliances or device is usually more helpful than placing it in the electric power supply of the counter. A separate ground to earth should be provided and used. Adequate space should be provided between shields and instruments to facilitate safe use and maintenance. No sources should be left or stored in counting rooms in order that the background may be kept as low as possible. Sources should be stored where they are secure from loss and do not constitute a radiation hazard.

With the shield in place, the detector mounted, and the electronics assembled, initial calibration can begin. The high voltage is usually adjusted to 1000 volts. Using a check source of cesium-137 or cobalt-60, the amplifier gain should be adjusted to produce pulses on the order of 5 volts, or approximately at half of maximum channel number on a multichannel analyzer. After the photomultiplier tube has had voltage applied for 1 to 3 days, a test should be made to see if the count rate is independent of small variations in applied voltage. First one turns on the analyzer. If the number of events being recorded in the lower channels of the analyzer is large, the low-level discriminator may need adjusting. If there are no counts being recorded it is possible that the low-level discriminator has been adjusted incorrectly. In this case the discriminator should be adjusted until low-energy events are being detected, and then adjusted until no low-level events are being detected. This will produce an approximate setting to be used for determining the correct bias on the detector. Using a gamma-emitting check source, adjust the voltage to 900 volts or 100 volts lower than the manufacturer's suggested operating voltage. Count the source for a convenient period of time and record the total number of counts in the full energy peak. At least 10,000 counts should be acquired. Increase the voltage by 10 volts, and re-count the source. Repeat until the high voltage has been increased to 1100 volts or 100 volts above the manufacturer's suggested operating voltage. If necessary, the gain on the main amplifier may need adjustment to keep the full energy peak in the range of the analyzer. A plot of the counts versus the applied voltage should be flat, or nearly so, for at least 100 volts. The appropriate high voltage is at the center of this plateau or at the manufacturer's suggested operating voltage. The bias should be adjusted to this value and left on continuously except for maintenance.

The next step is to correctly calibrate the system for energy. To do this, a source with two gamma rays differing significantly in energy, or two sources with differing gamma-ray energies are used. A practicable energy per channel should be chosen. Ten keV per channel is extremely convenient, but twenty keV per channel can be used. A calibration at five keV per channel may be used advantageously for identifying spectral components below 200 keV. Other energies per channel can be used, but should only be used by experienced investigators. Ten keV per channel will cover 0 to 2.56 Mev for a 256-channel analyzer, which is a good range for environmental monitoring. Bismuth-207 or a combination of cesium-137 and cobalt-60 are convenient sources for energy calibration.

Once the check sources are chosen, and the energy range is selected, the gain of the amplifier is adjusted to put one peak in the correct channel for that peak. The other peak is located. If it is too close to the other peak, more gain and more low-level discrimination is indicated and vice versa. By alternately adjusting the gain and a low-level discriminator or the zero to the analog to digital converter (ADC), both peaks can be placed in their proper channels. It is possible to estimate peak positions accurately to within 0.1 channel using a parabolic fit to the data. The peak is located by finding the channel with the most counts. A set of data is then obtained consisting of the channel number and the counts in that channel. The first set, the channel below the peak channel, is labeled $(0, N_0)$, the peak channel is labeled $(1, N_1)$, and the third channel, the channel above the peak, is labeled $(2, N_2)$. For ease of calculation, the minimum count of N_0 and N_2 is subtracted from N_0, N_1 and N_2. Thus three pairs of numbers are obtained. For convenience in this derivation assume N_2 be the minimum.

$$(0, N_0')$$

$$(1, N_1')$$

$$(2, 0)$$

where

$$N_0' = N_0 - N_2$$

$$N_1' = N_1 - N_2$$

$$N_2' = N_2 - N_2 = 0$$

These are then used in the equation for a parabola

$$y = ax^2 + bx, + c \qquad \text{(Eq. 26)}$$

where x is the first number, and y is the second number in the pairs of numbers so far determined. Using these pairs, three equations are obtained.

$$N_0' = c$$

$$N_1' = a + b + c$$

$$0 = 4a + 2b + c$$

These equations are then solved for a, b, and c, e.g.,

$$N_1' - N_0' = a + b$$

$$- N_0' = 4a + 2b$$

$$a = -\tfrac{1}{2}(2N_1' - N_0') \qquad \text{(Eq. 27)}$$

$$b = N_1' - N_0' - a \qquad \text{(Eq. 28)}$$

The peak is found by differentiating the parabolic equation (dy/dx) and solving the derivation for dy/dx = 0, e.g.,

$$\frac{dy}{dx} = 2a\,x + b \qquad \text{(Eq. 29)}$$

$$x = -\frac{b}{2a} \qquad \text{(Eq. 30)}$$

The peak then is located at the channel called 0 plus the value of x, or the peak channel previously found minus 1 plus the value for x.

With persistence, both peaks should be brought to within 0.1 channel of the proper location. After this is accomplished, a third peak should be determined to verify the energy calibration. The energy calibration should be verified daily and records of verification kept as part of an ongoing quality assurance program. It is recommended that a source, or sources, be made for this purpose.

The next phase involves establishing a background rate, checking time, and determining reproducibility. Backgrounds should be measured daily for at least 20 days and nights to determine expected fluctuations in the rate. Backgrounds should be determined at various times of the day and for night counting. Long counts, as well as counts for the expected or usual analysis time, are needed to verify any pattern or to obtain statistical accuracy. A 100-minute background measured with a 10.2-cm by 10.2-cm NaI(Tl) detector is shown in Figure 13. Six prominent peaks appear in this spectrum. The 0.511 MeV peak arises from annihilation radiation of cosmic positrons. The 0.61, 0.72, 1.13, and 1.76 MeV peaks are due to radon daughter products. Potassium-40 accounts for the 1.46 MeV peak. Any other prominent peaks in the background indicate nearby sources which should be removed, or contamination of the counting area which needs to be decontaminated. The shape of the background shown in Figure 15 shows the typical higher count rate at lower energies that occurs naturally.

The time base on the analyzer should be checked with the same check sources used in determining the energy alignment. Counts for all time periods (usually 10 to 400 minutes) are taken, and the count rate determined. The count rate (counts/unit time) should be the same for all time periods used. A calibrated pulse generator can be used for this check. Pulsers that use 60-cycle alternating current for their signal are commonly used and are quite accurate. These not only check consistency in the analyzer timing, but can indicate the accuracy of the absolute timing of the analyzer.

Timing tests should be conducted at moderate count rates, i.e., 200 counts per second (cps), and with the analyzer set in the "live time" mode. A

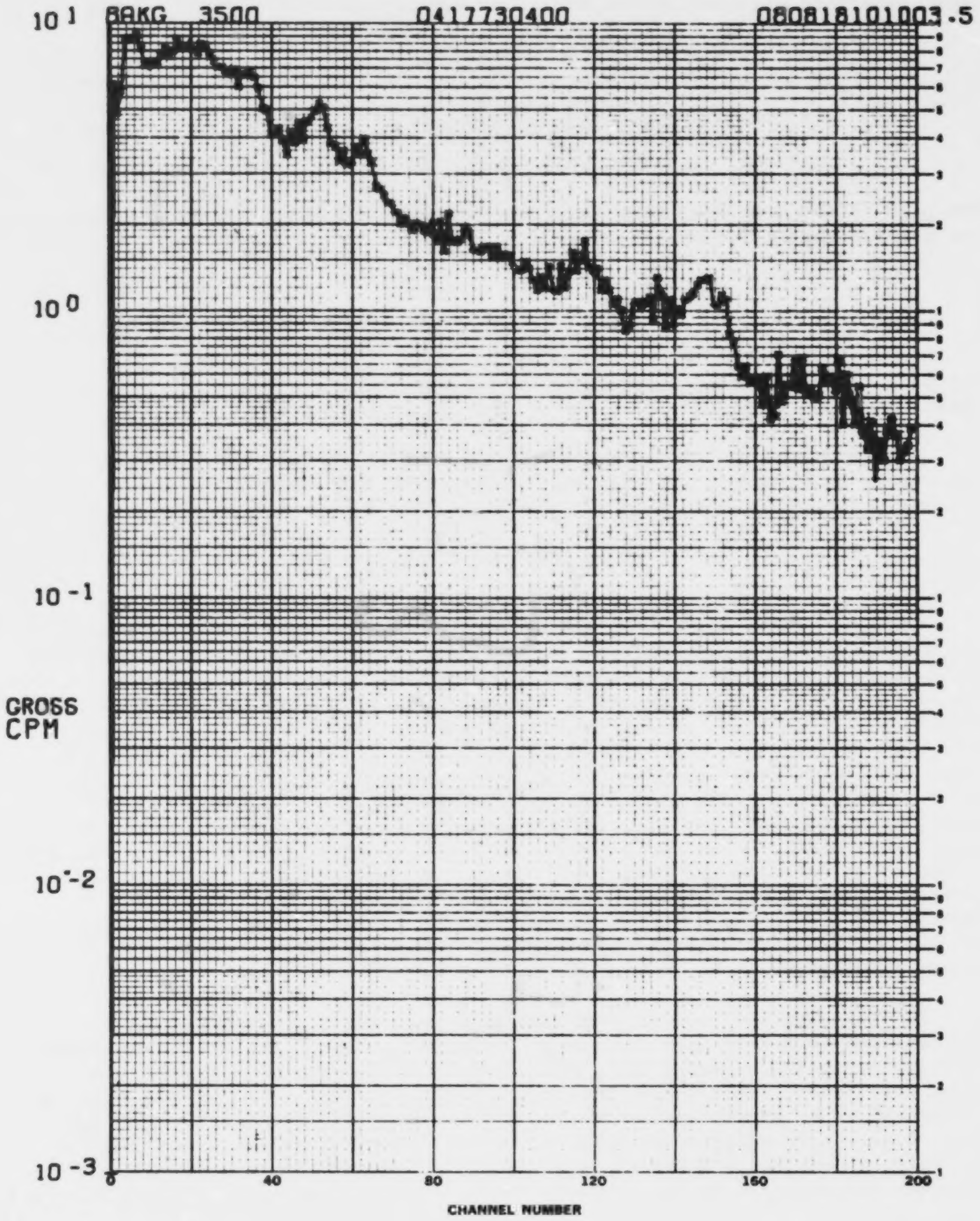

Figure 13. 400-minute background spectrum measured with a 10.2-cm × 10.2-cm NaI(Tl) detector.

weak high energy source having a half-life sufficiently long that a decay correction need not be used, e.g., zinc-65 should be used for this test. After the timer accuracy has been established, a "live time" test should be made. The most probable error in a live timer will be at high count rates which should not be encountered in environmental monitoring, but might occasionally occur when counting standards have too much activity. The live-timer test is based on the following reasoning: if the live timer works accurately for a particular setting, the analyzer will be "alive"--that is, in readiness to accept signal pulses--for the same accumulated time regardless of count rate. Therefore, if a weak source and a hot (high activity) source are counted simultaneously, the total counts of the weak source recorded should be the same as if the weak source were being counted by itself. A hot low-energy source and a weak high-energy source are used for the live-timer test. Typical sources used are mercury-203 (15,000 cps) and zinc-65 (200 cps).

First, the hot source and weak source are counted simultaneously. Next, the weak source is counted alone. The counts in the photopeak of the weak source are totaled for both runs. A comparison of the totals indicates the accuracy of the live timer. A pulser can be used in the place of the weak source and thereby eliminate the uncertainty due to the error in integration of the weak source photopeak. However, consideration should be given to the possibility of errors due to momentary lock-in of the pulser with the analyzer live timer. If there is a simple test or check for random coincidence, it would be of interest. Live timers of analyzers evaluated by other laboratories have shown inaccuracies ranging from 12 percent down to less than 0.5 percent for input rates up to 30,000 pulses per second. (1).

CONTROL CHARTS

Before initiating calibration procedures for quantitative work, quality control charts should be prepared and a routine should be established for maintaining the control charts. A daily plot of the gross background per unit time is the first chart to prepare. Any statistically significant deviation from the average rate should be investigated, and the reason for the change eliminated. Short (10 to 15 minutes) repetitive counting on a given day will, in fact, produce background rates with the expected standard deviation, as will short repetitive counts of a check source. Long counts (400 minutes to 1000 minutes) taken over a long period of time generally will show fluctuations in the background rate larger than counting statistics would indicate. These fluctuations arise mainly because of changes in radon levels in the counting room. However, one can still determine the observed standard deviation, and this deviation should then be used to prepare the quality control chart.

The standard deviation (σ) for N counts is $\pm \sqrt{N}$. The control chart, therefore, has days for the horizontal axis and counts for the vertical axis. Horizontal lines at N, $N \pm 1\sigma$, $N \pm 2\sigma$, and $N \pm 3\sigma$ should be drawn on the chart. As the number of determinations is increased, the number of points plotted between N and $N \pm 1\sigma$ should approach 68 percent of the total number of points; the number of points between N and $N \pm 2\sigma$ should be close to 95 percent of the total number of points. There should be almost no (less than 0.2 percent) data points outside of the lines indicating 3σ deviation from the average. Any point outside this range is suspect, and an immediate redetermination of the background should be made. If the redetermination is also out of the control limits the cause for the change in the background should be determined and corrective action taken. If the change is an increase in the count rate, a source has been left in the counting area, the counting area has become contaminated and should be decontaminated, or the electronics is adding counts. A cause for a decrease in the background rate could be electronics or the presence of material in the counting area which is acting as a further shield for the counting system. Backgrounds for each type of sample and sample configuration to be analyzed should be documented and plotted on the control charts, as they can be quite different.

Similar charts should be made for each of the two peaks which are used for determining energy calibration. The total number of counts in each peak is determined and this becomes the center line for the graph. Again, $\pm 1\sigma$, $\pm 2\sigma$, and $\pm 3\sigma$ lines are indicated and the data plotted daily. Any number outside of the $\pm 3\sigma$ control limits indicates that corrective action is needed. Background should be subtracted from the counts accumulated in the analyzer. The section on data analysis explains how to determine the total number of counts in each peak.

Other parameters that should be plotted on the control charts are peak position of each peak (channel number), and the full width at half-maximum for each peak. To determine full width at half-maximum, the number of counts in the peak channel is determined. Then the adjacent channels above and below the peak that have counts less than and greater than one-half of the peak intensity are found. Assuming linearity, the half-maximum points are found by linear interpolation. The difference in the channel numbers plus 1 is then the full width half-maximum. Data can be plotted as number of channels, percent of energy, or in keV.

When all of the sample data remain within the control limits, it may seem like a waste of time to continue obtaining control data on a daily basis. However, if the data go out of control, the immediate identification of a problem will be extremely gratifying. Also, the first unusual analysis of an environmental sample will not require a recalibration for confirmation. The continuing effort in maintaining these quality control charts is the cheapest insurance available for assuring precise and accurate data from the counting system.

DATA ANALYSES

If the pulse height spectrum from an environmental measurement is relatively simple, a straightforward hand analysis can be made. Areas of each photo peak are determined as described earlier. Then the activity of each radionuclide is given by

$$A_o = \frac{A}{\varepsilon \beta} \qquad \text{(Eq. 31)}$$

where A_o is the calculated activity, A the count rate observed, ε is the efficiency of the detector at the energy of the gamma ray producing the full energy peak, and β is the fraction of gamma rays emitted per disintegration. This method is adequate for simple spectra that have only a few well-separated full energy peaks. Care must be used to determine A consistently. ε has to be defined carefully. In the simplest case, ε is determined directly by calibration with a standard. If ε is determined from an ε-versus-energy plot, care must be taken to account for all events giving the full energy peak. Escape losses at low energy should be considered. A more common problem is that of losses due to coincidence gamma rays. If the gamma ray is part of a cascade, there is a good chance that the full energy peak will be smaller than it should be and that there will be a coincidence sum peak in the spectrum. Analyses of coincidence is somewhat more complicated and generally a computer will be needed to correct for coincidence losses.

The so-called "matrix" method is widely used for more complex spectra. This method requires that the background be stable and well known, and that good reference samples have been prepared and measured. The matrix method has been used satisfactorily for analyses of up to eight radionuclides. It is amenable to calculation by hand for four or less radionuclides, but a computer is recommended for analyses of five to eight radionuclides.

Deciding on the number of radionuclides and selecting them constitute the first step. Good standards should then be obtained and single radionuclide spectra run for each of the geometries with the appropriate sample matrix. The background should be removed from each of the spectra.

The next step is to select a full energy peak for each radionuclide. Care should be taken in the selection. Often the strongest gamma ray should be used, but on occasion, two gamma rays will overlap and another line should be used. After selecting the full energy peaks, select the channels which will be summed to determine the area of the peak. Generally, it is best to use the full peak area, rather than the peak as defined at 1/3 or 1/2 peak height. Normalize each spectrum so that the area of the full energy peak is equal to 1 (unity).

Determine the area for every full energy peak of the interfering radionuclides that lie in that portion of the spectrum in which the full energy peak of the radionuclide of interest is found. This area is then called the interference factor, F_{ab}.

F_{ab} is the ratio of the area of radionuclide b to the full energy peak of radionuclide b in the area of the full energy peak of radionuclide a.

Once the set of interference factors is determined, the matrix can be set up. Two examples are described below.

Assume radionuclide a gives the spectrum labeled A in Figure 14 and radionuclide b gives the spectrum labeled B in Figure 14 after the background has been removed. Areas under each region are labeled.

If the two radionuclides were put in the same sample, under reasonable conditions the resulting spectrum would be that labeled C in Figure 14. The count rates are given by

$$N_1 = C_a + F_{ab}C_b \qquad \text{(Eq. 32)}$$

$$N_2 = F_{ba}C_a + C_b \qquad \text{(Eq. 33)}$$

Solving for C_a and C_b we have

$$C_a = \frac{\begin{vmatrix} N_1 & F_{ab} \\ N_2 & 1 \end{vmatrix}}{\begin{vmatrix} 1 & F_{ab} \\ F_{ba} & 1 \end{vmatrix}}$$

and

$$C_b = \frac{\begin{vmatrix} 1 & N_1 \\ F_{ba} & N_2 \end{vmatrix}}{\begin{vmatrix} 1 & F_{ab} \\ F_{ba} & 1 \end{vmatrix}}$$

or

$$C_a = \frac{N_1 - F_{ab}N_2}{1 - F_{ab}F_{ba}} \qquad \text{(Eq. 34)}$$

and

$$C_b = \frac{N_2 - F_{ba}N_1}{1 - F_{ab}F_{ba}} \qquad \text{(Eq. 35)}$$

then if the activity of radionuclide a is in picocuries per gram (pCi/g) = E_aC_a and that of radionuclide b is in picocuries per gram (pCi/g) = E_bC_b where E_a and E_b are previously determined efficiencies for radionuclides a and b, we are able to determine the activities of radionuclide a and b when they are in the sample together.

For four radionuclides, the set of linear equations will look like this:

$$N_1 = C_1 + F_{12}C_2 + F_{13}\,C_3 + F_{14}C_4 \qquad \text{(Eq. 36)}$$

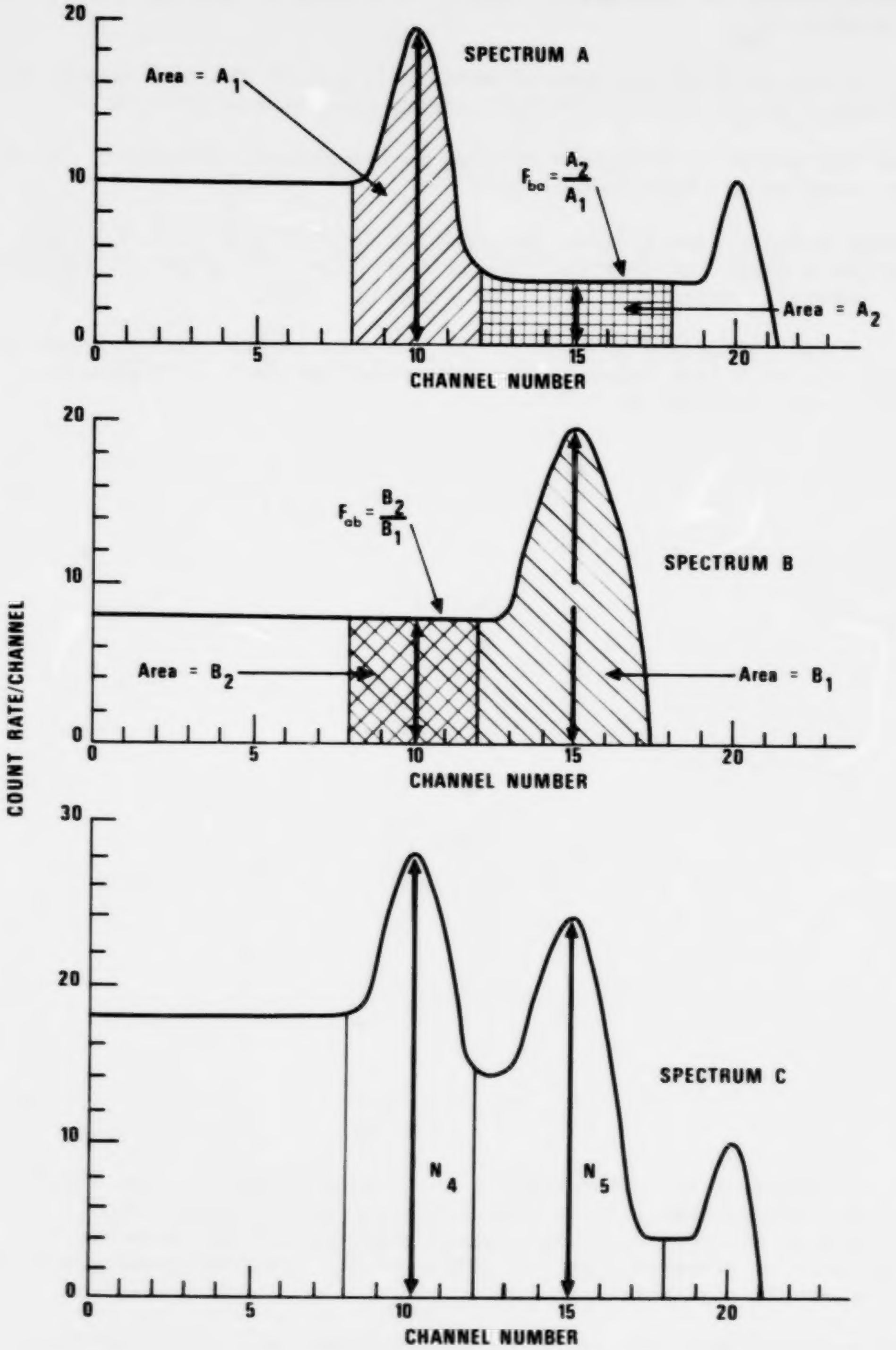

Figure 14. Idealized spectra illustrating interference factors and summation of gamma rays in a gamma-ray spectrometer.

$$N_2 = F_{21}C_1 + C_2 + F_{23}C_3 + F_{24}C_4 \qquad \text{(Eq. 37)}$$

$$N_3 = F_{31}C_1 + F_{32}C_2 + C_3 + F_{34}C_4 \qquad \text{(Eq. 38)}$$

$$N_4 = F_{41}C_1 + F_{42}C_2 + F_{43}C_3 + C_4 \qquad \text{(Eq. 39)}$$

Where F_{ij} = the fractional area of isotope $\underline{j}$ in the region used to define the full energy peak of isotope $\underline{i}$, and

C_i = the count rate of isotope $\underline{i}$.

The solution to these sets of equations is:

$$\begin{aligned} C_1 = \{ & N_1[(1-F_{43}F_{34}) - F_{32}(F_{23}-F_{43}F_{24}) + F_{42}(F_{23}F_{34}-F_{24})] \\ & - N_2[F_{12}(1-F_{43}F_{34}) - F_{32}(F_{13}-F_{43}F_{14}) + F_{42}(F_{13}F_{34}-F_{14})] \\ & + N_3[F_{12}(F_{23}-F_{43}F_{24}) - (F_{13}-F_{43}F_{14}) + F_{42}(F_{13}F_{24}-F_{23}F_{14})] \\ & - N_4[F_{12}(F_{23}F_{34}-F_{24}) - (F_{13}F_{34}-F_{14}) + F_{32}(F_{13}F_{24}-F_{23}F_{14})]\}/\Delta \qquad \text{(Eq. 40)} \end{aligned}$$

$$\begin{aligned} C_2 = \{ & -N_1[F_{21}(1-F_{43}F_{34}) - F_{31}(F_{23}-F_{43}F_{24}) + F_{41}(F_{23}F_{34}-F_{24})] \\ & + N_2[(1-F_{43}F_{34}) - F_{31}(F_{13}-F_{43}F_{14}) + F_{41}(F_{13}F_{34}-F_{14})] \\ & - N_3[(F_{23}-F_{43}F_{24}) - F_{21}(F_{13}-F_{43}F_{14}) + F_{41}(F_{13}F_{24}-F_{23}F_{14})] \\ & + N_4[(F_{23}F_{34}-F_{24}) - F_{21}(F_{13}F_{34}-F_{14}) + F_{31}(F_{13}F_{24}-F_{23}F_{14})]\}/\Delta \qquad \text{(Eq. 41)} \end{aligned}$$

$$\begin{aligned} C_3 = \{ & N_1[F_{21}(F_{32}-F_{42}F_{34}) - F_{31}(1-F_{42}F_{24}) + F_{41}(F_{34}-F_{32}F_{24})] \\ & - N_2[(F_{32}-F_{42}F_{34}) - F_{31}(F_{12}-F_{42}F_{14}) + F_{41}(F_{12}F_{34}-F_{32}F_{14})] \\ & + N_3[(1-F_{42}F_{24}) - F_{21}(F_{12}-F_{42}F_{14}) + F_{41}(F_{12}F_{24}-F_{14})] \\ & - N_4[(F_{34}-F_{32}F_{24}) - F_{21}(F_{12}F_{34}-F_{32}F_{14}) + F_{31}(F_{12}F_{24}-F_{14})]\}/\Delta \qquad \text{(Eq. 42)} \end{aligned}$$

$$\begin{aligned} C_4 = \{ & -N_1[F_{21}(F_{32}F_{43}-F_{42}) - F_{31}(F_{43}-F_{42}F_{23}) + F_{41}(1-F_{32}F_{23})] \\ & + N_2[(F_{32}F_{43}-F_{42}) - F_{31}(F_{12}F_{43}-F_{42}F_{13}) + F_{41}(F_{12}-F_{32}F_{13})] \\ & - N_3[(F_{43}-F_{42}F_{23}) - F_{21}(F_{12}F_{43}-F_{42}F_{13}) + F_{41}(F_{12}F_{23}-F_{13})] \\ & + N_4[(1-F_{32}F_{23}) - F_{21}(F_{12}-F_{32}F_{13}) + F_{31}(F_{12}F_{23}-F_{13})]\}/\Delta \qquad \text{(Eq. 43)} \end{aligned}$$

Where

$$\begin{aligned} \Delta = {} & (1-F_{43}F_{34}) - F_{32}(F_{23}-F_{43}F_{24}) + F_{42}(F_{23}F_{34}-F_{24}) \qquad \text{(Eq. 44)} \\ & - F_{21}[F_{12}(1-F_{43}F_{34}) - F_{32}(F_{13}-F_{43}F_{14}) + F_{42}(F_{13}F_{34}-F_{14})] \end{aligned}$$

$$+ F_{31}[F_{12}(F_{23}-F_{43}F_{24}) - (F_{13}-F_{43}F_{14}) + F_{42}(F_{13}F_{24}-F_{23}F_{14})]$$

$$- F_{41}[F_{12}(F_{23}F_{34}-F_{24}) - (F_{13}F_{34}-F_{14}) + F_{32}(F_{13}F_{24}-F_{23}F_{14})]$$

Another form for the solution of these equations can be found using the Gauss Reduction.

Rewriting equations 36 through 39, after dividing by the coefficient of C_1 we get

$$C_1 + F_{12}C_2 + F_{13}C_3 + F_{14}C_4 = N_1 \qquad \text{(Eq. 45)*}$$

$$C_1 + \frac{1}{F_{21}} C_2 + \frac{F_{23}}{F_{21}} C_3 + \frac{F_{24}}{F_{21}} C_4 = \frac{N_2}{F_{21}} \qquad \text{(Eq. 46)}$$

$$C_1 + \frac{F_{32}}{F_{31}} C_2 + \frac{1}{F_{31}} C_3 + \frac{F_{34}}{F_{31}} C_4 = \frac{N_3}{F_{31}} \qquad \text{(Eq. 47)}$$

$$C_1 + \frac{F_{42}}{F_{41}} C_2 + \frac{F_{43}}{F_{41}} C_3 + \frac{1}{F_{41}} C_4 = \frac{N_4}{F_{41}} \qquad \text{(Eq. 48)}$$

Subtracting equation 46 from 45, equation 47 from 46, and equation 48 from 47, we get

$$X_1C_2 + X_2C_3 + X_3C_4 = X_4 \qquad \text{(Eq. 49)}$$

$$X_5C_6 + X_6C_3 + X_7C_4 = X_8 \qquad \text{(Eq. 50)}$$

$$X_9C_2 + X_{10}C_3 + X_{11}C_4 = X_9 \qquad \text{(Eq. 51)}$$

Where

$$X_1 = F_{12} - \frac{1}{F_{21}}$$

$$X_2 = F_{13} - \frac{F_{23}}{F_{21}}$$

$$X_3 = F_{14} - \frac{F_{24}}{F_{21}}$$

$$X_4 = N_1 - \frac{N_2}{F_{21}}$$

$$X_5 = \frac{1}{F_{21}} - \frac{F_{32}}{F_{31}}$$

$$X_6 = \frac{F_{23}}{F_{21}} - \frac{1}{F_{31}}$$

$$X_7 = \frac{F_{24}}{F_{21}} - \frac{F_{34}}{F_{31}}$$

$$X_8 = \frac{N_2}{F_{21}} - \frac{N_3}{F_{31}}$$

$$X_9 = \frac{F_{32}}{F_{31}} - \frac{F_{42}}{F_{41}}$$

$$X_{10} = \frac{1}{F_{31}} - \frac{F_{43}}{F_{41}}$$

$$X_{11} = \frac{F_{34}}{F_{31}} - \frac{1}{F_{41}}$$

$$X_{12} = \frac{N_3}{F_{31}} - \frac{N_4}{F_{41}}$$

---

*Equation 36 divided by F_{11} which is 1.

Continuing the process

$$C_2 + \frac{X_2}{X_1} C_3 + \frac{X_3}{X_1} C_4 = \frac{X_4}{X_1} \qquad \text{(Eq. 52)}$$

$$C_2 + \frac{X_6}{X_5} C_3 + \frac{X_7}{X_5} C_4 = \frac{X_8}{X_5} \qquad \text{(Eq. 53)}$$

$$C_2 + \frac{X_{10}}{X_9} C_3 + \frac{X_{11}}{X_9} C_4 = \frac{X_{12}}{X_9} \qquad \text{(Eq. 54)}$$

Subtracting equation 53 from 52 and equation 54 from 53 leaves

$$X_{13}C_3 + X_{14}C_4 = X_{15} \qquad \text{(Eq. 55)}$$

$$X_{16}C_3 + X_{17}C_4 = X_{18} \qquad \text{(Eq. 56)}$$

Where

$$X_{13} = \frac{X_2}{X_1} - \frac{X_6}{X_5} \qquad X_{16} = \frac{X_6}{X_5} - \frac{X_{10}}{X_9}$$

$$X_{14} = \frac{X_2}{X_1} - \frac{X_7}{X_5} \qquad X_{17} = \frac{X_7}{X_5} - \frac{X_{11}}{X_9}$$

$$X_{15} = \frac{X_4}{X_1} - \frac{X_8}{X_5} \qquad X_{18} = \frac{X_8}{X_5} - \frac{X_{12}}{X_9}$$

Again, continuing the process, we obtain

$$C_4 = \frac{\dfrac{X_{15}}{X_{13}} - \dfrac{X_{18}}{X_{16}}}{\dfrac{X_{14}}{X_{13}} - \dfrac{X_{17}}{X_{16}}} \qquad \text{(Eq. 57)}$$

By putting C_4 in equation 55, we can solve for C_3, then putting C_3 and C_4 in equation 52 we solve for C_2. C_1 is determined by putting the values determined for C_2, C_3 and C_4 in equation 45.

CALIBRATION OF THE SYSTEM

After the method of data analysis has been selected, the final steps in calibrating the counting system are the selection of sample types having suitable geometries and the preparation of calibration standards containing the isotopes that are expected to be found in the various types of samples. Geometries should be chosen that are easily prepared and are readily reproducible. Fewer geometries facilitate the ease of calibration but limit the samples that can be analyzed. Some sample types commonly used, each having its own peculiar geometry, are:

1. Marinelli beaker, 4-liter
2. Plastic container, 400-ml
3. Plastic container, 200-ml
4. Air filter, 5.1-cm
5. Air filter, 10.2-cm
6. Liquid scintillation counting vial, 20-ml
7. Ampul, 5-ml
8. Point sources
9. Charcoal cartridges
10. Filters, 2.54-cm

These sample types are shown in Figure 15. Except for the Marinelli beaker, source holders should be fabricated for the other geometries to assure reproducible counting on a routine basis. The source holders can also be used for protecting the NaI(Tl) crystal from accidental contamination from a leaky or improperly prepared source. Over a period of time many laboratories make small variations in their laboratory technique and/or sample preparation technique without verifying carefully the changes in calibration due to these minor changes. These changes can result in a systematic change in the counting and lead to large systematic errors in reported data. Because of the low levels of activity usually encountered, most counting is done with the source as close as possible to the detector. Great care must be used in positioning samples near the detector for the reason that small variations in the geometry enormously affect the counting efficiency of the detector. Also, the samples should always be at room temperature, unless special precautions have been taken to avoid sudden thermal changes in the crystal which can crack it.

The accumulation of radionuclides for the calibration library is a formidable task. There are more than 115 different radionuclides reported to be emitted by nuclear reactors. Sixty-six of these have half-lives greater than 2.5 days and 55 emit gamma rays. Also, the number of naturally-occurring radionuclides is not small. The sample type can be used to select those radionuclides which can be considered for analysis. Appendix A lists some, but not all, of the gamma-emitting radionuclides most likely to occur in the samples obtained.

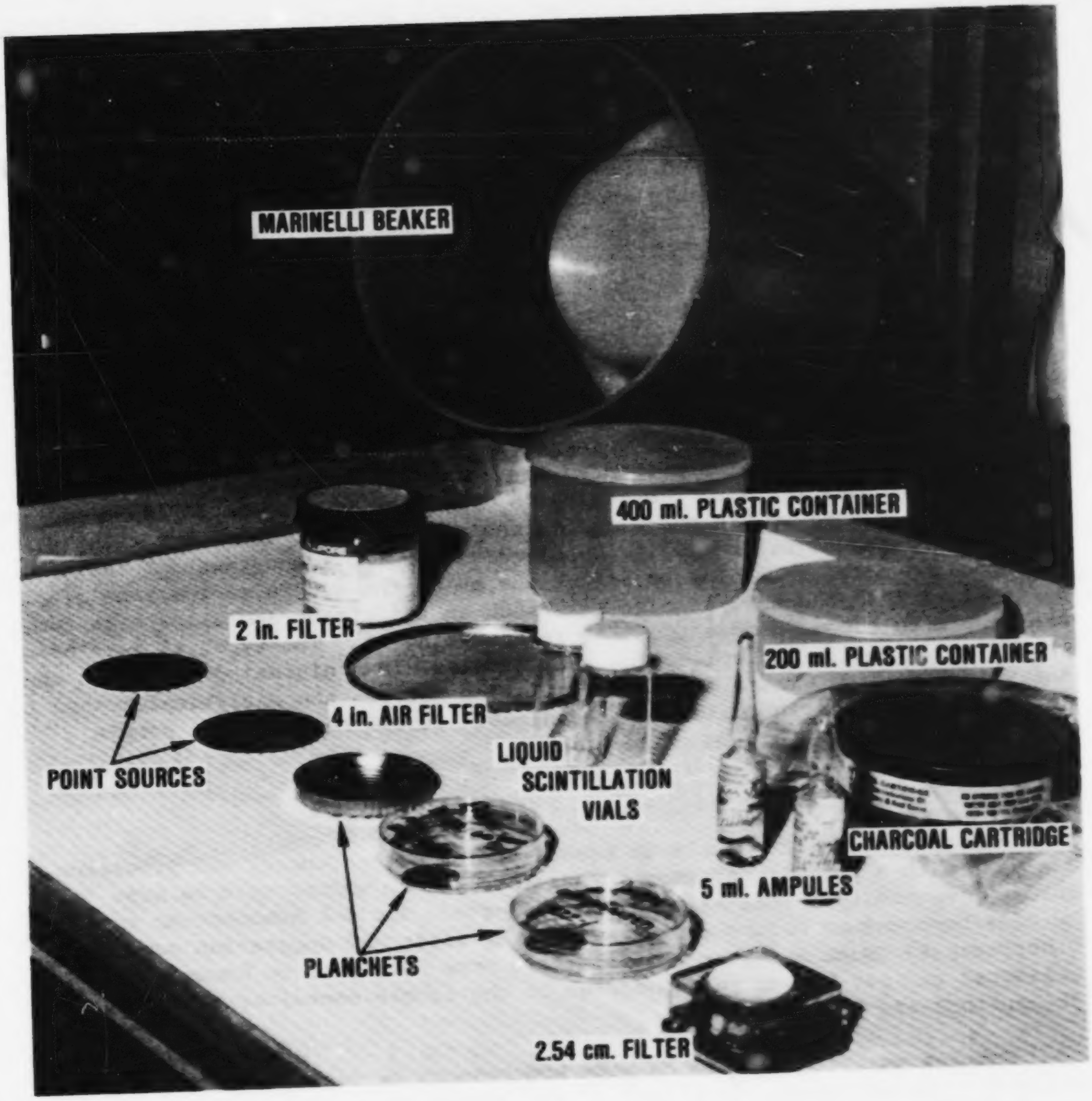
MARINELLI BEAKER
400 ml. PLASTIC CONTAINER
2 in. FILTER
200 ml. PLASTIC CONTAINER
4 in. AIR FILTER
LIQUID
SCINTILLATION
VIALS
POINT SOURCES
CHARCOAL CARTRIDGE
5 ml. AMPULES
PLANCHETS
2.54 cm. FILTER

Figure 15. Common sample holders.

Calibrated radionuclides need to be obtained. These calibrated radionuclides in turn are used to prepare calibration samples for analysis. Each radionuclide is prepared for each sample type and geometry. The preparation entails careful work and should be done using the best analytical techniques available. Generally, the calibrated radionuclide should be diluted gravimetrically and the carrier content and chemical form of the sample maintained. The calibration sample should simulate the type of matrix to be analyzed as nearly as possible. The calibration sample has to be homogeneous and stable. At least one background or "unspiked" sample should be prepared for each geometry and sample matrix. These calibration samples are then counted and the data abstracted for the calibration library. Activity levels should be adjusted to give count rates no more than 100 times the activity of the samples to be analyzed, but preferably about 10 times the activity levels expected.

SAMPLES AND STANDARDS PREPARATION

Sample Collection

It seems imperative that something be said about the collection of samples in this section on sample preparation. If a proper method or technique of sample collection is not used, the collected sample will not be representative of the environmental area or medium being monitored. A great deal of thought and care must be exercised in the collection of samples. There are several situations in which the analyst's treatment of the sample is--or should be--dictated by the technique of the sample collection. For example, if an environmental water sample is collected for the measurement of radioisotopes and nothing is done to adjust the pH of the sample at the time of collection, then the analyst must make such an adjustment and allow time for the sample to become homogeneous before analyzing it. The type, if any, of preservative added when collecting milk samples, is a dictating factor in the analytical method. There must be correlation between the analytical method to be used and the sample collection technique. It can be said that sample preparation begins with its collection.

Homogeneity of Sample

Homogeneity of the sample is essential for both accuracy and precision of analysis with a NaI(Tl) detector. Therefore, every effort must be made to insure homogeneity. Some samples, as collected, are not homogeneous and must be made homogeneous before analysis (such as soils and vegetation samples). Other samples (such as water and milk) are more likely to be homogeneous when collected but may become inhomogeneous in the sample container unless special precautions are taken.

Samples such as soil can be made homogeneous by sieving, grinding, resieving, and regrinding, until all of the sample can be passed through a 170 mesh--or finer--screen and then thoroughly blended.

Water samples collected in any kind of container may lose significant fractions of their radioisotope and trace elements content to the walls of the container, thus changing the activity of the sample and making it nonrepresentative of its source. Such changes in the sample can be avoided in most cases by lowering the pH of the sample to below a pH of 1. An acid such as hydrochloric or nitric which gives soluble salts with most cations should be used (167 ml of concentrated HCl or 125 ml of concentrated HNO_3 added to a 1-gallon (3.78-liter) sample will give a sample solution an acidity of 0.3N-0.5N). It is best to add acid at the time of sample collection. If acid is not added until the sample reaches the laboratory, there is some uncertainty as to the time for desorption from the container walls, in which case a waiting period of at least overnight should be allowed between acid addition and sample analysis. For the addition of acid to samples at the time of collection, fractions of concentrated acid should be measured into polyethylene bottles with Poly-Seal® caps in a laboratory just before going to the field for sample collection. Concentrated nitric acid should not be stored in polyethylene bottles for more than just a few days. In a few cases, the addition of carriers to the sample may be necessary.

Homogeneity of a sample is demonstrated by analyzing at least three aliquots of the sample and checking results for precision. Homogeneity for any sample should never be assumed without some mixing just prior to taking aliquots for analysis.

Stability of Sample

The stability of a sample relates to the physical, chemical, or biological state of the sample and often affects its homogeneity. Samples that are both chemically and physically stable should remain quite homogeneous once they are mixed. Acid added to water samples and formaldehyde or some other preservative added to milk act as stabilizers and help maintain homogeneity.

The chemical and physical form of some elements or radioisotopes as they exist in nature need to be known beforehand in order to stabilize the sample from the time it is collected until the time it is analyzed. In fact, for some kinds of analyses the stability of some samples upon removal from their environmental source may be so questionable as to dictate analysis at the site of the source.

Standards and Reference Samples

The concept of standards and reference samples may vary somewhat from laboratory to laboratory so that for the sake of discussion here some definition is needed. A standard source is here defined as an amount of an element or compound in some stable form, the content of which is traceable to National Bureau of Standards (NBS) source materials. The definition is here extended to include solutions of standard source materials, as it is possible for solutions of many materials to be made quite stable.

Many times standard source materials received from NBS or another supplier must be diluted for specific uses. The greatest of care must be taken in making such dilutions to maintain the integrity of the diluted standard source. The diluent must be physically and chemically the same as the standard source matrix.

®Registered trade name

A weight-to-weight dilution in contrast to a weight-to-volume or a volume-to-volume dilution should result in a more accurate diluted standard source and thus help to insure its integrity.

A particularly useful aid in making weighed deliveries of standard source solutions is the polyethylene doll's baby bottle with the neck drawn out to provide a small opening. Standard source solutions can be drawn into the bottle and weighed deliveries made from the bottle (delivered amounts determined by weight differences). Solutions can also be stored in the bottles by simply sealing the tip of the bottle with a mild flame. Water loss through the walls of these bottles is no more than 3%-5% per year at ambient temperatures.

Once a dilution of a standard source material has been made, then making the diluted standard source a homogenous source is of utmost importance. Just as the integrity of the original standard source material rests with its stability and homogeneity, so also rests the integrity of the diluted standard source. Solutions of diluted standard source materials should be shaken vigorously and inverted at least 10 times to insure thorough mixing.

In contrast to a standard source, a reference sample is here defined as a known quantity of sample matrix to which has been added a measured amount of a standard source (also, often called a control sample). These samples are taken through the same analytical procedure as other samples and they give results from which yield factors are determined.

Reference samples are made from measured aliquots of homogenous sample materials. After the addition of standard source material, the sample should be mixed thoroughly so that the standard source material will be subjected to the same sample matrix influences throughout the analytical procedure as other samples being analyzed.

STATISTICS AND UNCERTAINTIES IN MEASUREMENTS

Experience and theory indicate that it is impossible to measure any physical quantity exactly, i.e., with no error. Refinement of theoretical and experimental methods will reduce, but not eliminate, the possible error of a measurement. A statement or other indication of the possible error must accompany any reported measurement of a physical quantity for the reason that there is always a gamble on its relative correctness.

In reporting the results of sample activity, the statement of uncertainty in the measurement should reflect both the uncertainty resulting from the statistical nature of radioactivity and a liberal estimate of all the systematic errors involved in the measurement. Definitions of the terms accuracy, precision, systematic errors, and random errors must be understood to adequately report on the uncertainties of physical measurements.

1. Accuracy is the comparison of a measurement to its true or accepted value. An accurate measurement is one which results in a value very close to the true value. An inaccurate measurement results in a value that is not close to the true value. In order to obtain accurate values the measurements have to be precise. In no way, however, does precision indicate accuracy.

2. Precision is only a measure of the degree of agreement of repeated measurements of the same property. Precision is expressed in terms of dispersion about the arithmetic mean of the results of repetitive testing.

3. Random errors are those that arise from:

   a. the statistical nature of radioactive decay,

   b. variations in sample size, source-detector geometry, yields in preparation, etc., about a mean value of the respective variable.

4. Systematic errors are those ubiquitous errors arising from assumptions that are not measured or evaluated. These are, without doubt, the most difficult to understand and correct. Systematic errors are present as uncertainties in the activities of the standards used, as limitations in gravimetric and volumetric apparatus and in other standards. For example, they are ever present as fluctuations in the concentration of radon in the detector environment and in the assumption that temperature, humidity and barometric pressure do not affect the measurements. Some systematic errors enter as gross personal errors, e.g., forgetting to convert seconds to minutes, dpm to picocuries, ad infinitum.

The inconsistencies presented in comparison data are remarkable in that the uncertainties indicated seldom overlap. An example of inconsistent expressions of uncertainties is indicated in Figure 16. Such figures are typical when measurements of a single quantity by different participants are compared. The data plotted are obviously in error for the reason that the uncertainty of a measurement must overlap the true value no matter how inaccurate the data.

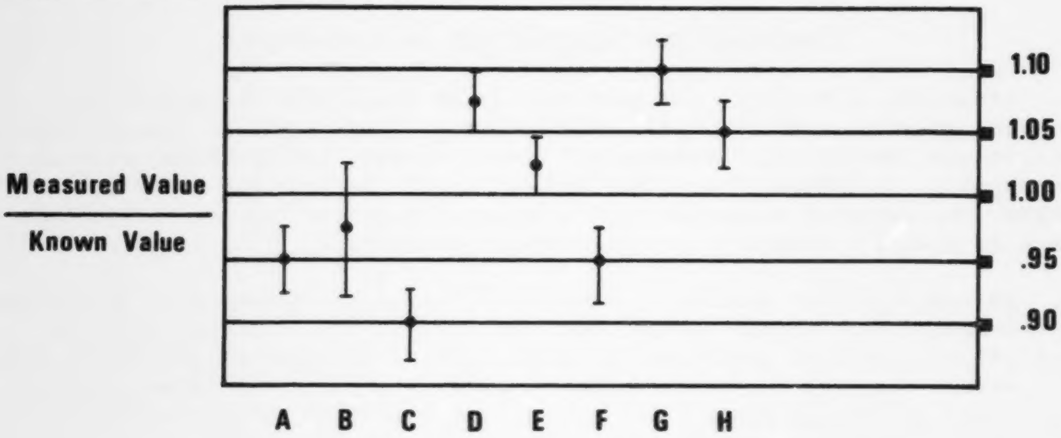

Figure 16. Comparison of analytical results from several participants when systematic results are not estimated correctly.

Figure 17 is a more realistic plot in which the range of uncertainty overlaps the true value. Figure 17 shows what is expected when all errors are indeed known and treated properly. Figure 16 arose from not describing or from leaving out systematic errors. The random numbers in a few cases are not treated correctly. There is an overwhelming tendency to treat counting errors as the systematic error because they can be determined easily, and they appear to be small. Systematic errors, however, tend to displace the mean whereas random numbers tend to establish the mean.

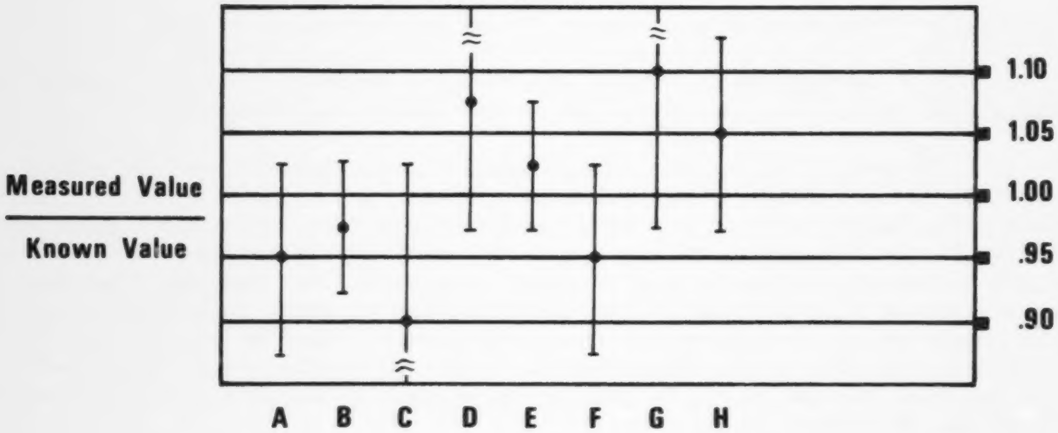

Figure 17. Comparison of analytical results from several participants with correct estimation of systematic errors.

In order to analyze the uncertainties in measurements, a knowledge of statistics and of compounding errors is essential. Two frequency distributions used in analyzing the results of measurements will be discussed. These are the normal distribution and the Poisson distribution. The normal distribution and the Poisson distribution are similar for large values of their respective parameters. Differences, however, still remain significant. It is very important to know what these differences are so that we can understand what our measurements are telling us and what they are not telling us. The conceptual differences remain significant.

The normal distribution applies to a continuously variable observed magnitude, such as that which results from making many measurements of the distance between two spectral lines. The Poisson distribution is applied to discontinuous variables, such as particle counting rates, which take on successive integer (whole number) values.

The normal distribution states that the probability (dP_x) that x will lie between x and $x + dx$ is

$$dP_x = \frac{1}{\sigma\sqrt{2}} e^{-\frac{(x-m)^2}{2\sigma^2}} dx \qquad \text{(Eq. 58)}$$

where e = 2.7183 (the base of the natural system of logarithms)
m = true value of the quantity whose measured values are x
σ = standard deviation, which is a parameter which describes the breadth of the distribution deviations (x-m) from the mean. The standard deviation is one of the two parameters, m and σ, of the normal distribution.

Figure 18 illustrates the general form of the normal distribution drawn for a mean value, m, of 100 and a standard deviation, σ, of 10. The ordinates are normalized so that the total area under the curve is unity [1]. Thus the area included between any two abscissas, X_1 and X_2, is the probability that a single measurement of x would lie between X_1 and X_2 while a very large number of measurements of x would have a mean value of m ($m = 100$ in Figure 18).

The maximum slope of the normal distribution curve falls at the points $x - m = \pm\sigma$. The value of this slope is:

$$\frac{1}{\sigma^2\sqrt{2\pi e}}$$

Tangents to the normal distribution curve at these inflection points intersect the x axis at $x - m = \pm 2\sigma$. The ratio of the ordinate y_σ at these symmetrical points of maximum slope to the maximum ordinate, y_m, is

$$Y_m = \frac{1}{\sigma\sqrt{2\pi}}$$

at $x = m$ is $y_\sigma/y_m = e^{-\frac{1}{2}} = 0.6065$. The half width is $\sigma\sqrt{2 \ln 2} = 1.177\sigma$ at $y = y_m/2$ (half maximum) and is $\sigma\sqrt{2} = 1.414\sigma$ at $y = y_m/e$ (1/e of maximum).

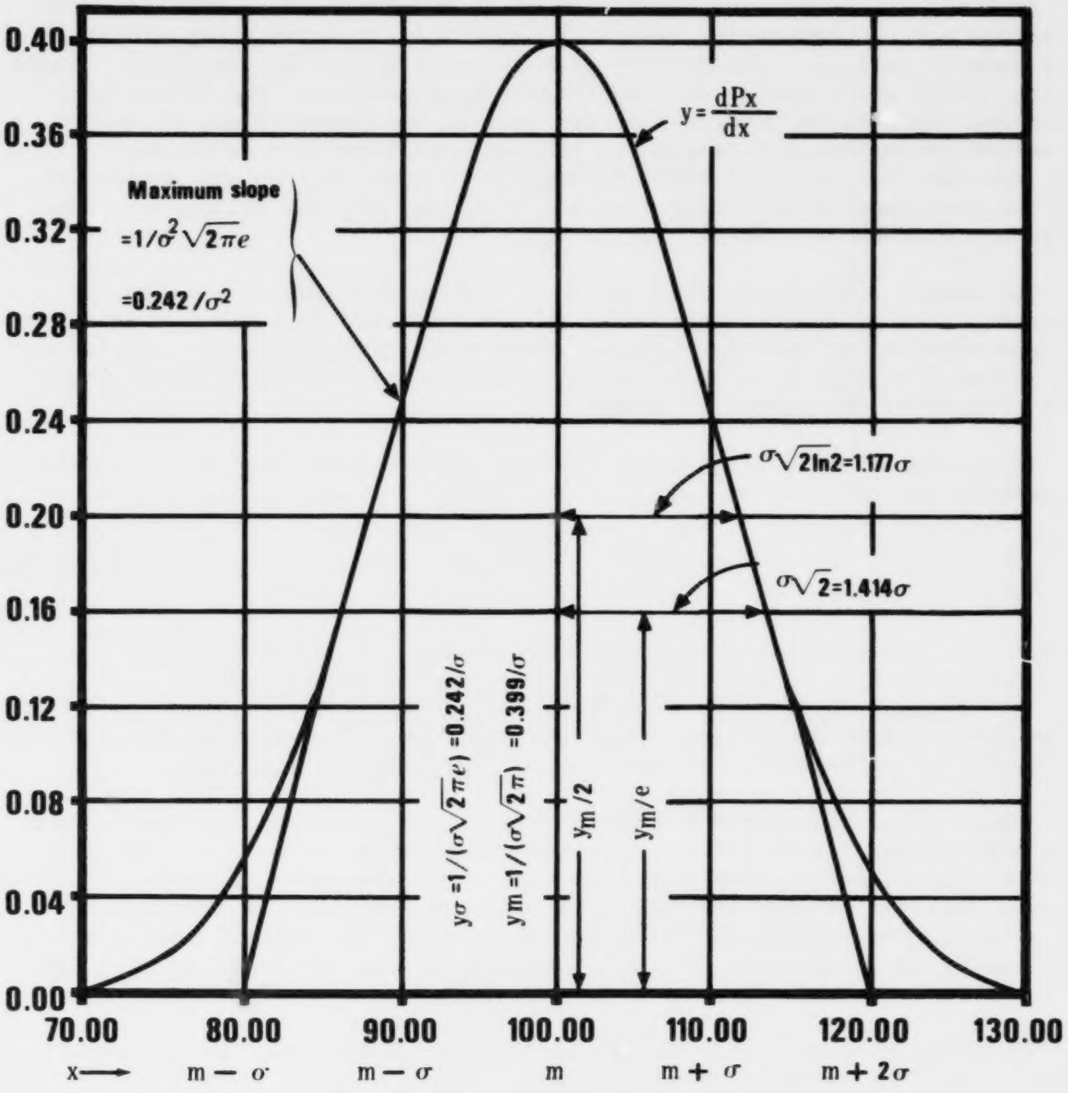

Figure 18. Normal distribution with a mean value, m, of 100 and a standard deviation, σ, of 10.

Poisson's distribution describes all random processes whose probability of occurrence is small and constant. Poisson's distribution has wide and diverse applicability and describes the fluctuations of such random processes as the disintegration of atomic nuclei, the emission of light quanta by excited atoms, and the appearance of cosmic ray bursts. The Poisson distribution applies to substantially all observations made in experimental gamma-ray spectroscopy.

The probability of observing a value, x, of a variable which has a Poisson distribution and a mean value, m, is given by

$$P_x = \frac{m^x}{x!} e^{-m} \qquad \text{(Eq. 59)}$$

where m may have any positive value and x is an integer. The Poisson distribution has only the parameter, m, in contrast to the two parameters of the normal distribution.

Provided one numerical evaluation of P_x has been made, other neighboring values may be computed quickly by using the following exact relationships:

$$P_{x-1} = \frac{x}{m} P_x \qquad \text{(Eq. 60)}$$

$$P_{x+1} = \frac{m}{x+1} P_x \qquad \text{(Eq. 61)}$$

$$P_o = e^{-m} \qquad \text{(Eq. 62)}$$

Some modern electronic calculators have programs that will compute P_x. It should be noted that for moderately large values of m (say 100) other values for P_x may be found quickly by determining a value of P_x and then using the above relationships to find P_{x+y}.

The Poisson distribution is slightly asymmetric favoring low values of x. Thus, substitution of $x = m$ in equation 60 shows that if the mean value is integer the probability of observing one less than the mean value is the same as the probability of observing the mean value.

A good approximation of P_x where $x > 10$ for any value m (do not confuse) is:

$$P_x \simeq \frac{1}{\sqrt{2\pi x}} \left(\frac{m}{x}\right)^x e^{-(m-x)} \qquad \text{(Eq. 63)}$$

The probability of actually observing the mean value in a series of observations of a random process of constant average value is zero. If, however, the integer nearest the mean value of a set of data is accepted in lieu of the mean, substitution of $x = m$ in equation 63 results in the following values:

m	P_m
10	0.127
100	0.040
1000	0.013

Note that the probability of observing $x = m$ is surprisingly small when the integer nearest the value of m is substituted.

The Poisson distribution must always be represented by a histogram because x can assume integer values only. Figure 19 illustrates the Poisson distribution for $m = 100$. The slight asymmetry of the Poisson histogram

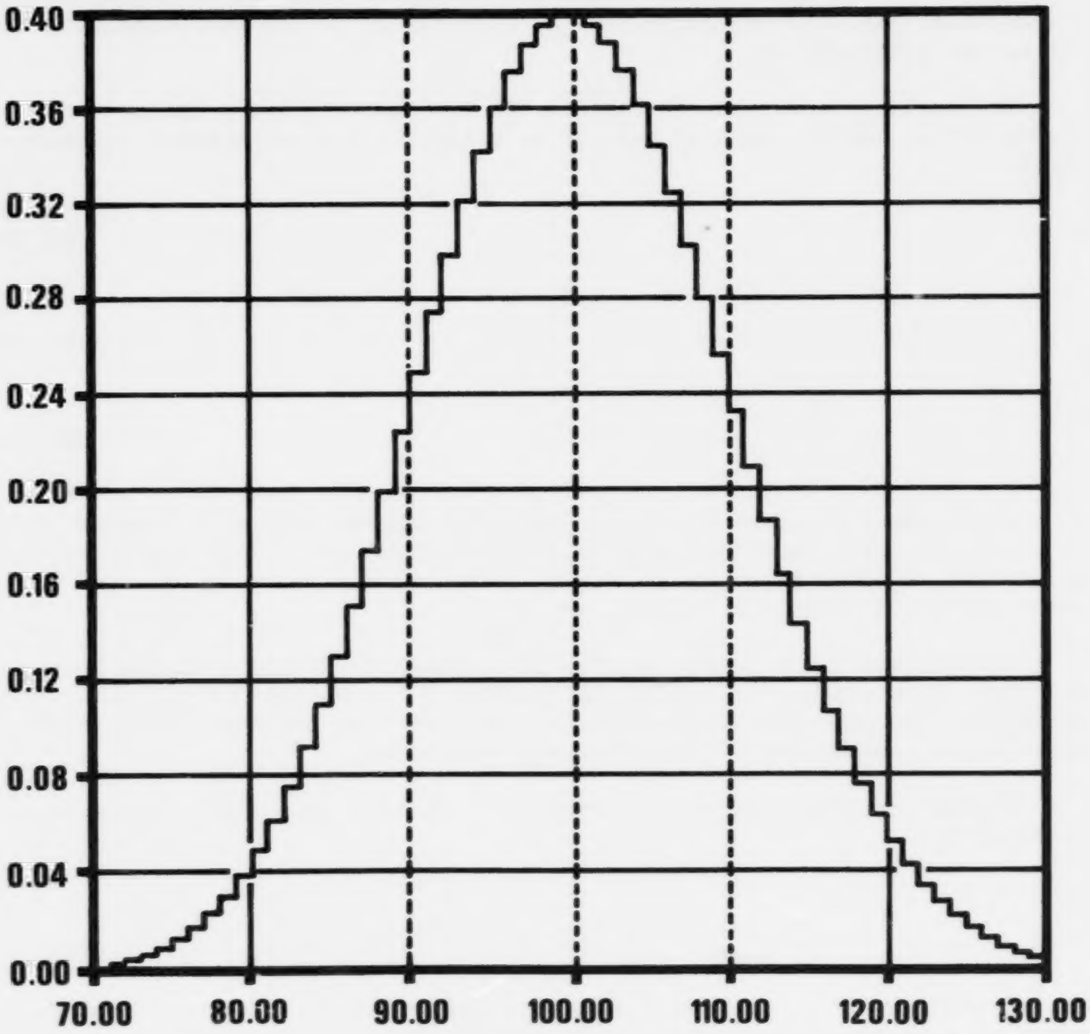

Figure 19. Poisson distribution with a mean value, m, of 100.

should be noted as well as the similarity between it and the symmetry of the normal distribution in Figure 20. For small values of m, say between m = 1 and m = 10, the Poisson distribution is very asymmetric and is not well approximated by the normal distribution.

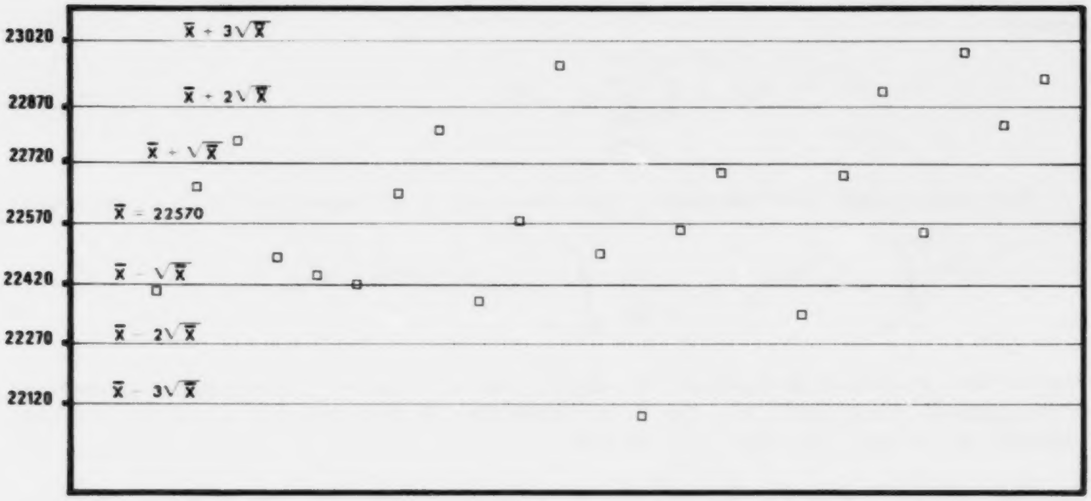

Figure 20. Control chart for low energy (0.57 MeV) peak from bismuth-207.

Only the mean of a random process can be approached for the reason that an infinite amount of data would have to be collected, whereas the data at hand, however large, are finite. The mean is a mathematical entity about which the data may be either symmetric or asymmetric depending upon the type of distribution. The decided asymmetry of the Poisson distribution for low values has been noted. The modal value (the most probable value) and the median (the value which is as frequently exceeded as not) are measures of central tendency, but are not weighted by each individual datum. Consequently, the best approximation to m is the arithmetic average, $\bar{x}$, of the n separate measurements, x_1, x_2, x_3 ..., X_n , which may be expressed

$$m \simeq \bar{x} = \frac{1}{n}\sum_{i=1}^{i=n} x_i \qquad \text{(Eq. 64)}$$

The "expectation value" of $\bar{x}$ is m when the above formula is applied to the data obtained from a large number of random trials.

The spread of random data about the mean value may be expressed by a parameter called the standard deviation, σ. The standard deviation (often abbreviated S.D.) is defined as the square root of the average value of the squares of the individual deviations (x - m) for a large number of observations. In a normal distribution, about 32 percent of a large series of individual observations will deviate from the mean value by more than $\pm\sigma$, thus 68 percent of the individual observations will lie within $\pm\sigma$.

The standard deviation for any frequency distribution may be obtained from the general formula

$$\sigma^2 = \sum_{x=-\infty}^{x=\infty} (x-m)^2 P_x \qquad \text{(Eq. 65)}$$

The general formula in terms of a large series of n measurements of x becomes

$$\sigma^2 = \frac{1}{n} \sum_{i=1}^{i=n} (x_i - m)^2 \qquad \text{(Eq. 66)}$$

For the normal distribution, the evaluation of equation 65 by integration gives

$$\sigma^2 = \int_{x=-\infty}^{x=\infty} (x-m)^2 dP_x = \frac{1}{\sigma\sqrt{2\pi}} \int_{x=-\infty}^{x=\infty} (x-m)^2 e^{-(x-m)/2\sigma^2} dx = \sigma^2$$

because the standard deviation is simply one of the two independent parameters of the normal distribution. As a consequence of the preceding material, the standard deviation may have any value.

The standard deviation for the Poisson distribution has a definite value because there is only one parameter. The expansion of equation 65 in terms of the parameter, m, for the Poisson distribution is

$$\sigma^2 = \sum_{x=0}^{x=\infty} \frac{(x-m)^2 m^x}{x!} e^{-m} = m \qquad \text{(Eq. 67)}$$

Therefore the standard deviation σ for the Poisson distribution is $\sqrt{m}$.

The value calculated for the standard deviation is actually an estimate because the number of observations, no matter how large, is finite. The best approximation of the standard deviation of a distribution in terms of a finite number of observations is

$$\sigma^2 \simeq \frac{n}{n-1} \frac{1}{n} \sum_{i=1}^{i=n} (x_i - \bar{x})^2 = \frac{1}{n-1} \sum_{i=1}^{i=n} (x_i - \bar{x})^2 \qquad \text{(Eq. 68)}$$

The $n-1$ term represents the reduction by 1 in the number of individual equations, and therefore degrees of freedom, that results when the distribution about $\bar{x}$ is considered. In the special case of a single observation, $x = \bar{x}$, the standard deviation is indeterminate.

When the distribution of n individual measurement of x about their estimated mean value $\bar{x}$ is approximately normal, we may assume that some 68 percent of the x_i values will lie within $\bar{x} \pm \sigma$. If one additional observation is made, it would have a 68 percent chance of lying within $\bar{x} \pm \sigma$. Therefore the standard deviation, σ, of the distribution is also the standard deviation of a single observation.

If one or more additional experiments are conducted under identical conditions and for which there will be n observations each, the respective means may be expected to have a much greater chance than 68 percent of lying within the band $(\bar{x} \pm \sigma_{\bar{x}})$. The means of a number of experiments would take on an essentially normal distribution in which some new mean value $\bar{x}_2$ will lie within the band $(\bar{x} \pm \sigma_{\bar{x}})$. The measure of the distribution of the means $\sigma_{\bar{x}}$ will be smaller than σ.

The theory of errors indicates that a series of K mean values, $\bar{x}$, $\bar{x}_2$, $\bar{x}_3$, ..., $\bar{x}_k$, in which each mean is determined from n observations, will tend to exhibit a normal distribution about their grand average $\bar{\bar{x}}$.* This will be true if n is sufficiently large even though the distribution of the parent population x_i is not normally distributed as in an asymmetric Poisson distribution. The distribution of mean values tends to be much more nearly normal than the distribution of the parent population. A theoretical justification of the relationship between σ and $\sigma_{\bar{x}}$ based on a normal distribution of $\bar{x}$ follows. When a large series of k measurements of the mean value $\bar{x}$, each of which has n measurements of x, the grand average, $\bar{\bar{x}}$, will approach the true mean, m. The standard deviation of $\bar{x}$ depends upon n in the following manner:

$$(\sigma_{\bar{x}})^2 = \frac{1}{k} \sum_{j=1}^{j=k} (\bar{x}_j - m)^2 = \frac{\sigma^2}{n} \qquad \text{(Eq. 69)}$$

Upon considering a single series of n measurements of x the result is reported as $(\bar{x} \pm \sigma_{\bar{x}})$ where

$$\bar{x} = \frac{1}{n} \sum_{i=1}^{i=n} x_i \qquad \text{(Eq.70)}$$

$$\sigma_{\bar{x}} = \frac{\sigma}{\sqrt{n}} \qquad \text{(Eq. 71)}$$

$$\sigma_{\bar{x}} = \sqrt{\frac{1}{n(n-1)} \sum_{i=1}^{i=n} (x_i - \bar{x})^2} \qquad \text{(Eq. 72)}$$

If a new series of n measurements is made, a different value for the mean would be obtained, but the chance that the new mean value would lie within $(\bar{x} \pm \sigma_{\bar{x}})$ is 68 percent. The standard deviation of the mean is also known as the standard error.

---

*It should be noted that the grand average $\bar{\bar{x}}_2$ of K mean values is not sound unless the number of observations n is the same for each mean x_i.

Equations 69 and 72 may be shown to be valid for the Poisson distribution. If a total, v , of

$$\sum_{1}^{n} x_i$$

random events is observed, the standard deviation by equation 65 in this single observation is

$$\sqrt{\sum_{i=1}^{i=n} x_i} \qquad \text{(Eq. 73)}$$

the result would be given as

$$v \pm \sigma = \sum_{i=1}^{i=n} x_i \pm \sqrt{\sum_{i=1}^{i=n} x_i} \qquad \text{(Eq. 74)}$$

The fractional standard deviation, F.S.D., would be

$$\text{F.S.D.} \equiv \frac{\sigma}{v} = \frac{1}{\sum_{i=1}^{i=n} x_i} \sqrt{\sum_{i=1}^{i=n} x} = \frac{1}{\sqrt{\sum_{i=1}^{i=n} x_i}} \qquad \text{(Eq. 75)}$$

Consider the total of a number of observations

$$\sum_{i=1}^{i=n} x_i$$

and the same observations in n groups of contiguous and equal intervals as

$$x_1 + x_2 + x_3 + \ldots + x_n = \sum_{i=1}^{i=n} x_i \; .$$

The average of the n groups would be

$$\bar{x} = \frac{1}{n} \sum_{i=1}^{i=n} x_i$$

and the standard deviation of the mean would be

$$\sigma = \sqrt{m} \simeq \sqrt{x}$$

$$\sigma_{\bar{x}} = \frac{\sigma}{\sqrt{n}} = \frac{1}{n} \sqrt{\sum_{i=1}^{i=n} x_i} \qquad \text{(Eq. 76)}$$

The result of the measurements would be reported as

$$\bar{x} \pm \sigma_{\bar{x}} = \frac{1}{n}\left(\sum_{i=1}^{i=n} x_i \pm \sqrt{\sum_{i=1}^{i=n} x_i}\right) \qquad \text{(Eq. 77)}$$

which has the same fractional standard deviation as Equation 75. This is the same as dividing equation 74 by the number of groups n into which the data were subdivided. The point is made that observation of a total

$$\sum_{i=1}^{i=n} x_i$$

randomly distributed events has a fractional standard deviation of

$$1\sqrt{\sum_{i=1}^{i=n} x_i}$$

As a consequence of this exercise one may observe that the standard deviation for 100 events is 10 percent and for 10,000 counts 1 percent. No manipulation of the same total data can reduce the size of the fractional uncertainty due purely to randomness.

INEFFICIENT STATISTICS*

The preceding work treats of efficient statistics by which the probable accuracy of a mathematical estimate is assured within the limits imposed by the quantity and distribution of data. The calculations for efficient statistics are often so time-consuming that preliminary estimates of statistical values are desirable. Techniques for obtaining preliminary estimates of statistical values have been given the term inefficient statistics. Application of inefficient statistical methods requires acceptance of certain assumptions, chiefly in regard to the type of distribution. The practical aspects of inefficient statistical methods result from either dealing with a limited quantity of random data or dealing with only a limited quantity of the total data that have been collected. Inefficient statistics may be subdivided as macrostatistics in which n is greater than 100 and microstatistics in which n is equal to or less than 10.

1. Macrostatistics ($n > 100$)

a. The estimate of the mean of a large symmetrical population based upon the median (50-percent point or the point where one-half the data lies below and the other half lies above) has an efficiency of 64 percent. This is to say the estimate would have the accuracy that would be obtained if only 0.64 of the data had been used. Thirty-six percent of the information, then, is ignored.

b. Another technique for estimating the mean is to take the average of the two observations which lie 29 percent inside the upper and lower extremes of the data collected. These observations are at the 29- and 71-percent points of the distribution. The result has the same accuracy as the mean calculated from 81 percent of the observations.

c. When the mean is estimated by choosing the average of the 20-, 50-, and 80-percent points, the loss of information is, effectually, 12 percent.

The estimate of the standard deviation for $n = 100$ based upon the 93-percent and 7-percent points utilizes approximately 65 percent of the information contained in the data. The formula is

$$\sigma = \frac{\text{(93-percent point) - (7-percent point)}}{3}$$

This estimate is based upon the approximation that 86 percent of the data in a normal distribution falls within $m = \pm 1.5\sigma$.

---

*(18, pp. 902-904)

2. Microstatistics ($n < 10$)

For $n \leq 10$, the median is a more accurate estimate of the mean than the average of the extreme data for all values of n other than 3 and 5. The median is taken as the value of the middle datum when n is odd and as the average of the middle score when n is even.

a. The efficiency of using the median as an estimate of the mean has an efficiency equal to or greater than 0.64 for all n.

b. The average of the third value from each end of a distribution $n = 7$ to 10 (and probably higher) has an efficiency about 0.84.

Estimates of the standard deviation of a small sample, in which n is from 2 to 20 may be made from the following:

Range $\equiv$ (largest observation) - (smallest observation)

$$\sigma \simeq \sqrt{\frac{\sum_{i=1}^{i=n} (x_i - \bar{x})^2}{n-1}}$$

$$\simeq \frac{\text{range}}{\sqrt{n}} \qquad \text{(Eq. 78)}$$

The efficiency for $n = 3$ is 99 percent and declines to about 85 percent for $n = 10$. The following table gives a few values for the denominator when $n > 10$.

n	10	15	20	30	50	100
Range/σ	3.08	3.47	3.73	4.09	4.50	5.02

The relative efficiency of range as an estimator of standard deviation decreases as n increases. By dividing the data into equal groups of seven or eight observations and using the average of the ranges of the groups it is possible to improve the estimate of the standard deviation.

An estimate of the standard error (standard deviation of the mean value) for a small sample is

$$\sigma_{\bar{x}} = \frac{\sigma}{\sqrt{n}} = \sqrt{\frac{\sum_{i=1}^{i=n} (x_i - \bar{x})^2}{n(n-1)}}$$

$$\simeq \frac{\text{range}}{n} \qquad \text{(Eq. 79)}$$

An estimate of chi-square for small samples having a Poisson distribution is

$$\chi^2 = \frac{1}{\bar{x}} \sum_{i=1}^{i=n} (x_i - \bar{x})^2 = \frac{n\sigma^2}{\bar{x}} \simeq \frac{(\text{range})^2}{\text{mean}} \qquad \text{(Eq. 80)}$$

Examples:

1. Find the probability P_x of observing the value 19 in a Poisson distribution whose mean is 15.

$$P_x = \frac{m^x}{x!} e^{-m} = P_{19} = \frac{15^{19}}{19!} e^{-15}$$

$$= \frac{2.217 \times 10^{22}}{1.216 \times 10^{17}} \times 3.059 \times 10^{-7}$$

$$= 5.577 \times 10^{-2} \quad \text{or} \quad \approx 5.6\%$$

2. Using $P_x = 5.577 \times 10^{-2}$ from Example 1, find P_{x-1}, P_{x+1}, and P_o.

a. $$P_{x-1} = \frac{x}{m} P_x = P_{19-1} = \frac{19}{15} \times 0.05577$$

$$= 0.0731 \quad \text{or} \quad \approx 7.3\%$$

b. $$P_{x+1} = \frac{m}{x+1} P_x = P_{19+1} = \frac{15}{19+1} \times 5.577 \times 10^{-2}$$

$$= \frac{15}{20} \times 5.577 \times 10^{-2} = 4.183 \times 10^{-2}$$

or $\approx 4.2\%$

c. $$P_0 = e^{-m} = e^{-15} = 3.059 \times 10^{-7}$$

or $\approx 0.0000306\%$

3. a. Find the probability P_x in a Poisson distribution that the next observation x will be 31 when the mean m is 34.

$$P_x \approx \frac{1}{\sqrt{2\pi x}} \left(\frac{m}{x}\right)^x e^{-(m-x)}$$

$$\approx \frac{1}{\sqrt{2\pi(31)}} \left(\frac{34}{31}\right)^{31} e^{-(34-31)}$$

$$\approx 7.165 \times 10^{-2} \times 1.752 \times 10^{1} \times 4.978 \times 10^{-2}$$

$$\approx 6.25 \times 10^{-2} \quad \text{or} \quad 6.3\%$$

b. Find the probability P_x in a Poisson distribution that the next observation will be $x = m = 34$.

$$P_x \simeq \frac{1}{\sqrt{2\pi x}} \left(\frac{m}{x}\right)^x e^{-(m-x)}$$

$$\simeq \frac{1}{\sqrt{2\pi(34)}} \left(\frac{34}{34}\right)^{34} e^{-(34-34)}$$

$$\simeq 6.842 \times 10^{-2} \times 1 \times 1 = 6.842 \times 10^{-2}$$

or 6.8%

4. Find the approximate mean by finding the arithmetic average of the following data: 8, 5, 7, 6, 7, 4, 9, 11, 5, 6.

$$m \simeq \bar{x} = \frac{1}{n} \sum_{i=1}^{i=n} x_i$$

by inspection, the number of observations n is 10.

$$m \simeq \bar{x} = \frac{1}{10} (8 + 5 + 7 + 6 + 7 + 4 + 9 + 11 + 5 + 6)$$

$$= 6.8$$

5. Using the data in Example 4, find the standard deviation in terms of a finite number of observations

$$\sigma^2 = \frac{1}{n-1} \sum_{i=1}^{i=n} (x_i - m)^2$$

Setting up a table for the data and results of calculations:

x_i	$\bar{x}$	$x_i-\bar{x}$	$(x_i-\bar{x})^2$
8	6.8	1.2	1.44
5	6.8	-1.8	3.24
7	6.8	0.2	0.04
6	6.6	-0.8	0.64
7	6.8	0.2	0.04
4	6.8	-2.8	7.84
9	6.8	2.2	4.84
11	6.8	4.2	17.64
5	6.8	-1.8	3.24
6	6.8	-0.8	0.64

$$\sum x_i = 68 \qquad \bar{x} = \frac{68}{10} = 6.8$$

$$\sum_{i=1}^{i=10} (x_i - \bar{x}) = 0 \qquad \sum_{i=1}^{i=10} (x_i - \bar{x})^2 = 39.6$$

$$\sigma^2 = \frac{1}{10-1} \times 39.6 = 4.4 \qquad \sigma = \sqrt{4.4} = 2.098$$

6. Estimate the standard deviation from the data in Example 4. By rearranging the data on the basis of largest to smallest (or by inspection), it is found that the range is 9 - 4 = 5 .

$$\sigma \simeq \frac{\text{range}}{\sqrt{n}} = \frac{5}{\sqrt{10}} = 1.581$$

7. Using the table value for n = 10, find the estimate of the standard deviation of the data in Example 4. From the table when n = 10 , range/σ = 3.08 .

$$\sigma \simeq \frac{9 - 4}{3.08} = \frac{5}{3.08} = 1.623$$

8. Using inefficient statistics, find the estimate of the standard deviation when n = 300 and the observed values at the 93- and 7-percent points are 61 and 44 respectively.

$$\sigma \simeq \frac{\text{(93-percent point)} - \text{(7-percent point)}}{3} = \frac{61 - 44}{3} = 5.667$$

9. Using inefficient statistics, find an estimate of the standard error using the data in Example 4.

$$\sigma_{\bar{x}} = \frac{\text{range}}{n} = \frac{9 - 4}{10} = 0.5$$

10. Using inefficient statistics, find the value of chi-square for the data in Example 4.

$$\chi^2 \simeq \frac{\text{range}}{\text{mean}} = \frac{9 - 4}{6.8} = 3.676$$

SUPERPOSITION OF SEVERAL INDEPENDENT RANDOM PROCESSES

A generalization of the Poisson distribution is required in gamma-ray spectroscopy because samples usually contain more than one gamma-emitting nuclide and all the gamma rays are detected during the period of measurement. Although the spectra of the radioactive background and the gamma emitters in the sample result from random events detected during the period of measurement, they may be treated as layer-upon-layer. Hence, the term superposition when considering the total spectrum made up of two or more spectra.

Referring to the matrices described in Chapter 10, the activity or counts due to radionuclide i can be written

$$C_{i1} = a_{i1}N_1 + a_{i2}N_2 + a_{i3}N_3 + a_{i4}N_4 + a_{i5}N_5 + a_{i6}N_6 \qquad \text{(Eq. 81)}$$

where the a's are the numbers found when the equation is solved.

Using values for a particular NaI(Tl) detector at the Quality Assurance Branch of the Environmental Monitoring and Support Laboratory-Las Vegas, Nevada, and the following conditions for a 4-liter Marinelli beaker containing 3.5 liters of water

Isotope	Channels for Interference Factors	Term for Sum of Channels	Efficiency (Counts/pCi)
^{51}Cr	28-36	N^{51}Cr	0.01392
^{106}Ru	47-56	N^{106}Ru	0.02252
^{137}Cs	62-72	N^{137}Cs	0.07850
^{134}Cs	74-86	N^{134}Cs	0.07190
^{65}Zn	104-120	N^{65}Zn	0.03339
^{60}Co	124-138	N^{60}Co	0.05483

the following formulas are obtained:

$$\begin{aligned}{}^{51}\text{Cr}\ \ (\text{cpm}/3.5\ \text{liter}) = {} & 1.000(N^{51}\text{Cr}) - 0.300254(N^{106}\text{Ru}) - 0.252904(N^{137}\text{Cs}) \\ & - 0.372847(N^{134}\text{Cs}) - 0.078011(N^{65}\text{Zn}) - 0.089156(N^{60}\text{Co}) \qquad \text{(Eq. 82)}\end{aligned}$$

$$\begin{aligned}{}^{106}\text{Ru}\ \ (\text{cpm}/3.5\ \text{liter}) = {} & 0.000(N^{51}\text{Cr}) + 1.093667(N^{106}\text{Ru}) - 0.145403(N^{137}\text{Cs}) \\ & - 0.656015(N^{134}\text{Cs}) - 0.111432(N^{65}\text{Zn}) + 0.092489(N^{60}\text{Co}) \qquad \text{(Eq. 83)}\end{aligned}$$

$^{137}\mathrm{Cs}$ (cpm/3.5 liter) =
$0.000(N^{51}\mathrm{Cr}) - 0.245768(N^{106}\mathrm{Ru}) + 1.003305(N^{137}\mathrm{Cs})$
$- 0.282704(N^{134}\mathrm{Cs}) - 0.072860(N^{65}\mathrm{Zn}) - 0.084018(N^{60}\mathrm{Co})$ (Eq. 84)

$^{134}\mathrm{Cs}$ (cpm/3.5 liter) =
$0.000(N^{51}\mathrm{Cr}) + 0.052171(N^{106}\mathrm{Ru}) + 0.006090(N^{137}\mathrm{Cs})$
$+ 1.077541(N^{134}\mathrm{Cs}) - 0.266478(N^{65}\mathrm{Zn}) - 0.191901(N^{60}\mathrm{Co})$ (Eq. 85)

$^{65}\mathrm{Zn}$ (cpm/3.5 liter) =
$0.000(N^{51}\mathrm{Cr}) - 0.085519(N^{106}\mathrm{Ru}) + 0.011547(N^{137}\mathrm{Cs})$
$+ 0.018941(N^{134}\mathrm{Cs}) + 1.017764(N^{65}\mathrm{Zn}) - 1.255153(N^{60}\mathrm{Co})$ (Eq. 86)

$^{60}\mathrm{Co}$ (cpm/3.5 liter) =
$0.000(N^{51}\mathrm{Cr}) - 0.004314(N^{106}\mathrm{Ru}) + 0.000515(N^{137}\mathrm{Cs})$
$- 0.071606(N^{134}\mathrm{Cs}) + 0.019198(N^{65}\mathrm{Zn}) + 1.013625(N^{60}\mathrm{Co})$ (Eq. 87)

Thus, for ^{65}Zn the values of the a's are:

$a_1 = 0.00000$
$a_2 = -0.085519$
$a_3 = +0.011547$
$a_4 = +0.018941$
$a_5 = +1.017764$
$a_6 = +1.255153$

The uncertainty in the value measured for C_i is expressed as

$$\sigma^2(C_i) = a_{i1}{}^2N_1 + a_{i2}{}^2N_2 + a_{i3}{}^2N_3 + a_{i4}{}^2N_4 + a_{i5}{}^2N_5 + a_{i6}{}^2N_6 \quad \text{(Eq. 88)}$$

or the variance σ^2 for the counts obtained for zinc-65 is

σ^2(cpm/3.5 liter 65Zn) =
$0.00731(N^{106}\mathrm{Ru}) + 0.000133(N^{137}\mathrm{Cs}) + 0.00359(N^{134}\mathrm{Cs})$
$+ 1.0359(N^{65}\mathrm{Zn}) + 1.575(N^{60}\mathrm{Co})$

and the uncertainty is, therefore, expressed as σ. For zinc-65, it is seen that the estimated uncertainty is very strongly influenced by the amount of cobalt-60 in the sample.

The terms in the preceding paragraph do not consider background to be a factor, but we should realize that backgrounds are important at the levels being measured. First, let us assume that gross counts are being measured such that we get a count M in a time t_M and a background count b in a measured time of t_b where b is the average background rate. The average background rate then is

$$B = bt_b \pm \sqrt{bt_b} \quad \text{(Eq. 89)}$$

$$B/t_b = b \pm \sqrt{b/t_b} \qquad \text{(Eq. 90)}$$

The count M can be estimated as being due to the sample count rate S and the background count rate B .

$$M/t_s = \frac{S + B}{t_s}$$

$$= \left[(S + b)t_s + \sqrt{(S + B)t_s}\right]\frac{1}{t_s}$$

$$= S + b \pm \sqrt{\frac{S}{t_s} + \frac{b}{t_s}} \qquad \text{(Eq. 91)}$$

If the count rate of the background is subtracted from the above the result is

$$\text{Sample Count Rate} = S + b \pm \sqrt{\frac{S}{t_s} + \frac{b}{t_s}} - b \pm \sqrt{\frac{b}{t_b}} \qquad \text{(Eq. 92)}$$

Remember that uncertainties are summed with the formula

$$R^2 = r_1{}^2 + r_2{}^2 + \ldots + r_n{}^2 \qquad \text{(Eq. 93)}$$

where $r_1, r_2, \ldots, r_n$ are the absolute values of the uncertainties in the mean values of the several quantities, and R is the final uncertainty in the mean value of a physical magnitude from the summation or the difference of several independent observations on two or more physical quantities (such as the number of counts in a region of a spectrum). The sample count rate then becomes

$$\text{Sample Count Rate} = S \pm \sqrt{\frac{S}{t_s} + \frac{b}{t_s} + \frac{b}{t_b}} \qquad \text{(Eq. 94)}$$

Keep in mind that S + b is equal to the observed count rate when the sample is counted.

The background uncertainty enters twice, once for any previous background determinations of blank or mock sources and again for the particular sample of interest. In the previous example of the count rate uncertainty for zinc-65, it is necessary to add the terms due to two background fluctuations for each of the regions of interest, one for the background if it has been subtracted from the spectra before the regions of interest are totalized and one for the standard background in these regions. If the standard background has been known to have uncertainties larger than counting statistics indicate, this uncertainty should be used.

In the preceding formulas for determining the activity and standard deviation of a radionuclide in a composite spectrum, it has been implicitly assumed that the background had been subtracted from all the measured spectra. To include the uncertainties due to fluctuations in backgrounds, a more detailed explanation follows.

Let the background be firmly determined by previous measurements. Then for each area chosen to represent a full energy peak or region of interest used in determining the interference factors we have a set of background numbers. Let us say that the backgrounds are represented by rates b_1 through b_6 . Now if a sample is counted, the gross count rates will be labeled $Y_i = N_i + B_i$ where region N_i is the net count, and $B_i = b_i t_s$ and t_s is the time required to accumulate the spectrum.

C_i is still determined by

$$C_i = a_{i_1}N_1 + a_{i_2}N_2 + a_{i_3}N_3 + a_{i_4}N_4 + a_{i_5}N_5 + a_{i_6}N_6$$

but the standard deviation is now given by

$$\sigma_i^2 = a_{i_1}{}^2N_1 + a_{i_2}{}^2N_2 + a_{i_3}{}^2N_3 + a_{i_4}{}^2N_4 + a_{i_5}{}^2N_5 + a_{i_6}{}^2N_6 + b_it_s + b_it_b$$

where t_b is a large time used during the establishment of the mean background rate. The count rate is then

$$SCR_i = C_i/t_s \pm \sqrt{\frac{a_{i_1}{}^2N_1 + a_{i_2}{}^2N_2 + \ldots + a_{i_6}{}^2N_6}{t_s} + \frac{b_i}{t_s} + \frac{b_i}{t_b}} \qquad \text{(Eq. 95)}$$

When analyzing the results of an experiment that involves several steps, two additional types of error analysis must be considered other than those fundamental uncertainties resulting from counting statistics. Uncertainties due to variations in sample size, counting geometry, etc., are easily observed when several measurements have been made. These uncertainties result from somewhat random, but measurable, events. Thus if a formula is used to calculate an activity that has several variables, a, b, c , the errors can be documented as probable error r_a, r_b, r_c , etc.

Suppose the activity calculation A is written as

$$A = \frac{abc}{def}$$

and we know the uncertainties r_a, r_b, r_c, r_d, r_e, r_f , the fractional error in A , (R/A), is determined as

$$\left(\frac{R}{A}\right)^2 \simeq \left(\frac{r_a}{a}\right)^2 + \left(\frac{r_b}{b}\right)^2 + \left(\frac{r_c}{c}\right)^2 + \left(\frac{r_d}{d}\right)^2 + \left(\frac{r_e}{e}\right)^2 + \left(\frac{r_f}{f}\right)^2$$

or

$$R = A\sqrt{\left(\frac{r_a}{a}\right)^2 + \left(\frac{r_b}{b}\right)^2 + \ldots\ldots + \left(\frac{r_f}{f}\right)^2}$$

There will, however, be a few steps in the making of every measurement where the uncertainty is not random and there is no way of controlling the error. Such errors may arise from not being able to fabricate a standard that simulates the sample to be analyzed. Example problems of non-random uncertainty in analyzing the radionuclides present on a charcoal cartridge (filter) are:

a. Distribution of radionuclides in the sample is not known.

b. A standard cannot be obtained for a particular radionuclide.

c. An unknown or a different radionuclide than anticipated occurs in the sample.

These errors should be added instead of combined in the manner that is done for random errors. Thus, if these errors are known as k, l, m, and n for the measurement of a sample, we should report the activity and the uncertainty as:*

$$A \pm \left(\sqrt{\frac{s+b}{t_s} + \frac{b}{t_b} + (r_a)^2 + (r_b)^2 + \ldots + (r_f)^2} + \frac{1}{3}(k + l + m + n)\right)$$

To determine the fractional error, let us assume that:

$$\left(\frac{s+b}{t_s} + \frac{b}{t_b}\right)^{-\frac{1}{2}} = 0.01$$

$$\frac{r_a}{a} = 0.02$$

$$\frac{r_b}{b} = 0.01$$

and $k = 0.03$, $l = 0.01$, $m = 0.02$, and $n = 0.03$; then the fractional error is

$$\begin{aligned}\frac{\sigma}{A} &= \pm\sqrt{(0.01)^2 + (0.02)^2 + (0.01)^2} + \frac{1}{3}(0.03 + 0.01 + 0.02 + 0.03)\\ &= \pm\sqrt{0.0006} + 0.03\\ &= \pm(0.024 + 0.03)\\ &= \pm 0.054 \text{ or } \pm 5.4\%\end{aligned}$$

We should state that this result is at the 1σ confidence level. In practice, it is best to account for each fractional error as it is determined and to combine fractional errors as the final values are tabulated.

---

*The factor 1/3 in estimating systematic errors is constant and independent of the number of terms included in estimating the total systematic error.

STATISTICAL TESTING FOR NORMAL AND NON-NORMAL DATA

In principle, the results of gamma-ray spectroscopy should follow statistical laws of distribution. Consequently, gamma-ray spectroscopy systems should be tested to determine if the data obtained have the desired distribution. The Poisson distribution is acknowledged as representative of random data, but the assumption of a normal distribution makes calculation easier. The error caused in using normal statistics over Poisson statistics is minimal unless the number of data is small. If checks indicate that results follow a normal distribution, it can be assumed that the instrument is capable of operating correctly. When checks indicate a non-normal distribution, the instrument must be repaired or the system modified. Some of the common causes leading to non-normal results are:

1. Change in the radon concentrations in the air surrounding the detector.
2. Line noise or faulty grounding.
3. Ground loops.
4. Temperature variations.
5. Detector failure.
6. Electronic malfunction.

An easy check of the normality of the distributions of results is to plot both the background and the performance standard results on a control chart for analysis. The tests described below should be repeated on a monthly or quarterly basis and will require little effort. Although the Poisson distribution is valid for gamma-ray detection, a NaI(Tl) detector will generally have count rates high enough that the Gaussian or normal distribution law is sufficiently accurate. Background counts will have larger fluctuations than are expected from counting statistics because of the lack of adequate controls and the relatively long counting times required. Generally, the background for a NaI(Tl) detector will fluctuate 3 to 10 times greater than a Poisson distribution would indicate during a time period of a year. The performance standard counted for a short time (10 to 15 minutes) will more closely approximate a Poisson distribution.

The relative normalcy of counting results is not obvious through inspection of a control chart or a series of numbers. The use of statistical tests is the only way that numbers representing counting results can be checked to assure that the spectrometer is operating correctly. The mean square of the successive differences (MSSD) is preferred over a chi-square analysis (16, pp. 385-390). The MSSD method is highly selective for a small number (5 to 25) of measurements. If values are taken at random from a normal population and classified in the order of appearance the variable (the Von Neuman statistic)

$$r = \frac{\sum_{i=1}^{i=(n-1)} (x_{i+1} - x_i)^2}{2 \sum_{i=1}^{i=n} (\bar{x}_i - \bar{x})^2} \qquad \text{(Eq. 96)}$$

has a probable value of 1. A value much below 1 points to either a drift or to abnormal groups, or both, while a value above 1 reveals abnormally rapid fluctuations. Table 2 presents the limiting values of r at the probability levels of 95 percent and 99 percent for n between 4 and 25. It should be kept in mind that a probability level of 95 percent means that 5 percent of the data will be rejected falsely and a probability level of 99 percent means that 1 percent of the data will be rejected falsely.

TABLE 2. LIMITING VALUES OF r AT PROBABILITIES OF 95% AND 99% FOR THE MEAN SQUARE OF THE SUCCESSIVE DIFFERENCES STATISTICAL TEST

n	0.01	0.05	0.95	0.99	n
4	0.313	0.390	1.610	1.687	4
5	0.269	0.410	1.590	1.731	5
6	0.281	0.445	1.555	1.719	6
7	0.307	0.468	1.532	1.693	7
8	0.331	0.491	1.509	1.668	8
9	0.354	0.512	1.488	1.646	9
10	0.376	0.531	1.469	1.624	10
11	0.396	0.548	1.452	1.604	11
12	0.414	0.564	1.436	1.586	12
13	0.431	0.578	1.422	1.569	13
14	0.477	0.591	1.409	1.553	14
15	0.461	0.603	1.397	1.539	15
16	0.475	0.614	1.386	1.525	16
17	0.487	0.624	1.376	1.513	17
18	0.499	0.633	1.367	1.501	18
19	0.510	0.642	1.358	1.490	19
20	0.520	0.650	1.350	1.480	20
21	0.530	0.657	1.343	1.470	21
22	0.539	0.665	1.335	1.461	22
23	0.548	0.671	1.329	1.452	23
24	0.556	0.678	1.322	1.444	24
25	0.564	0.684	1.316	1.436	25

Table 3 shows an example selected from one of the author's instruments. It is noted that this particular instrument failed catastrophically 1 month after the end of the period in which these data were acquired. The column captioned "Count Low" is the number of counts accumulated in 10 minutes from the 570 keV gamma ray from bismuth-207 check source. For the low energy peak, the average count accumulated was 22569.6, the expected spread was 150.23, the observed σ was 260.54 and r was 0.58. From Table 2 we find for $n = 25$ and

TABLE 3. MSSD TEST APPLIED TO COUNTS OF A Bi-207 SAMPLE OBTAINED WITH A MULTICHANNEL GAMMA-RAY SPECTROMETER

x_i (Count Low)	$(x_{i+1}-x_i)^2$	$(x_i - \bar{x})^2$	x_i (Count High)	$(x_{i+1}-x_i)^2$	$(x_i - \bar{x})^2$
22056		263785	8982		209324
22119	3969	203040	9114	17424	105963
22403	80656	27756	9386	73984	2864
22666	69169	9293	9502	13456	3904
22772	11236	40966	9571	4761	17287
22487	81225	6823	9440	17161	0
22445	1764	15525	9322	13924	13811
22416	841	23593	9346	576	8746
22646	52900	5837	9537	36481	9502
22800	23716	53084	9651	12996	44724
22374	181476	38259	9383	71824	3195
22572	39204	6	9467	7056	755
22963	152881	154764	9659	36864	48171
22491	222784	6187	9396	69169	1894
22091	160000	229058	8854	293764	342834
22557	217156	159	9425	326041	211
22688	17161	14019	9555	16900	13336
22499	35721	4984	9346	43681	8746
22341	249621	52258	9374	784	4293
22694	124609	15475	9583	43681	20587
22890	38416	102656	9664	6561	50391
22544	119716	655	9480	33856	1639
22991	199809	177578	9675	38025	55451
22813	31684	59244	9690	225	62740
22922	11881	124186	9586	10816	21456
564240	1902938	1629190	235988	1190010	1051824

$\bar{x} = 564240/25 = 22569.6$

$\sqrt{x} = 150.23$

$\sigma = 260.54 \quad \sigma^2 = 67882$

$r = \frac{1902938}{2 \times 1629190}$

$= 0.58$ (non-normal)

$\bar{x} = 235988/25 = 9439.52$

$\sqrt{x} = 97$

$\sigma = 209.35 \quad \sigma^2 = 43827$

$r = \frac{1190010}{2 \times 1051824}$

$= 0.57$ (non-normal)

a 95 percent probability, $0.684 \leq r \leq 1.316$. The value obtained for r lies outside of this range, thus indicating that the instrument is either drifting or has abnormal groupings of data. In this particular case, the instrument was drifting. Figures 20 (page 51) and 21 are sections of a control chart using these data. The drift shown to exist by this test is not obvious through visual inspection of the control chart. Data accumulated for the 1063 keV peak show similar behavior.

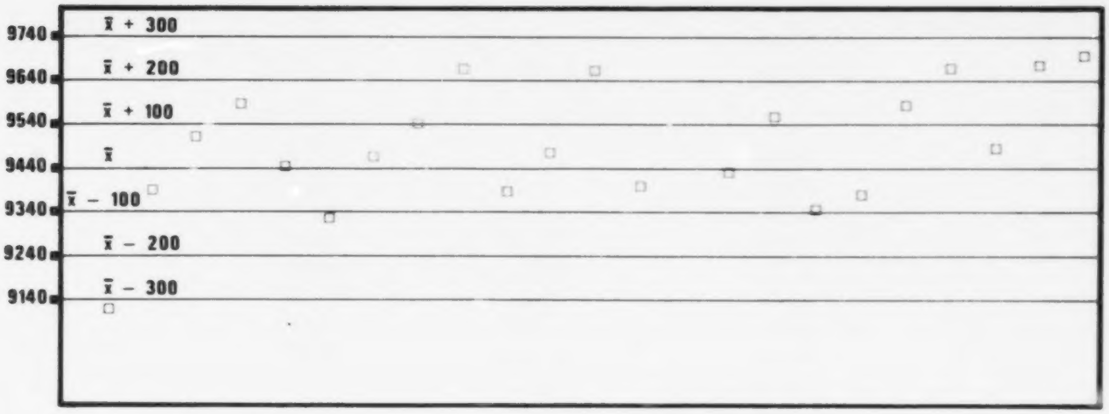

Figure 21. Control chart for high energy (1.063 MeV) peak from Bi-207.

Table 4 illustrates the test used in the preceding example for nine background measurements obtained from the same instrument system. Those nine measurements were taken in one afternoon which prevented the observation of long term drifts. The average of the background counts for the 10-minute counting interval was $\bar{x} = 6342$. The standard deviation was calculated as $\sigma = 75.5$ which was within normal limits of $\sqrt{\bar{x}} = 79.6$. In this case $r = 133017/(2 \times 45603) = 1.46$. From Table 2, using values for $n = 9$, and a probability of 95 percent, the limiting values of r become $0.512 \leq r \leq 1.488$. The calculated value for r lies within the limiting values, indicating that the data are probably random.

The recommended test for normality is the Kolmogorov-Smirnov test (also known as the "vodka test")(19). This test, used in conjunction with the plotting of data on probability paper, is fairly easily performed and will add to the documentation of data taken for the control charts. Using the data from Table 5, the first step is to place the numbers in order beginning with the smallest. Let $x_1, x_2, \ldots, x_n$ designate these ordered sample values. The distribution function $S_i(x)$ is then defined as:

$$S_i(x) = \frac{i}{n} \qquad x_i \leq x \leq x_{i+1}$$

Tables 5 and 6 show the rearrangement of the control data x_i presented in Table 3. The fifth columns of Tables 5 and 6 show the distribution function of S_{25}. The fifth column of Table 7 shows the distribution function of S_9.

TABLE 4. MSSD TEST FOR BACKGROUND MEASURMENTS
OF A 10.2-CM BY 10.2-CM NaI(Tl) DETECTOR

10 Minute Counts	$(x_{i+1}-x_i)^2$	$(x_i - \bar{x})^2$
6408		4356
6397	121	3025
6218	32041	15376
6426	43264	7056
6250	30976	8464
6331	6561	121
6294	1369	2304
6412	13924	4900
6343	4761	1
57079	133017	45603

Σx = 57078

$\bar{x}$ = 6342

$\sqrt{x}$ = 79.64

σ = 75.50

$$r = \frac{133017}{2 \times 45603} = 1.46 \text{ (normal)}$$

TABLE 5. KOLMOGOROV-SMIRNOV TEST ON LOW ENERGY (0.57 MeV) GAMMA RAYS FROM Bi-207

x_i (Count Low)	$\frac{x_i - m}{\sigma}$	$f(x_i)$	$F(x_i)$	$S_i(x)$	D_i	D'_i
22056	-1.97	0.06	0.02	0.04	0.02	
22091	-1.83	0.07	0.03	0.08	0.05	0.06
22119	-1.73	0.09	0.04	0.12	0.08	0.09
22341	-0.88	0.27	0.19	0.16	0.03	0.12
22374	-0.75	0.30	0.23	0.20	0.03	0.01
22403	-0.64	0.33	0.26	0.24	0.01	0.01
22416	-0.59	0.34	0.28	0.28	0.00	0.02
22445	-0.48	0.36	0.32	0.32	0.00	0.04
22487	-0.31	0.38	0.38	0.36	0.02	0.04
22491	-0.30	0.38	0.38	0.40	0.02	0.02
22499	-0.27	0.38	0.39	0.44	0.05	0.06
22544	-0.10	0.40	0.46	0.48	0.02	0.09
22557	-0.50	0.40	0.48	0.52	0.04	0.06
22572	0.01	0.40	0.50	0.56	0.06	0.08
22646	0.30	0.38	0.62	0.60	0.02	0.10
22666	0.37	0.37	0.64	0.64	0.00	0.02
22688	0.46	0.36	0.68	0.68	0.00	0.04
22694	0.48	0.36	0.68	0.72	0.04	0.04
22772	0.78	0.29	0.78	0.76	0.02	0.08
22800	0.89	0.27	0.81	0.80	0.01	0.02
22813	0.94	0.26	0.83	0.84	0.01	0.03
22890	1.23	0.19	0.89	0.88	0.01	0.05
22922	1.35	0.16	0.91	0.92	0.01	0.03
22963	1.51	0.13	0.93	0.96	0.03	0.05
22991	1.62	0.11	0.95	1.00	0.05	0.07

TABLE 6. KOLMOGOROV-SMIRNOV TEST ON HIGH ENERGY (1.063 MeV) GAMMA RAYS FROM Bi-207

x_i (Count High)	$\frac{x_i - m}{\sigma}$	$f(x_i)$	$F(x_i)$	$S_i(x)$	D_i	D'_i
8854	-1.95	0.06	0.03	0.04	0.01	
8982	-1.49	0.13	0.07	0.08	0.02	0.03
9114	-1.02	0.24	0.15	0.12	0.03	0.07
9322	-0.28	0.38	0.39	0.16	0.23	0.27
9346	-0.19	0.39	0.42	0.24	0.18	0.26
9346	-0.19	0.39	0.42	0.24	0.18	0.18
9374	-0.09	0.40	0.46	0.28	0.18	0.22
9383	-0.06	0.40	0.48	0.32	0.16	0.20
9386	-0.05	0.40	0.48	0.36	0.12	0.16
9397	-0.01	0.40	0.50	0.40	0.10	0.14
9425	0.09	0.40	0.59	0.44	0.10	0.14
9440	0.14	0.40	0.56	0.48	0.08	0.12
9467	0.24	0.39	0.59	0.52	0.07	0.09
9480	0.29	0.38	0.61	0.56	0.05	0.09
9502	0.37	0.37	0.64	0.60	0.04	0.10
9537	0.49	0.35	0.69	0.64	0.05	0.09
9555	0.55	0.34	0.71	0.68	0.03	0.07
9571	0.61	0.33	0.73	0.72	0.01	0.05
9538	0.65	0.32	0.74	0.76	0.02	0.02
9586	0.67	0.32	0.75	0.80	0.05	0.01
9651	0.90	0.27	0.82	0.84	0.02	0.01
9659	0.93	0.26	0.82	0.88	0.06	0.02
9664	0.94	0.26	0.83	0.94	0.09	0.05
9675	0.98	0.25	0.84	0.98	0.12	0.08
9690	1.04	0.23	0.85	1.00	0.15	0.11

TABLE 7. KOLMOGOROV-SMIRNOV TEST ON BACKGROUND MEASUREMENTS OF A 10.2-CM BY 10.2-CM NaI(Tl) DETECTOR

x_i	$\frac{x_i - m}{\sigma}$	$f(x_i)$	$F_\gamma(x_i)$	$S_i(x)$	$S_{i+1}(x)$	D_i	D_i'
6218	-1.64	0.10	0.05	0.11	0.10	0.06	
6250	-1.22	0.19	0.11	0.22	0.20	0.11	0.00
6294	-0.64	0.33	0.26	0.33	0.30	0.07	0.04
6331	-0.15	0.39	0.44	0.44	0.40	0.00	0.11
6343	0.01	0.40	0.50	0.56	0.50	0.06	0.06
6397	0.73	0.31	0.77	0.67	0.60	0.10	0.21
6408	0.87	0.29	0.81	0.78	0.70	0.00	0.11
6412	0.93	0.26	0.82	0.89	0.80	0.07	0.04
6426	1.11	0.22	0.87	1.00	0.90	0.13	0.02

$\bar{x}$ = 6342

$\sqrt{x}$ = 79.64

σ = 73.50

The next step is to plot $S_i(x)$ versus counts/time on probability paper (e.g., K & E Probability × 90 divisions, #46 8000) as in Figures 22, 23, and 24. A plot of "normal" data will produce a straight line on this paper. The mean value is that value having a probability of 50 percent. Thus, from Figure 22, the mean value is 22557. From Figure 23, the mean value is 9467, and from Figure 24, the mean value is 6343. While the standard deviation can be determined as the inverse of the slope as a function of confidence levels (1σ = 84.13 and 15.86, 2σ = 97.73 and 2.27) it is easier, generally, to calculate its value.

Real data do not generally produce a straight line. The Kolmogorov-Smirnov test, however, will indicate whether or not the data are acceptable as a sample from a normal distribution. By using the mean value m and standard deviation σ, normal data are created from a data set from which probability values may be generated using the following formula:

$$F(x_i) = \int_{t=-\infty}^{t=x_i} \frac{e^{-(t-m)^2/2\sigma^2}}{\sqrt{2\pi}}\, dt \qquad \text{(Eq. 97)}$$

$$F(x_i) = \int_{s=-\infty}^{s=\frac{x_i-m}{\sigma}} \frac{e^{-s^2/2}}{\sqrt{2\pi}}\, ds \qquad \text{(Eq. 98)}$$

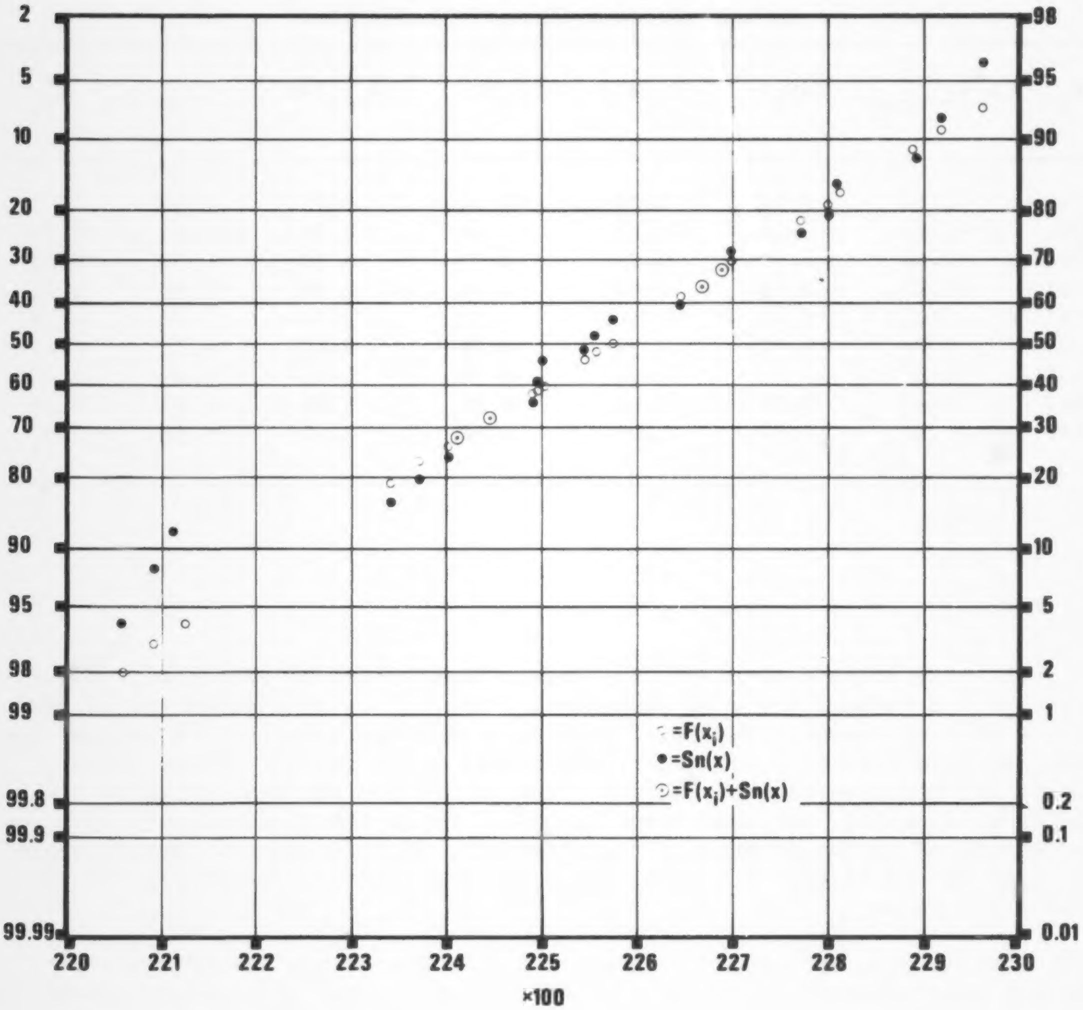

Figure 22. Probability plot for low-energy (0.57 MeV) peak from Bi-207.

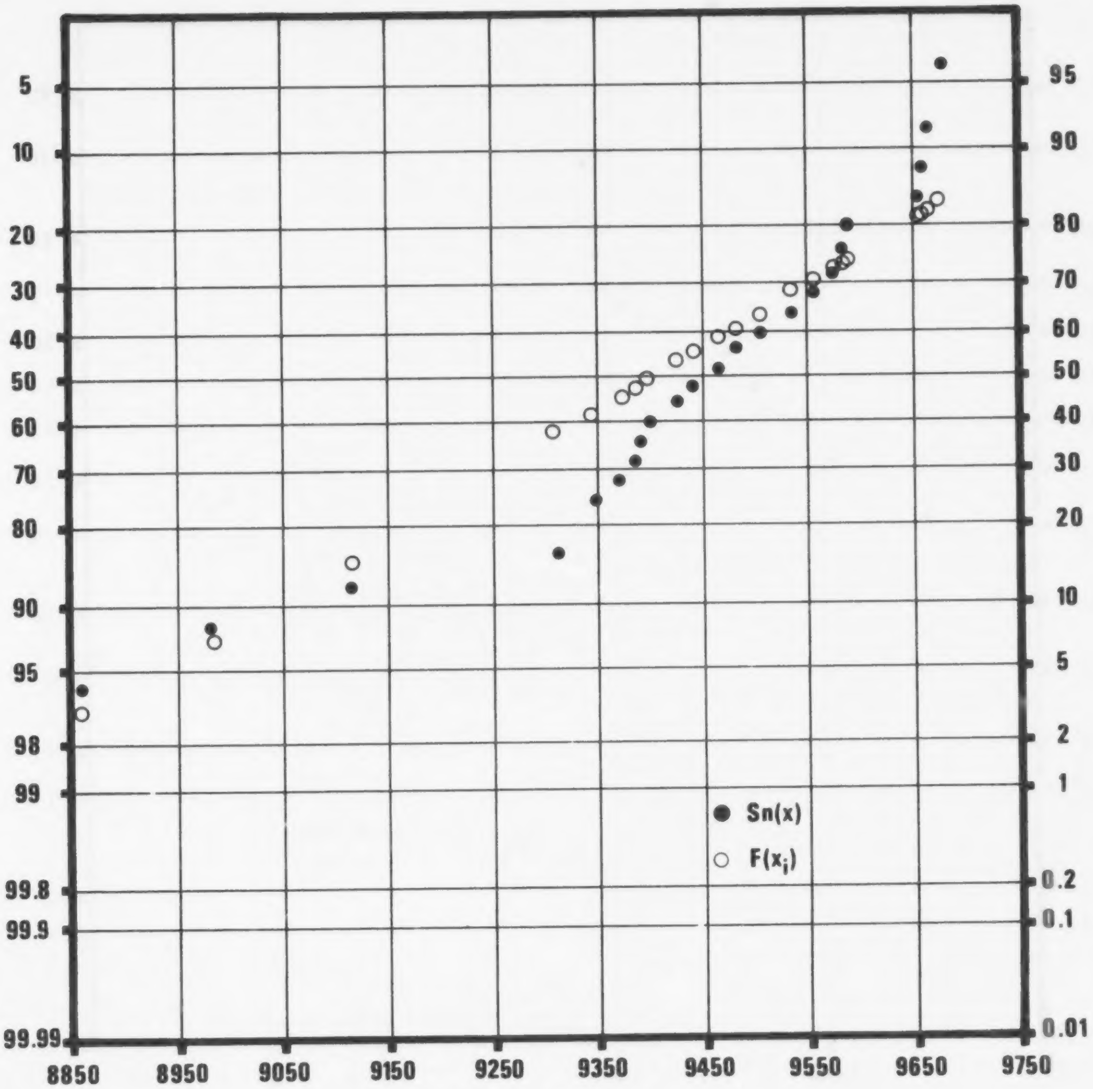

Figure 23. Probability plot for high-energy (1.063 MeV) peak from Bi-207.

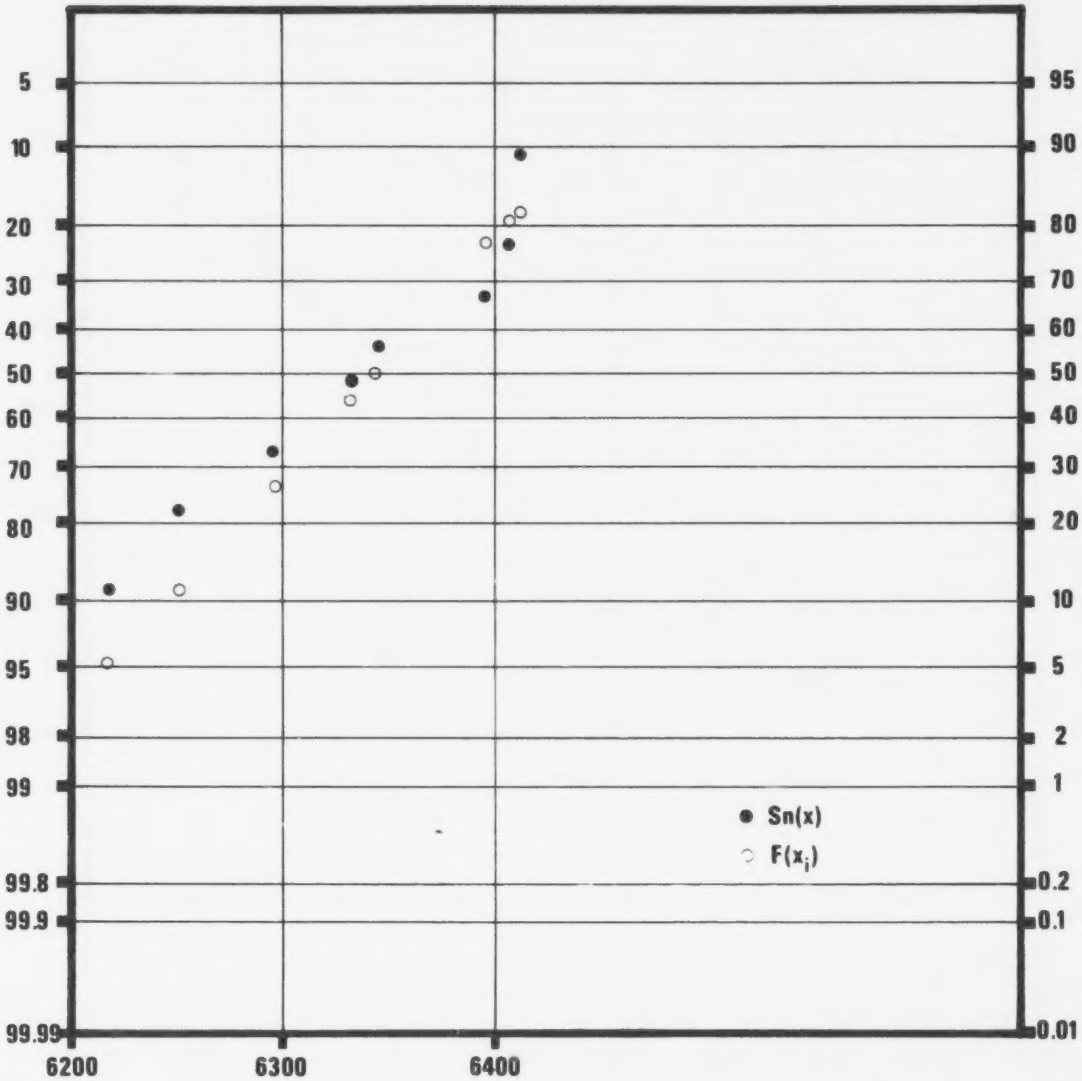

Figure 24. Probability plot for 10-minute background counts measured with a 10.2-cm by 10.2-cm NaI(Tl) detector.

The second column at each table gives the value of $(x_i - m)/\sigma$ for each data point, the third column gives the value $f(x) = (1/\sqrt{2\pi})^{\frac{1}{2}} \exp(-S^2/2)$ and the fourth column gives the probability $F(x_i)$ for each data point. $F(x)$ can be obtained using some modern programmable calculators, or found in standard tables (e.g., C.R.C. Handbook of Chemistry and Physics). For the examples of this section, the values of F(x) are also plotted in Figures 22, 23, and 24.

The test is completed by determining the absolute values

$$D_i = |F_{(x_i)} - S_i(x_i)| \text{ and } D_i' = |F_{(x_i)} - S_{i-1}(x_{i-1})|.$$

The largest value of D_i or D_i' is then compared to the critical values D_α in Table 8. If the maximum D_i or D_i' is less than D_α for the number of determinations taken (n), then the data are acceptable and will not be rejected. If the D_i value is larger than D_α then we know how often the data are falsely rejected.

The maximum value for D in Table 5 is 0.12 which is far below any critical value D_i for $n = 25$ found in Table 8. We conclude that these data, then, are normal. However, the maximum value for D in Table 6 is 0.27 and there is a second value of D equal to 0.26. The critical value of D_α at the 95 percent confidence level for $n = 25$ from Table 8 is 0.27. Thus if we reject these data, we expect to conclude falsely 5 times out of 100 that these data are not normal. To conclude that these data are normal without further measurements requires a great deal of optimism.

From Table 7, the maximum value for D is found to be 0.21, which is much smaller than a critical value D_α for $n = 9$ found in Table 8. Thus it is seen that the instrument is capable of producing normal data on any given day provided the measurements are made fairly rapidly and in a short time period. Needless to say at this point the instrument must also be calibrated daily, even to produce data of dubious validity.

TABLE 8. LIMITING VALUES FOR D_α IN THE KOLMOGOROV-SMIRNOV TEST

Two-Sided Test

α =	0.80	0.90	0.95	0.98	0.99
n = 1	0.900	0.950	0.975	0.990	0.995
2	0.684	0.776	0.842	0.900	0.929
3	0.565	0.636	0.708	0.785	0.829
4	0.493	0.565	0.624	0.689	0.734
5	0.447	0.509	0.563	0.627	0.669
6	0.410	0.468	0.519	0.577	0.617
7	0.381	0.436	0.483	0.538	0.576
8	0.358	0.410	0.454	0.507	0.542
9	0.339	0.387	0.430	0.480	0.513
10	0.323	0.369	0.409	0.457	0.489
11	0.308	0.352	0.391	0.437	0.468
12	0.296	0.338	0.375	0.419	0.449
13	0.285	0.325	0.361	0.404	0.432
14	0.275	0.314	0.349	0.390	0.418
15	0.266	0.304	0.338	0.377	0.404
16	0.258	0.295	0.327	0.366	0.392
17	0.250	0.286	0.318	0.355	0.381
18	0.244	0.279	0.309	0.346	0.371
19	0.237	0.271	0.301	0.337	0.361
20	0.232	0.265	0.294	0.329	0.352
n = 21	0.226	0.259	0.287	0.321	0.344
22	0.221	0.253	0.281	0.314	0.337
23	0.216	0.247	0.275	0.307	0.330
24	0.212	0.242	0.269	0.301	0.323
25	0.208	0.238	0.264	0.295	0.317
26	0.204	0.233	0.259	0.290	0.311
27	0.200	0.229	0.254	0.284	0.305
28	0.197	0.225	0.250	0.279	0.300
29	0.193	0.221	0.246	0.275	0.295
30	0.190	0.218	0.242	0.270	0.290
31	0.187	0.214	0.238	0.266	0.285
32	0.184	0.211	0.234	0.262	0.281
33	0.182	0.208	0.231	0.258	0.277
34	0.179	0.205	0.227	0.254	0.273
35	0.177	0.202	0.224	0.251	0.269
36	0.174	0.199	0.221	0.247	0.265
37	0.172	0.196	0.218	0.244	0.262
38	0.170	0.194	0.215	0.241	0.258
39	0.168	0.191	0.213	0.238	0.255
40	0.165	0.189	0.210	0.235	0.252
Approximation for N > 40	$\frac{1.07}{\sqrt{n}}$	$\frac{1.22}{\sqrt{n}}$	$\frac{1.36}{\sqrt{n}}$	$\frac{1.52}{\sqrt{n}}$	$\frac{1.63}{\sqrt{n}}$

LOWER LIMIT OF DETECTION

Gamma-ray spectrometers may be used to detect and analyze single or multi-radionuclide samples. The randomness of the background count, the randomness of the net sample count, and the similarities of some gamma spectra indicate that there is a gross count below which it is not possible to satisfactorily demonstrate a net count for a particular radionuclide. The net count of a radioactive sample is proportional to sample activity when all other factors pertaining to the detector system and sample are constant. Consequently, there is a limit of sample activity below which it is not possible to satisfactorily demonstrate the presence of a particular radionuclide. The lower limit of detection (LLD) is defined as the smallest amount of sample activity that will yield a net count sufficiently large to imply its presence.

The numerical value for a LLD is not absolute, but depends upon several factors of which the following are principle(20):

1. The preselected statistical risk one is willing to take of concluding falsely a particular sample activity is present (α).

2. The predetermined degree of confidence in assuming that the presence of a particular radionuclide has been detected ($1-\beta$).

3. The similarities and dissimilarities of the background and radionuclide gamma spectra to the spectrum of the particular radionuclide under consideration.

4. The concentration of the radionuclide to be detected and the concentrations of any other radionuclides in the sample.

The simplest case of finding LLD is that in which the gross count in a single channel is the sum of the count of a single radionuclide and the background count. It is assumed that the background and sample count rates occurring in a fixed time are sufficiently large that their distribution can be adequately approximated by a normal distribution having a mean and variance equal to the expected number of counts. The following symbols will be used in this discussion:

S = source strength in counts

γ = calibration constant to convert counts into activity A

$A = \gamma S$ = source activity which may be expressed in terms of pCi or other suitable units

C_B = measured background count

C_{B+S} = measured sample-plus-background count

K_α = value (upper percentile of the standardized normal variate) corresponding to the preselected risk for concluding falsely that activity is present (α) (Table 9)

K_β = value (upper percentile of standardized normal variate) coresponding to the predetermined degree of confidence for detecting the presence of activity ($1 - \beta$) (Table 9)

The LLD is approximately equal to:

$$LLD \simeq \gamma(K_\alpha + K_\beta)\sqrt{2\ C_B} \text{ when } K_\alpha/C_B << 1 \qquad \text{(Eq. 99)}$$

TABLE 9. RISK AND CONFIDENCE VALUES

α	$1-\beta$	K
0.01	0.99	2.327
0.05	0.95	1.645
0.10	0.90	1.282
0.15	0.85	1.036
0.20	0.80	0.842
0.25	0.75	0.675
0.30	0.70	0.524
0.35	0.65	0.385
0.40	0.60	0.253
0.45	0.55	0.126

α is the probability for concluding falsely that activity is present. If we will accept the risk that 10 percent of our measurements of samples without activity will be reported as showing activity, then K = 1.282.

$1-\beta$ is the probability for concluding correctly that activity is present. If we want 95 percent of the measurements of samples containing activity reported as containing activity, then K = 1.645.

Two convenient formulas for approximating an LLD are:

$$LLD \simeq \gamma(K_\alpha + K_\beta)\ (C_{B+S} + C_B)^{\frac{1}{2}} \qquad \text{(Eq. 100)}$$

which may be used when a sample count has been taken near the LLD.

$$LLD \simeq \gamma(K_\alpha + K_\beta)\left(\frac{C_{B+S}}{t^2} + \frac{C_B}{r^2}\right)^{\frac{1}{2}} \qquad \text{(Eq. 101)}$$

which may be used when the counting time, t , for the sample plus background differs from the counting time r , for the background alone. In both formulas, the expressions under the square root sign represent either the estimated standard deviation of the net count or the estimated standard deviation of the net count rate.

Another formula for the LLD can be derived realizing that the standard deviation, S_d, found when the activity of the sample is near the LLD approaches the standard deviation, S_o, when no activity is present. The approximation for the LLD derived from a more vigorous analysis (20) results in:

$$\text{LLD} = K_\alpha S_o + K_\beta S_d \qquad \text{(Eq. 102)}$$

Assuming $S_d \simeq S_o$ the lower limit of detection can be approximated by

$$\text{LLD} \simeq (K_\alpha + K_\beta) S_o \qquad \text{(Eq. 103)}$$

The standard error S_o for a net activity is the root mean square of the standard error of the background. Therefore,

$$S_o = \sqrt{S^2_{\text{sample + background}} + S^2_{\text{background}}} \qquad \text{(Eq. 104)}$$

for very low activity

$$S^2_{\text{sample + background}} \simeq S^2_{\text{background}}$$

and

$$S_o = S_{\text{background}} \sqrt{2}$$

and lower limit of detection becomes

$$\text{LLD} \simeq (K_\alpha + K_\beta) S_b \sqrt{2} \qquad \text{(Eq. 105)}$$

The standard error of an estimated radionuclide concentration parameter depends upon the counting times of the sample and the background, the relationships between the spectrum and of a particular radionuclide and other spectra in the library, the background, and the other radionuclides in the sample.

Three typical counting situations in which the LLD must be considered are:

1. Determining the LLD when the library contains the spectrum of the radionuclide of interest and no other radionuclides are known to be present.

2. Determining the LLD for a particular radionuclide when other radionuclides are included in the library, but do not occur in the sample.

3. Determining the LLD for a particular radionuclide when other known radionuclides in the sample are assumed to be present at fixed levels and the library contains the spectra for all radionuclides present.

The following procedures are used to obtain the LLD for the three preceding cases:

Case 1. (Library contains the radionuclide of interest and no other radionuclides are known to be present.) Obtain a series of background pulse height distributions for the analyzer system to be employed using a blank sample identical to the sample type that will be routinely used. Obtain the average counts in the photopeak area selected to generate the matrix for analysis. For a single radionuclide, the activity can be found by $A = EC$ where A is the activity in some appropriate unit (e.g., picocurie), C is the net count rate, and E is the efficiency (pCi/count per unit time). If no activity is present, the gross count (G) will be

$$\begin{aligned} G &= C.t_c + Bt_c \\ &= Bt_c \end{aligned}$$

and the standard deviation will be

$$\sigma^2 = \frac{\varepsilon^2 \cdot g \cdot c}{t_c} + \frac{B}{t_b}$$

$$\sigma = \sqrt{\frac{\varepsilon^2 B}{t_c} + \frac{B}{t_b}} \qquad \text{(Eq. 106)}$$

and the lower limit of detection will be

$$\text{LLD} = (k_\alpha + k_\beta)\sqrt{\frac{\varepsilon^2 B}{t_c} + \frac{B}{t_b}} \qquad \text{(Eq. 107)}$$

Case 2. (Other radionuclides in the library, but not in the samples.) The procedure is similar to that of Case 1. Let $b_1 \ldots b_n$ be the count rate in each region of interest for a blank sample, and let the activity for each region be given as before

$$C_1 = a_{1_1}N_1 + a_{1_2}N_2 + \ldots + a_{1N}N_n$$

$$C_i = a_{i_1}N_1 + a_{i_2}N_2 + \ldots + a_{in}N_n$$

Now for a given analysis time t_c

$$C_i = a_{i_1}n_1t_c + a_{i_2}n_2t_c + \ldots + a_{in}n_nt_c$$

where n_n represents the count rate. From the discussion on the previous chapter, the standard deviation is given by

$$\begin{aligned} \sigma_i^2 &= a_{i_1}{}^2N_1 + \ldots + a_{in}^2N_n + B_1 + \ldots + B_n \\ &= a_{i_1}{}^2n_1t_c + \ldots + a_{in}^2n_nt + B_1 + \ldots + B_n \end{aligned}$$

If no activity is present in the sample then

$$\sigma_i^2 = a_{i_1}{}^2b_it_c + \ldots + a_{in}{}^2n_nt_c + B_1 + \ldots B_n$$

and the lower limit of detection becomes

$$\mathrm{LLD} \approx (k_\alpha + k_\beta)\sqrt{\frac{a_{i_1}{}^2 b_1}{t_c} + \ldots \frac{a_{in}{}^2 b_n}{t_c} + \frac{b_1}{t_b} + \ldots + \frac{b_n}{t_b}} \qquad \text{(Eq. 108)}$$

Case 3. (Other known radionuclides in sample are present at fixed levels and library contains spectra for all radionuclides present.) The procedure is similar to the preceding cases with the following modifications. A mock sample is prepared to contain fixed concentrations of the nuclides assumed to be present in the sample exclusive of the radionuclide of interest whose concentration must be zero. Again, all interference terms must be included. In this case we must still add the interference from the added radionuclides in the mock sample and a term for the background.

As in case 2 we see that

$$C_i = a_{i_1} N_1 + \ldots + a_{in} N_n$$

and

$$\sigma_i{}^2 = a_{i_1}{}^2 n_1 t_c + \ldots + a_{in}{}^2 n_n t_c + B_1 + \ldots + B_n$$

In this case, however, the n_i will be larger than the background measured in Case 2, and the standard deviation is dependent on the concentration of the radionuclides added to the blank.

Also, the lower limit for detection of one nuclide is dependent on the combination and amount of the rest of the nuclides included in the set. The lower limit of detection is given by

$$\mathrm{LLD} \approx (k_\alpha + k_\beta)\sqrt{\frac{a_{i_1}{}^2 n_1 + \ldots + a_{in}{}^2 n_n}{t_c} + \frac{b_1 + \ldots b_n}{t_b}} \qquad \text{(Eq. 109)}$$

Note that as the number of radionuclides present increases there will be an increase in the size of the standard deviation and in the lower limit of detection. The amount of the increase will depend upon the multiple correlation of the spectrum for the radionuclide of interest with the radionuclides of the added library spectra.

Pasternak and Harley (20) have made a thorough review of the theoretical aspects of detection limits for radionuclides in multicomponent samples. Their experimental data were collected by a 20- by 10-cm sodium iodide detector and a 400-channel analyzer located in a room shielded with 11 cm of steel. The estimated limits for detecting ^{65}Zn, ^{60}Co, and ^{137}Cs in single radionuclide samples were as low as 15 to 31 picocuries for 30-minute counts from which 30-minute background counts were subtracted, and 10 to 22 picocuries for 30-minute counts from which backgrounds obtained from 1000-minute counts were substracted. The variation resulted principally from the effects of gamma peaks in the background spectra. When any two of the aforementioned radionuclides or all three occurred in a sample, the precision of detection near the lower limits was found to be materially less. Furthermore, there are wide variations in the lower limits of detection for different radionuclide mixtures because their spectra vary in the amounts of overlapping in the regions of spectral interest.

The detection limits for radionuclides which had little spectral interference from other radionuclides were not materially affected in samples having three nuclides in the library. When the library contained 10 radionuclides, the lower limits of detection increased markedly over a sample (as much as 5 to 10 times) which had only 3 radionuclides. Lower limits of detection for radioisotopes having a low yield per nuclear event were much higher than those which had a higher yield. Beryllium-7 for example, has a principal spectral peak produced by a photon yield of only 10 percent for each nuclear event. By contrast, ^{65}Zn has a principal spectral peak produced by a photon yield of 49 percent and ^{60}Co has a photon yield of 100 percent for each of its two spectral peaks.

REFERENCES

1. Crouch, D. F., and R. L. Heath. 1963. Routine Testing and Calibration Procedures for Multichannel Pulse Analyzers and Gamma-Ray Spectrometers. 22nd Edition. U.S. Atomic Energy Commission Research and Development Report, Physics, IDO-16923. TID-4500, 25 pp.

2. Heath, R. L., R. G. Helmer, L. A. Schmittroth and G. A. Gazier. 1965. The Calculation of Gamma-Ray Shapes for Sodium Iodide Spectrometers. U.S. Atomic Energy Commission Research and Development Report, Physics. Computer Program and Experimental Problems. IDO-17017. 158 pp.

3. Heath, R. L. 1964. Scintillation Spectrometry Gamma-Ray Spectrum Catalogue. 2nd Edition. U.S. Atomic Energy Commission Research and Development Report. IDO-16880-1. Vol. 2 of 2. 364 pp.

4. Ibid. 1964. IDO-16880-2. Vol. 2 of 2. 264 pp.

5. Douglas, Geneva S., Editor. 1967. Radioassay Procedures for Environmental Samples. Public Health Service publication No. 999-RH-27. Washington, D.C. 520 pp.

6. Crouthamel, E. C. 1970. Applied Gamma-Ray Spectrometry. 2nd Edition. (Revised by F. Adams and R. Dams). Pergamon Press, New York, New York. 753 pp.

7. Siegbahn, Kai, Editor. 1965. Alpha-, Beta-, and Gamma-Ray Spectroscopy. North Holland Publishing Co., Amsterdam, The Netherlands. Vol. 1. 862 pp.

8. National Environmental Research Center. 1975. Radioactivity Standards Distribution Program. National Environmental Research Center, Las Vegas, Nevada. EPA-680/4-75-002a. 19+ pp.

9. Environmental Monitoring and Support Laboratory. 1975. Environmental Radioactivity Laboratory Intercomparison Studies Program. Environmental Monitoring and Support Laboratory, Las Vegas, Nevada. EPA-680/4-75-002b.

10. Lederer, C. M., J. M. Hollander and I. Perlman. 1967. Table of Isotopes. 6th Edition. John Wiley & Sons. New York, New York. 594 pp.

11. Nuclear Data Group, Editors. 1965-76. Nuclear Data Sheets (successor in part to Nuclear Data, U.S. ISSN 0029-5477). Academic Press, New York, New York.

12. Martin, M. J., Editor. 1976. Nuclear Decay Data for Selected Radionuclides. Oak Ridge National Laboratory. ORNL-5114, VC-34c-Nuclear Physics. 54 pp.

13. Way, Katherine, Editor. 1966-76. Nuclear Data Tables. Sec. A. (Successor in part to Nuclear Data, U.S. ISSN 0029-5477). Academic Press, New York, New York.

14. Nuclear Data Group, Editors. 1975. Nuclear Data Sheets. Academic Press, New York, New York. Vol. 15, No. 3, p. 350.

15. Storm, Ellery, and Harvey I. Israel. 1967. Photon Cross Sections from 0.001 to 100 MeV for Elements 1 Through 100. Los Alamos Scientific Laboratory. LA-3753, UC-34, Physics. TID-4500. 257 pp.

16. Kodt, L. 1973. "Radionuclide metrology," in *Nucl. Instrum. Methods.* Siegbahn, K. Editor. North Holland Publishing Co., Amsterdam, The Netherlands. Vol. 112, pp. 245-251.

17. Energy Research and Development Administration. "Standard Nuclear Instrument Modules." TID-20893(Rev.3, 1969). Superintendent of Documents, U.S. Government Printing Office, Washington, D.C.

18. Evans, Robley D. 1975. The Atomic Nucleus. McGraw-Hill Book Company, Inc. New York, New York. 972 pp.

19. Siegel, Sidney. 1956. Nonparametric Statistics for the Behavioral Sciences. McGraw-Hill Book Company, Inc. New York, New York. 312 pp.

20. Pasternak, B. S., and H. H. Harley. 1971. *Nucl. Instrum. Methods.* North Holland Publishing Co., Amsterdam, The Netherlands. Vol. 91. pp. 530-540.

21. Way, Katherine, Editor. 1970. Nuclear Data Tables. Academic Press, New York, New York. Sec. A., Vol. 8, Nos. 1-2.

22. Nuclear Data Group, Editors. 1970. Nuclear Data Sheets. Academic Press, New York, New York. Sec. B., Vol. 4, Nos. 3-4.

23. Ibid. 1971. Sec. B, Volume 6, No. 1.

24. Ibid. 1971. Sec. B, Volume 5, No. 5.

25. Ibid. 1974. Volume 11, No. 4.

26. Ibid. 1975. Volume 15, No. 2.

27. Ibid. 1975. Volume 14, No. 4.

28. Ibid. 1972. Sec. B, Volume 8, No. 5.

29. Ibid. 1971. Sec. B, Volume 5, No. 3.

30. Ibid. 1971. Sec. B, Volume 6, No. 3.

31. Ibid. 1970. Sec. B, Volume 4, No. 6.

32. Way, Katherine, Editor. 1974. Atomic Data and Nuclear Data Tables. Academic Press, New York, New York. Vol. 13, Nos. 2-3.

33. Nuclear Data Group, Editors. 1977. Nuclear Data Sheets. Academic Press, New York, New York. Vol. 20, No. 2.

34. Ibid. 1976. Volume 17, No. 3.

35. Ibid. 1972. Sec. B, Volume 8, No. 2.

36. Ibid. 1971. Sec. B, Volume 5, No. 3.

37. Ibid. 1971. Sec. B, Volume 5, No. 6.

38. Amersham Searle Corporation. 1975. Research Products Catalogue. Arlington Heights, Illinois.

BIBLIOGRAPHY

Hodgman, Charles D., Editor. 1959. C.R.C. Standard Mathematical Tables. 12th Edition. Chemical Rubber Publishing Company. Cleveland, Ohio. 525 525 pp.

International Atomic Emergency Agency. 1960. Metrology of Nuclides. International Atomic Energy Agency. Vienna, Austria. 472 pp.

International Atomic Energy Agency. 1967. Standardization of Radionuclides. International Atomic Energy Agency. Vienna, Austria. 742 pp.

National Bureau of Standards. 1961. A Manual of Radioactivity Procedures. NBS Handbook No. 80. U.S. Department of Commerce. Washington, D.C. 159 pp.

National Bureau of Standards. 1963. Radioactivity Recommendations of the International Commission on Radiologic Units and Measurements. NBS Handbook No. 86. U.S. Department of Commerce. Washington, D.C. 53 pp.

National Center for Radiological Health. 1967. Radionuclide Analysis by Gamma Spectroscopy. U.S. Department of Health, Education and Welfare. Rockville, Maryland. 373+ pp.

Putnam, Marie, R. G. Helmer, D. H. Gipson, and R. L. Heath. 1965. A Nonlinear Least-squares program for the Determination of Parameters of Photopeaks by the Use of a Modified Gaussian function. U.S. Atomic Energy Commission Research and Development Report, Physics. IDO-17016. TID-4500 (43rd Edition). 85 pp.

Stevenson, P. C. 1966. Processing of Counting Data. Subcommittee on Radiochemistry. National Academy of Sciences-National Research Council. National Bureau of Standards. U.S. Department of Commerce. Clearinghouse for Federal Scientific and Technical Information. Springfield, Virginia. 167 pp.

Subcommittee on Radiochemistry and the Subcommittee on the Use of Radioactivity Standards. 1974. User's Guide for Radioactivity Standards. Technical Information Center, Office of Information Services, U.S. Atomic Energy Commission. NAS-NS-3115. 85 pp.

APPENDIX A. BASIC DATA FOR SELECTED GAMMA RAY-EMITTING RADIONUCLIDES

Radionuclide	Half-Life	Ref	Energy of Principal Gamma Ray (MeV)	Gamma-Ray Intensity* F(%)	Ref	Remarks
Be-7	53.3 d	21	0.477	10.3	21	
Na-22	2.602 y	12	0.511	180.58	12	
			1.274	99.95	21	
K-40	1.28 × 10^9 y	21	1.461	10.7	21	
			†1.461	†(3.30 γ/s/g of potassium)	21	
Sc-46	83.8 d	12	0.889	100	22	
			1.120	100		
Cr-51	27.704 d	12	0.320	9.80	12	
Mn-54	312.5 d	12	0.835	99.978	21	
			0.511		21	
Co-56	77.3 d	21	0.847	99.974	21	
			1.038	12.9		
			1.238	70		
			1.771	15.6		
			2.035	7.4		
			2.599	16.8		
			3.254	7.6		
Co-57	270.9 d	12	0.122	85.6	12	
			0.136	10.6		
Co-58	70.8 d	12	0.511	30	12	
			0.811	99.45		
Fe-59	44.6 d	12	1.099	56.1	12	
			1.292	43.6		

APPENDIX A. BASIC DATA FOR SELECTED GAMMA RAY-EMITTING RADIONUCLIDES (continued)

Radionuclide	Half-Life	Ref	Energy of Principal Gamma Ray (MeV)	Gamma-Ray Intensity* F(%)	Ref	Remarks
Co-60	5.271 y	12	1.173	99.90	12	
			1.333	100		
Zn-65	244.1 d	12	0.511	2.92	12	
			1.115	50.75		
Se-75	120 d	12	0.121	16.7	12	
			0.136	56.8		
			0.265	59.5		
			0.280	25.1		
			0.401	11.8		
Sr-85	64.85 d	12	0.514	98.0	12	
Y-88	107 d	12	0.898	93.4	12	
			1.836	99.35		
Zr-95	65.5 d	21	0.724	43.5	21	
			0.757	54.3		
Nb-95	35.1 d	21	0.755	99.8	21	The ratio of Nb-95 activity to that of its parent, Zr-95, is given as a function of time, t, by 2.155[1 - exp (-0.00916t)] where t is in days and the Nb-95 activity is zero at t = 0.
Ru-103	39.35 d	12	0.497	86.4	12	
			0.610	5.3		

APPENDIX A. BASIC DATA FOR SELECTED GAMMA RAY-EMITTING RADIONUCLIDES (continued)

Radionuclide	Half-Life	Ref	Energy of Principal Gamma Ray (MeV)	Gamma-Ray Intensity* F(%)	Ref	Remarks
Ru-106—Rh-106	369 d	21	0.512	20.6	21	Rh-106 is assumed to be in equilibrium with Ru-106.
			0.622	9.94		
Cd-109	453 d	12	0.088	3.72	12	
Ag-110m	250.8 d	12	0.658	94.6	12	
			0.678	10.6		
			0.707	16.4		
			0.764	22.4		
			0.885	73.0		
			0.937	34.4		
			1.384	24.7		
			1.505	13.3		
Sn-113—In-113m	114.9 d	12	0.392	64.9	12	In-113 is assumed to be in equilibrium with Sn-113 after 17 hours.
Sb-124	60.2 d	12	0.603	97.9	12	
			0.646	7.21		
			0.723	11.26		
			1.691	48.8		
			2.091	5.58		
Sb-125	2.77 y	21	0.176	6.3	21	
			0.428	29.6		
			0.464	10.0		
			0.601	18.4		
			0.607	5.2		
			0.636	11.2		
I-131	8.04 d	12	0.284	6.06	12	
			0.364	81.2		
			0.637	7.27		

APPENDIX A. BASIC DATA FOR SELECTED GAMMA RAY-EMITTING RADIONUCLIDES (continued)

Radionuclide	Half-Life	Ref	Energy of Principal Gamma Ray (MeV)	Gamma-Ray Intensity* F(%)	Ref	Remarks
Ba-133	10.5 y	12	0.276	7.3	12	
			0.302	18.66		
			0.356	62.4		
			0.382	8.86		
Cs-134	2.062 y	12	0.563	8.38	12	
			0.569	15.43		
			0.605	97.6		
			0.796	85.4		
			0.802	8.73		
Cs-137	30.0 y	12	0.662	85.0	12	
Ce-139	137.65 d	12	0.165	80.0	12	
Ba-140	12.8 d	21	0.163	6.2	21	The ratio of La-140 activity to that of its parent, Ba-140, is given as a function of time, t, by 1.153 [1-exp -(0.516t)] where t is in days and the La-140 activity is taken to be zero at t = 0.
			0.305	4.5		
			0.424	3.2		
			0.438	2.1		
			0.538	23.8		
La-140	40.27 h	21	0.329	21	21	
			0.433	3.3		
			0.487	45		
			0.752	4.4		
			0.816	23.1		
			0.868	5.5		
			0.920	2.5		
			0.925	6.9		
			1.597	95.6		
			2.522	3.3		
Ce-141	32.50 d	12	0.145	48.0	12	

APPENDIX A. BASIC DATA FOR SELECTED GAMMA RAY-EMITTING RADIONUCLIDES (continued)

Radionuclide	Half-Life	Ref	Energy of Principal Gamma Ray (MeV)	Gamma-Ray Intensity* F(%)	Ref	Remarks
Ce-144	284 d	21	0.134	10.8	21	
Ta-182	115 d	25	0.100	40.2	25	
			0.152	20.5		
			0.222	21.6		
			0.229	10.4		
			0.264	10.4		
			1.121	100		
			1.189	47		
			1.221	78.3		
			1.230	33.1		
Au-195	183 d	26	0.099	12	26	
Hg-203	46.59 d	12	0.279	81.5	12	
Bi-207	38 y	12	0.570	97.8	12	
			1.064	74.3		
			1.770	7.3		
Ra-226	1600 y	21	0.186	3.3	21	ΦEquilibrium intensities (after 38 days with no loss of radon)
			0.295	18Φ		
			0.351	35Φ		
			0.609	43Φ		
			0.120	14Φ		
			1.765	16.6Φ		
U-235	7.1 × 10^8 y	28	0.143	1.7Φ	28	ΦNormalized to give 54 photons/100 α for 0.1861 γ
			0.163	4.6Φ		
			0.186	54Φ		
			0.205	5.0		
U-238	4.49 × 10^9 y	29				

APPENDIX A. BASIC DATA FOR SELECTED GAMMA RAY-EMITTING RADIONUCLIDES (continued)

Radionuclide	Half-Life	Ref	Energy of Principal Gamma Ray (MeV)	Gamma-Ray Intensity* F(%)	Ref	Remarks
Th-232	1.405×10^{10} y	21	0.239	40 Φ	21	*Equilibrium intensity
			0.337	11 Φ		
			0.510	∿ 8.0 Φ		
			0.583	30 Φ		
			0.727	7.1 Φ		
			0.909	30 Φ		
			0.967	27 Φ		
			1.596	5.6 Φ		
			2.615	35.93Φ		
Am-241	433 y	21	0.0596	35.3	21	

* Intensity is measured as gamma rays emitted per disintegration.
d - day
h - hour
y - year

APPENDIX B. THORIUM-232 SERIES DECAY DATA

Nuclide and Half-Life	Type of Decay	Reference	Particle Energy (MeV)	Transition Probability (%)	Electromagnetic Transition Photon energy (MeV)	Electromagnetic Transition Photons emitted (%)
Thorium-232 1.405 × 10^{10} y	α	33	3.830	0.20	0.591	0.15
			3.953	23.3		
			4.010	77.3		
Radium-228 5.75 y	β^-	34	0.046	100		
Actinium-228 6.13 h		34	0.45	4.9	0.057	0.5
			0.49	5.6	0.099	1.4
			0.62	5.7	0.129	2.9
			0.99	7.3	0.154	1.0
			1.02	4.0	0.209	4.6
			1.12	6.5	0.270	3.8
			1.17	33	0.328	3.4
			1.76	20	0.338	12.
			2.10	13	0.409	2.2
					0.463	4.6
					0.562	1.
					0.727	0.8
					0.755	1.1
					0.772	1.6
					0.782	0.5
					0.794	4.8
					0.830	0.6
					0.835	1.8
					0.840	1.
					0.904	0.9
					0.911	29.
					0.964	5.5
					0.986	17.
					1.247	0.6
					1.459	1.
					1.495	1.
					1.501	0.6
					1.580	0.7
					1.587	3.7
					1.630	1.9
					1.638	0.5

APPENDIX B. THORIUM-232 SERIES DECAY DATA (continued)

Nuclide and Half-Life	Type of Decay	Reference	Particle Energy (MeV)	Transition Probability (%)	Electromagnetic Transition	
					Photon energy (MeV)	Photons emitted (%)
Thorium-228	α	34	5.340	27	0.084	1.2
1.913 y			5.423	73	0.131	0.11
					0.166	0.08
					0.216	0.27
Radium-224	α	34	5.449	4.9	0.241	3.9
3.66 d			5.685	95.1		
Radon-220	α	34	6.288	100	0.550	0.1
55.6 s						
Polonium-216	α	34	6.778	100		
0.15 s						
Lead-212	β^-	35	0.155	5.1	0.115	0.6
10.64 h			0.332	83	0.239	44.9
			0.571	13	0.300	3.4
Bismuth-212	α†	35	6.090	26.8	0.039	1
60.55 min			6.051	70.2	0.727	6.6
(α to ^{208}Tl is 35.93%)			5.768	1.67	0.785	1.12
			5.607	1.12	1.620	1.5
	β^-‡		0.085	5		
(β^- to ^{212}Po is 64.07%)			0.445	1		
			0.630	3		
			0.738	2		
			1.524	7		
			2.251	86		
Polonium-212	α	35	8.785	100		
0.305 μs						
Thallium-208			0.64	4.5	0.277	6.9
3.07 min			1.032	2.7	0.511	23.
			1.285	24	0.583	86.
			1.518	21	0.736	1.8
			1.795	50	0.860	12.3
					2.615	100.

† Relative alpha intensity per 100 alpha decays

‡ Relative beta intensity per 100 beta decays

NOTE: Percentages relate to the disintegrations of the individual nuclides. Complete decay schemes are available in the Nuclear Data Sheets.

APPENDIX C. URANIUM-238 SERIES DECAY DATA

Nuclide and Half-Life	Type of Decay	Reference	Particle Energy (MeV)	Transition Probability (%)	Electromagnetic Transition	
					Photon energy (MeV)	Photons emitted (%)
Uranium-238	α	31	4.195	77		
4.49×10^9 y			4.145	23		
Thorium-234	β^-	31	0.100	12	0.063	5.7
24.1 d			0.101	21	0.092	3.2
			0.193	67	0.093	3.6
Protactinium-234		31	2.30	90	0.767	0.2
1.17 min	β^-		1.50	9	1.001	0.6
			0.58	1		
Uranium-234	α	31	4.773	72.5	0.053	0.12
2.48×10^5 y			4.723	27.5	0.121	0.04
Thorium-230	α	33	4.687	76.3	0.068	0.4
7.7×10^4 y			4.621	23.4		
Radium-226	α	33	4.602	5.5	0.186	3.3
1600 y			4.784	94.5		
Radon-222	α	21	5.486	100		
3.824 d						
Polonium-218	α	21	6.000	~100		
3.05 min						
Lead-214	β^-	21	0.20	2.2	0.242	7.4
26.8 min			0.51	1.3	0.295	18
			0.69	46	0.352	35
			0.75	43		
			1.04	7		
Bismuth-214	β^-	21	0.82	2.9	0.609	43
19.8 min			1.08	6.6	0.768	4.6
			1.15	4.9	0.806	1.2
					0.934	3.1
			1.27	4.5	1.112	14
			1.39	1.6	1.155	1.7
			1.43	8.7	1.238	6.4
			1.51	18	1.2811	1.6

APPENDIX C. URANIUM-238 SERIES DECAY DATA (continued)

Nuclide and Half-Life	Type of Decay	Reference	Particle Transition		Electromagnetic Transition	
			Energy (MeV)	Probability (%)	Photon energy (MeV)	Photons emitted (%)
Bismuth-214(continued)			1.55	17	1.3778	4.6
					1.3854	1.
			1.62	1.2	1.4017	1.7
			1.74	3.5	1.4080	2.8
			1.86	1.0	1.5095	2.2
					1.723	3.2
			1.90	8.6	1.7647	16.6
			3.28	19	1.8477	2.2
					2.119	1.3
					2.204	5.4
					2.448	1.77
Polonium-214 162 μs	α	21	7.688	100		
Lead-210 22.3 y	β^-	37	0.017	80	0.046	4.1
			0.061	20		
Bismuth-210 5.012 d	α	37	4.697	1.3×10^{-4}		
	β^-		1.161	~100		
Polonium-210 138.38 d	α	37	5.3048	~100		

NOTE: Percentages relate to the disintegrations of the individual nuclides. Complete decay schemes are available in the Nuclear Data Sheets.

APPENDIX D. URANIUM-235 SERIES DECAY DATA

Nuclide and Half-Life	Type of Decay	Reference	Particle Energy (MeV)	Transition Probability (%)	Electromagnetic Transition Photon energy (MeV)	Electromagnetic Transition Photons emitted (%)
Uranium-235	α	30			0.109	2.5
7.1×10^{8} y					0.144	11
					0.163	5
			4.598	4	0.185	54
			4.556	3	0.202	5
			4.502	1.4		
			4.444	1.5		
			4.430	1.5		
			4.417	2		
			4.398	56		
			4.374	6		
			4.368	12		
			4.345	1		
			4.325	3		
			4.216	6		
Thorium-231	β^-	30	0.140	2	0.026	12
25.52 h			0.203	11	0.084	5.1
			0.213	1.6		
			0.298	~85		
Protactinium-231		30	5.058	11	0.0273	7
3.248×10^{4} y	α		0.27	20	0.283	1.6
			5.027	25.4		
			5.013		0.300	2.3
			4.986	1.4	0.303	2.3
			4.950	22.8	0.330	1.3
			4.933	3	0.407	3.6
			4.851	1.4		
			4.733	8.4		
			4.712	1		
			4.680	1.5		
Actinium-227	α	38	4.938	0.5		
21.8 y			4.951	0.7		
	β^-		0.019	~10		
			0.034	~35		
			0.044	~54		

APPENDIX D. URANIUM-235 SERIES DECAY DATA (continued)

Nuclide and Half-Life	Type of Decay	Reference	Particle Energy (MeV)	Transition Probability (%)	Electromagnetic Transition	
					Photon energy (MeV)	Photons emitted (%)
Thorium-227	α	38	5.707	8.2		
18.5 d			5.712	4.9	0.050	~10
			5.755	20.3	0.236	12.5
			5.976	23.4	0.256	6.3
			6.037	24.5		
Francium-223	β^-	38	0.78	2.7	0.050	43
22 min			0.914	15.5	0.080	10.8
			1.069	12.5	0.205	1.4
			1.099	68	0.235	4.3
Radium-223	α	38	5.534	9.2	0.122	~1
11.4 d			5.603	24.2	0.144	~3
			5.712	52.5	0.154	~5
			Others	14.1	0.270	~14
					0.324	~3
					0.338	~2.5
Radon-219	α	38	6.423	7.5	0.271	9.9
4.0 s			6.551	11.5	0.402	6.5
			6.817	81		
Polonium-215	α	38	7.384	100		
1.78 ms						
Lead-211	β^-	29	0.544	5	0.405	3.8
36.1 min			0.971	1.4	0.427	1.8
			1.376	93	0.832	3.6
Bismuth-211	α	29	6.622	84	0.351	13.3
2.13 min			6.277	16		
Thallium-207	β^-	29	1.431	~100	0.898	~0.27
4.77 min						

NOTE: Percentages relate to the disintegrations of the individual nuclides. Complete decay schemes are available in the Nuclear Data Sheets.

APPENDIX E. PULSE HEIGHT SPECTRA OF SELECTED RADIONUCLIDES

The net pulse height spectra plotted in the figures of Appendix E were obtained using a 10.2-cm by 10.2-cm NaI(Tl) crystal. The energy calibration of the spectrometer system was either 10 or 20 keV per channel, as indicated in each figure title. Spectra marked with an asterisk were obtained using a NaI(Tl) well crystal.

Figure		Page
E-1.	Beryllium-7 net pulse height spectrum calibrated at 10 keV per channel.	103
E-2.	Sodium-22 spectrum with an energy calibration of 10 keV per channel.	104
E-3.	Potassium-40 spectrum calibrated at 10 keV per channel.	105
E-4.	Scandium-46 spectrum calibrated at 10 keV per channel.	106
E-5.	Scandium-46 spectrum calibrated at 20 keV per channel.*	107
E-6.	Chromium-51 spectrum calibrated at 10 keV per channel.	108
E-7.	Manganese-54 spectrum calibrated at 10 keV per channel.	109
E-8.	Cobalt-56 spectrum calibrated at 20 keV per channel.	110
E-9.	Cobalt-57 spectrum calibrated at 10 keV per channel.	111
E-10.	Cobalt-58 spectrum calibrated at 10 keV per channel.	112
E-11.	Cobalt-58 spectrum calibrated at 10 keV per channel.*	113
E-12.	Iron-59 spectrum calibrated at 10 keV per channel.	114
E-13.	Cobalt-60 spectrum calibrated at 10 keV per channel.	115
E-14.	Cobalt-60 spectrum calibrated at 20 keV per channel.*	116
E-15.	Zinc-65 spectrum calibrated at 10 keV per channel.	117
E-16.	Selenium-75 spectrum calibrated at 10 keV per channel.	118
E-17.	Strontium-85 spectrum calibrated at 10 keV per channel.	119
E-18.	Yttrium-88 spectrum calibrated at 20 keV per channel.*	120
E-19.	Zirconium-95 spectrum calibrated at 10 keV per channel.	121
E-20.	Niobium-95 spectrum calibrated at 10 keV per channel.	122
E-21.	Ruthenium-103 spectrum calibrated at 10 keV per channel.	123
E-22.	Ruthenium-106 spectrum calibrated at 10 keV per channel.	124
E-23.	Cadmium-109 spectrum calibrated at 10 keV per channel.	125

APPENDIX E. PULSE HEIGHT SPECTRA OF SELECTED RADIONUCLIDES (continued)

Figure | Page

E-24. Silver-110m spectrum calibrated at 10 keV per channel. 126
E-25. Silver-110m spectrum calibrated at 20 keV per channel.* 127
E-26. Tin-113 spectrum calibrated at 10 keV per channel. 128
E-27. Antimony-124 spectrum calibrated at 10 keV per channel. 129
E-28. Antimony-125 spectrum calibrated at 10 keV per channel. 130
E-29. Iodine-131 spectrum calibrated at 10 keV per channel. 131
E-30. Barium-133 spectrum calibrated at 10 keV per channel. 132
E-31. Cesium-134 spectrum calibrated at 10 keV per channel. 133
E-32. Cesium-134 spectrum calibrated at 20 keV per channel.* 134
E-33. Cesium-137 spectrum calibrated at 10 keV per channel. 135
E-34. Cerium-139 spectrum calibrated at 10 keV per channel. 136
E-35. Barium-140 spectrum calibrated at 10 keV per channel. 137
E-36. Cerium-141 spectrum calibrated at 10 keV per channel. 138
E-37. Cerium-144 spectrum calibrated at 10 keV per channel. 139
E-38. Gold-195 spectrum calibrated at 10 keV per channel. 140
E-39. Mercury-203 spectrum calibrated at 10 keV per channel. 141
E-40. Bismuth-207 spectrum calibrated at 10 keV per channel. 142
E-41. Radium-226 spectrum calibrated at 10 keV per channel. 143
E-42. Natural uranium spectrum calibrated at 10 keV per channel. 144
E-43. Thorium-232 spectrum calibrated at 10 keV per channel. 145
E-44. Americium-241 spectrum calibrated at 10 keV per channel. 146
E-45. Background spectrum calibrated at 10 keV per channel. 147

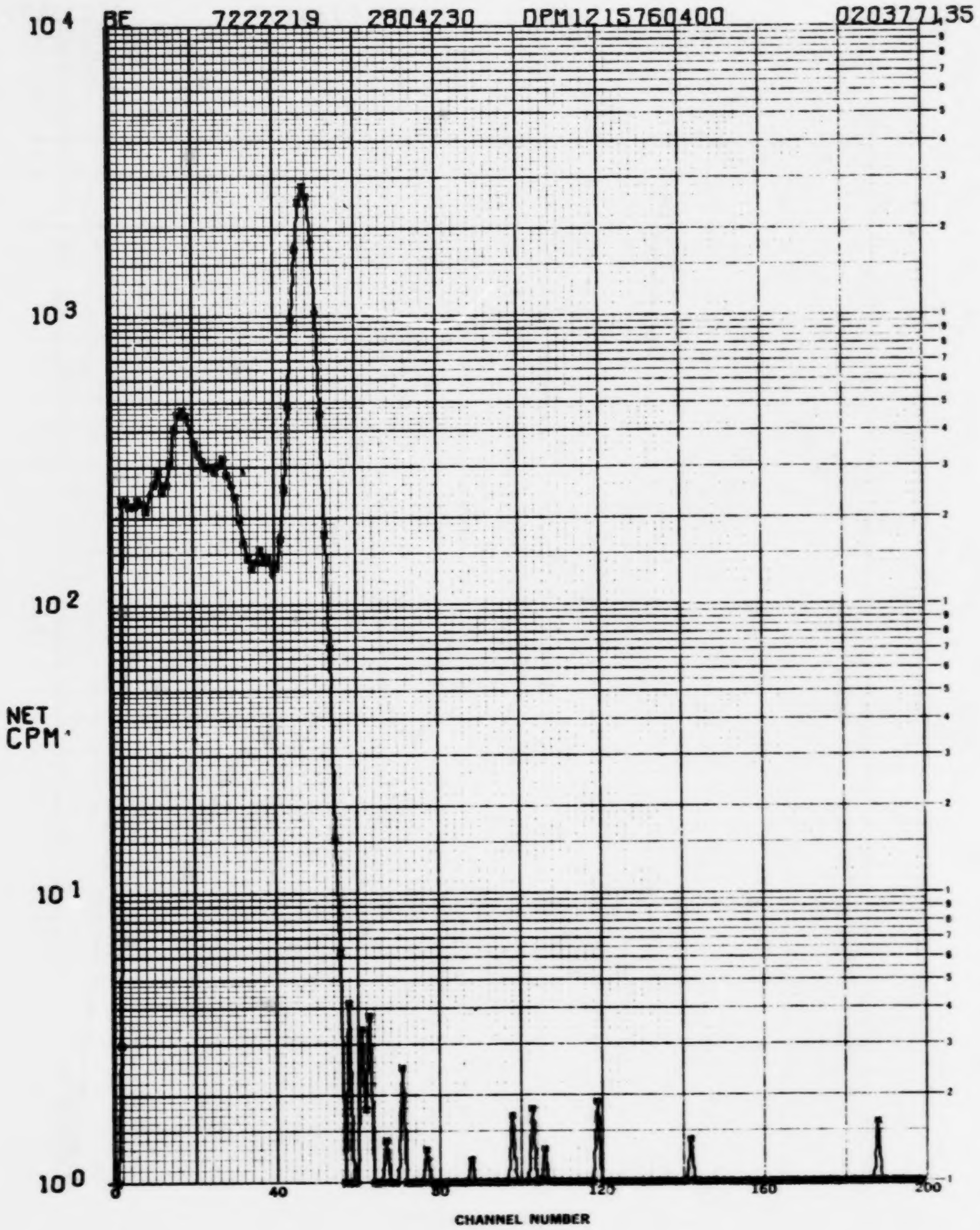

Figure E-1. Beryllium-7 net pulse height spectrum calibrated at 10 keV per channel.

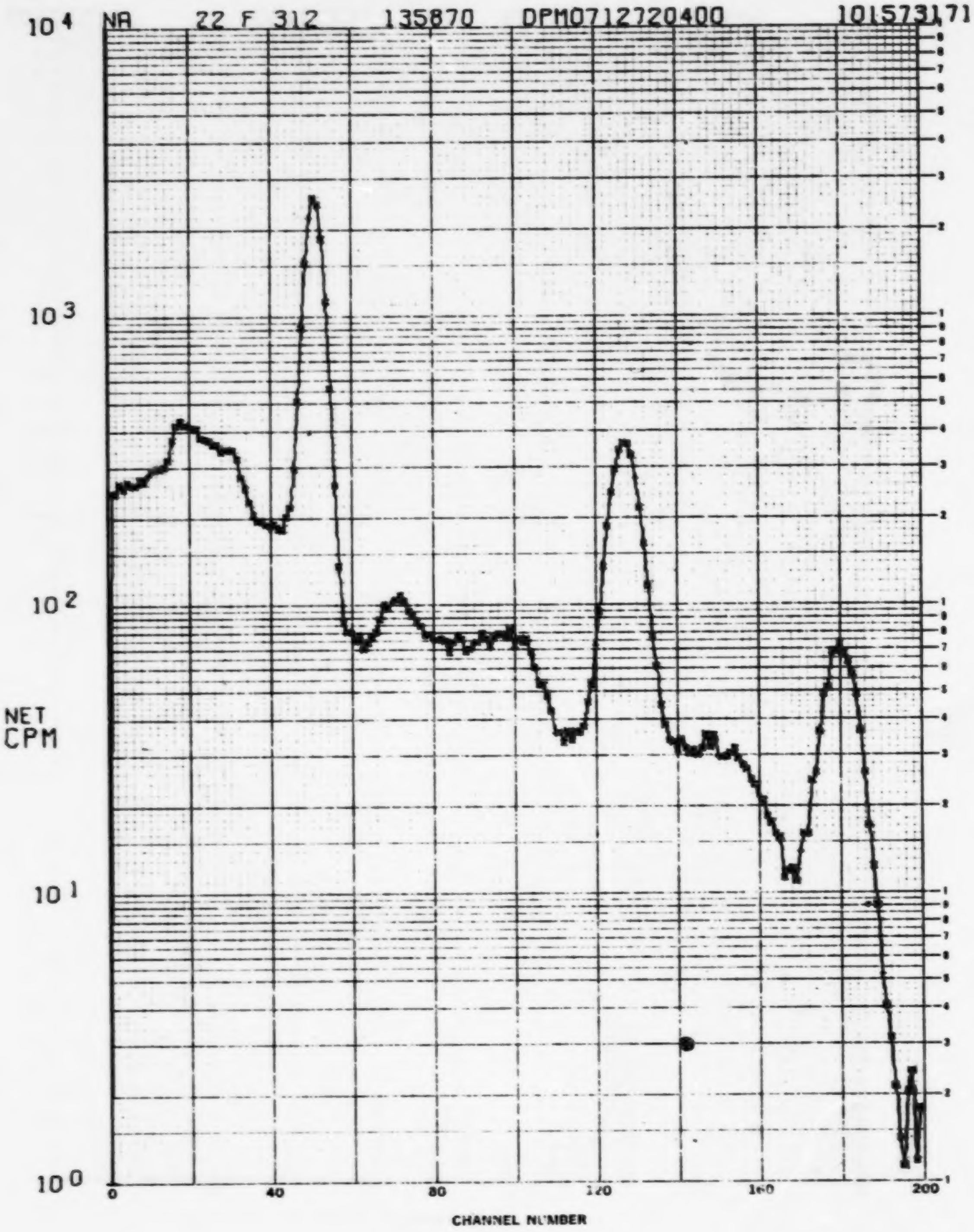

Figure E-2. Sodium-22 spectrum with an energy calibration of 10 keV per channel.

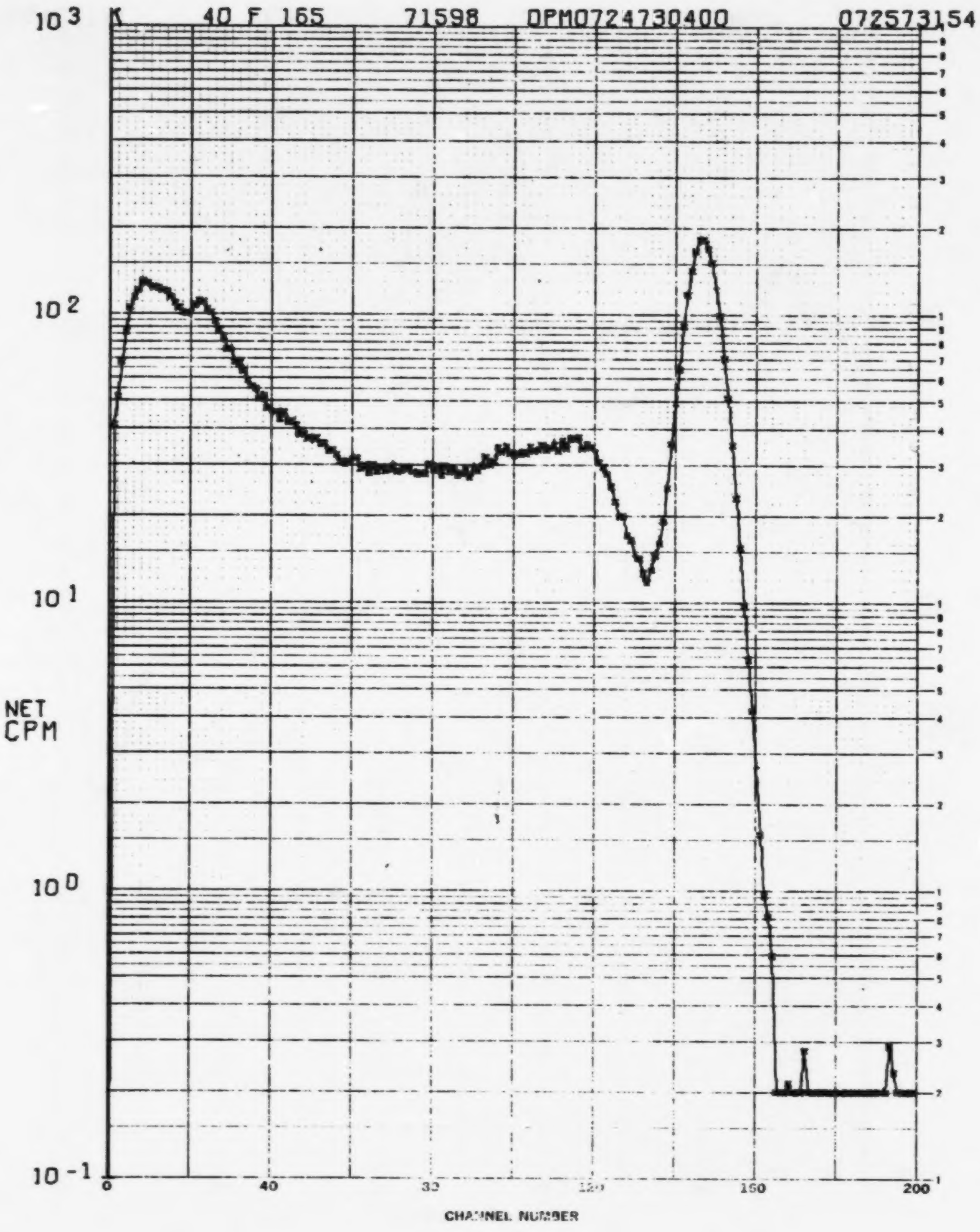

Figure E-3. Potassium-40 spectrum calibrated at 10 keV per channel.

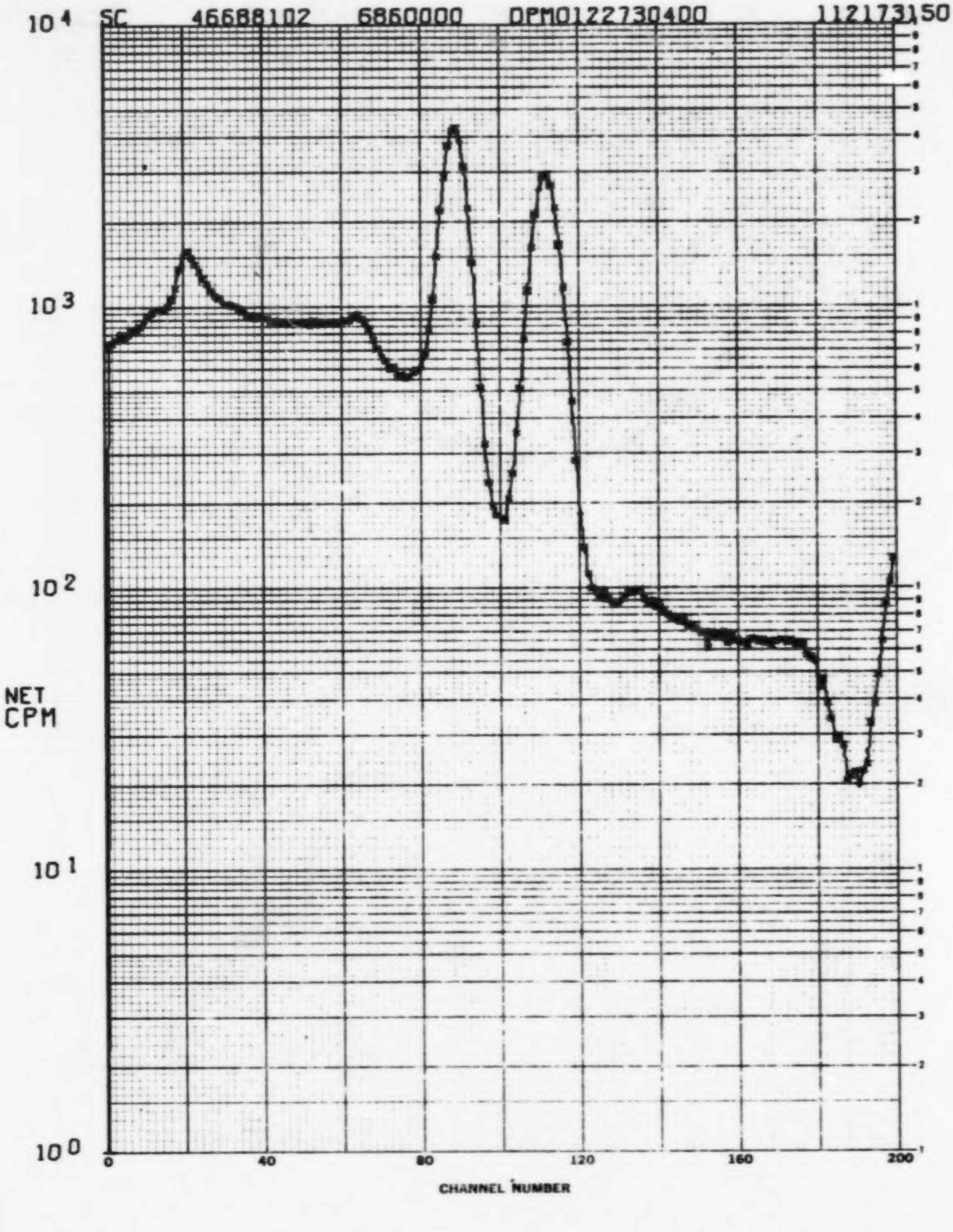

Figure E-4. Scandium-46 spectrum calibrated at 10 keV per channel.

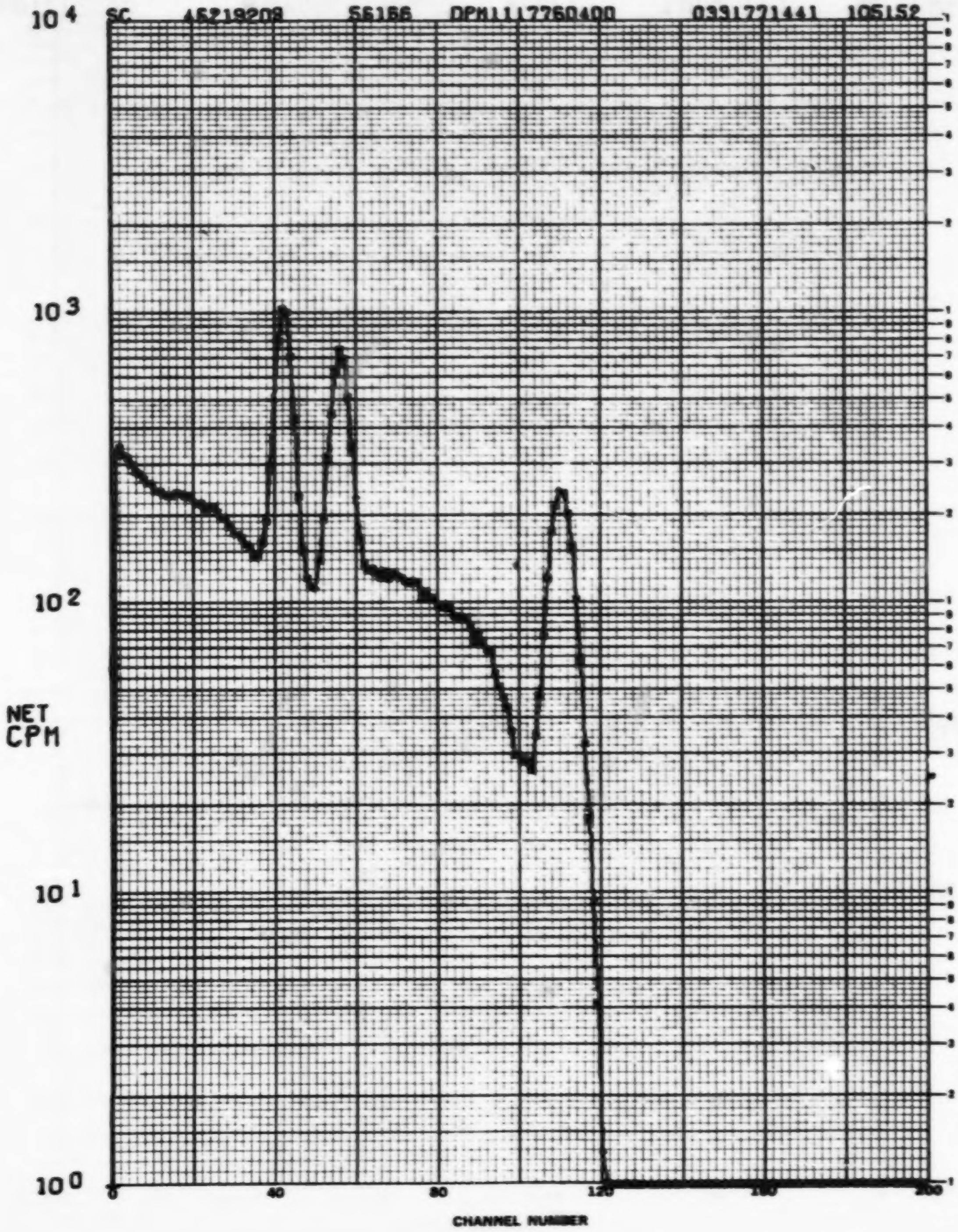

Figure E-5. Scandium-46 spectrum calibrated at 20 keV per channel.*

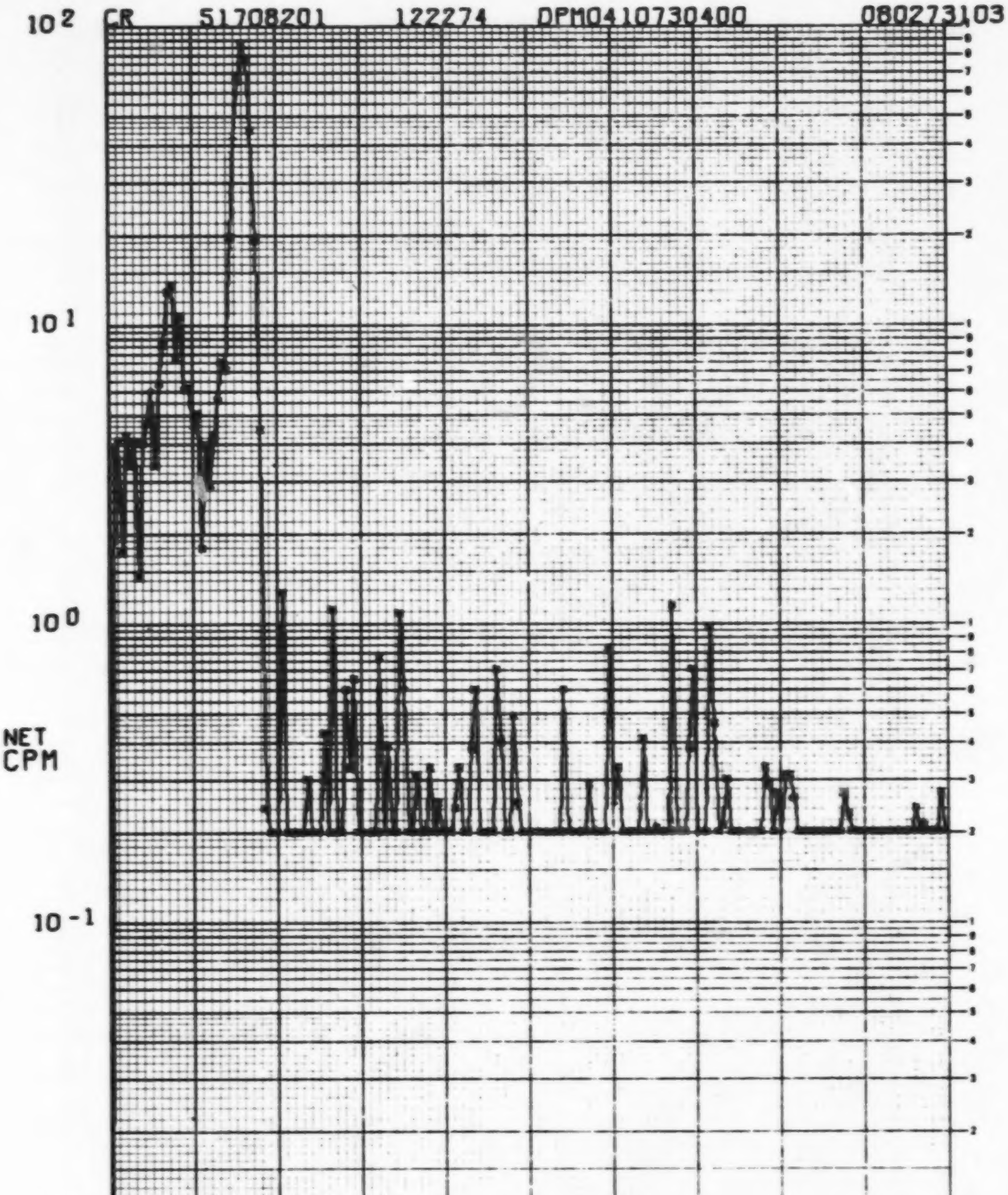

Figure E-6. Chromium-51 spectrum calibrated at 10 keV per channel.

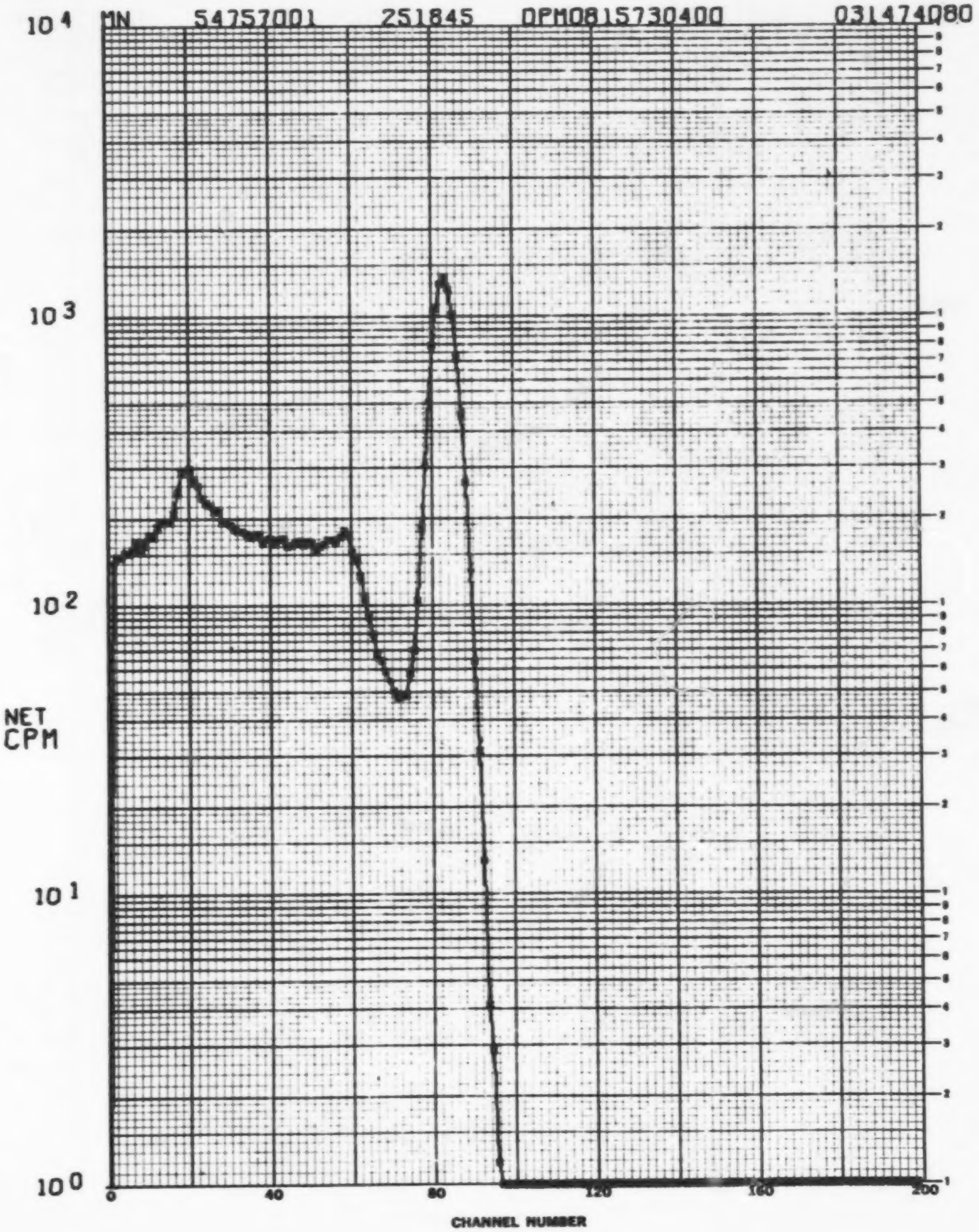

Figure E-7. Manganese-54 spectrum calibrated at 10 keV per channel.

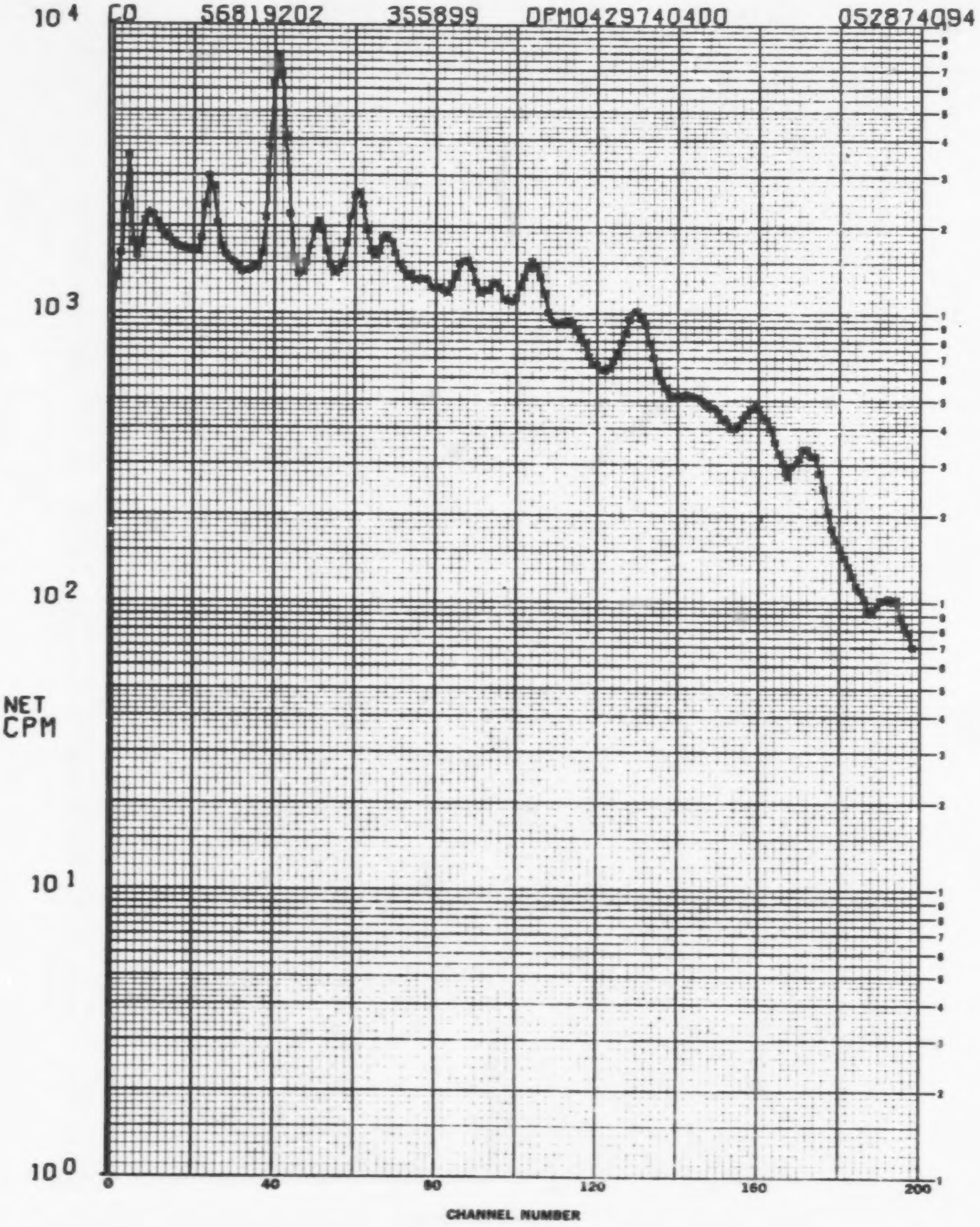

Figure E-8. Cobalt-56 spectrum calibrated at 20 keV per channel.

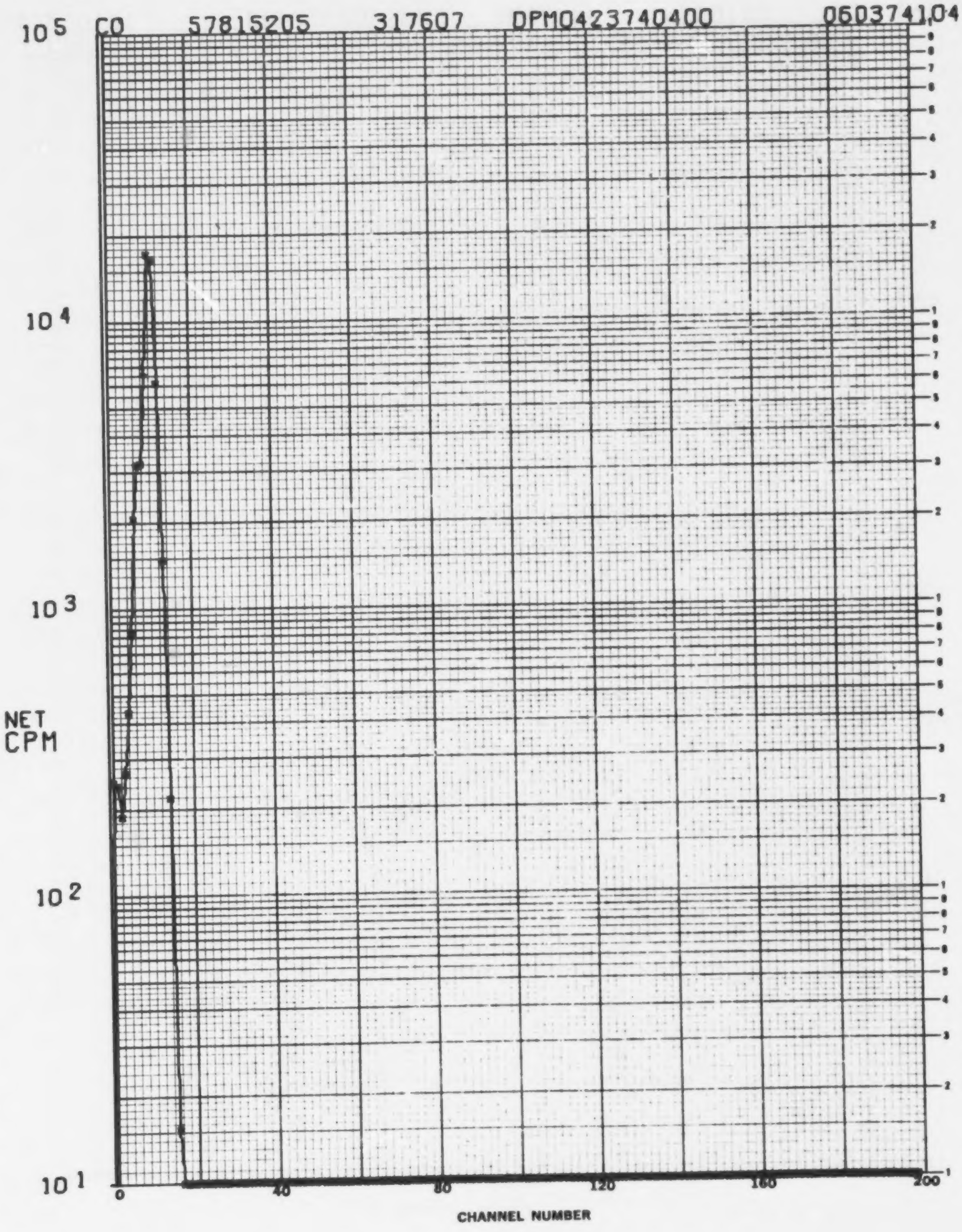

Figure E-9. Cobalt-57 spectrum calibrated at 10 keV per channel.

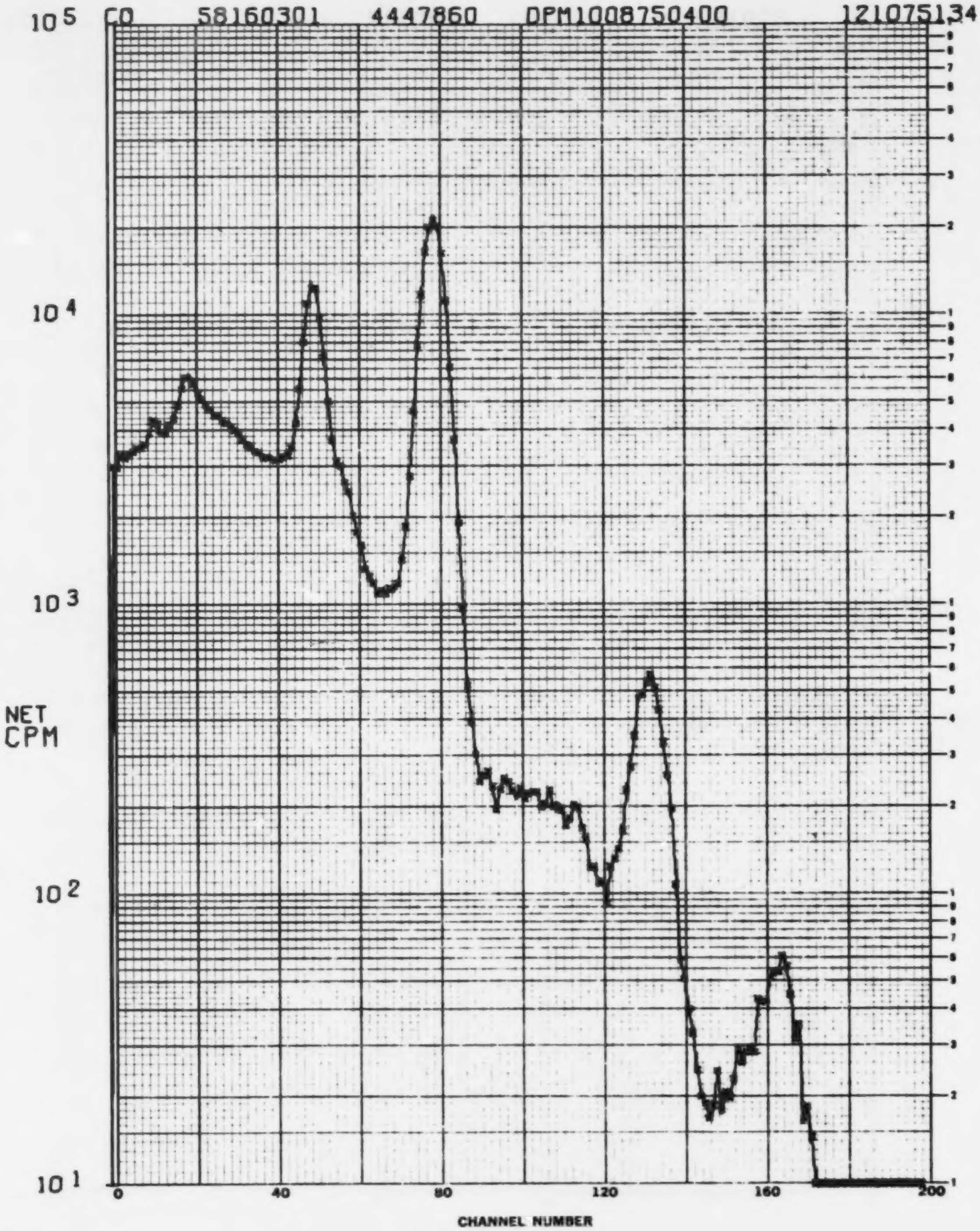

Figure E-10. Cobalt-58 spectrum calibrated at 10 keV per channel.

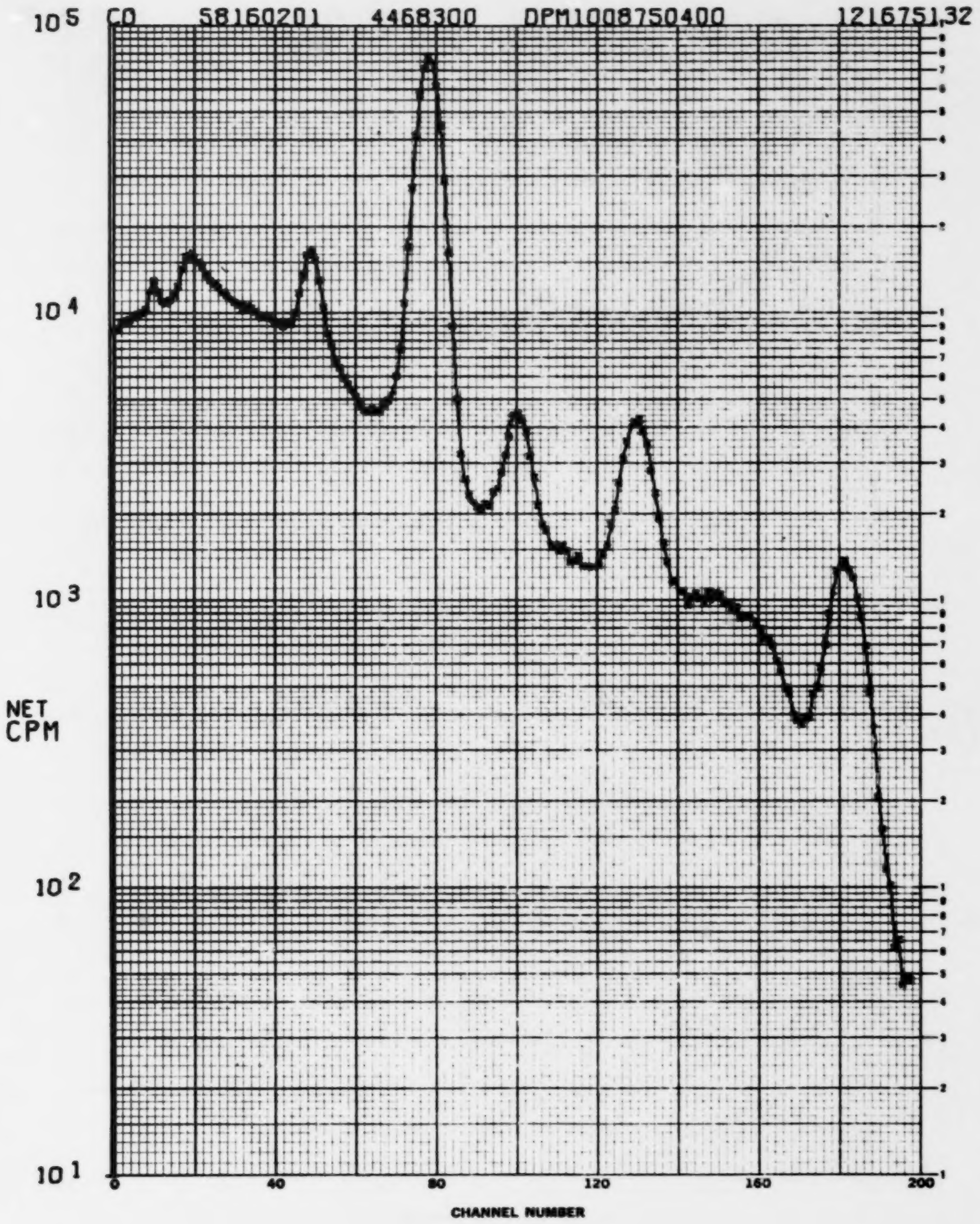

Figure E-11. Cobalt-58 spectrum calibrated at 10 keV per channel.*

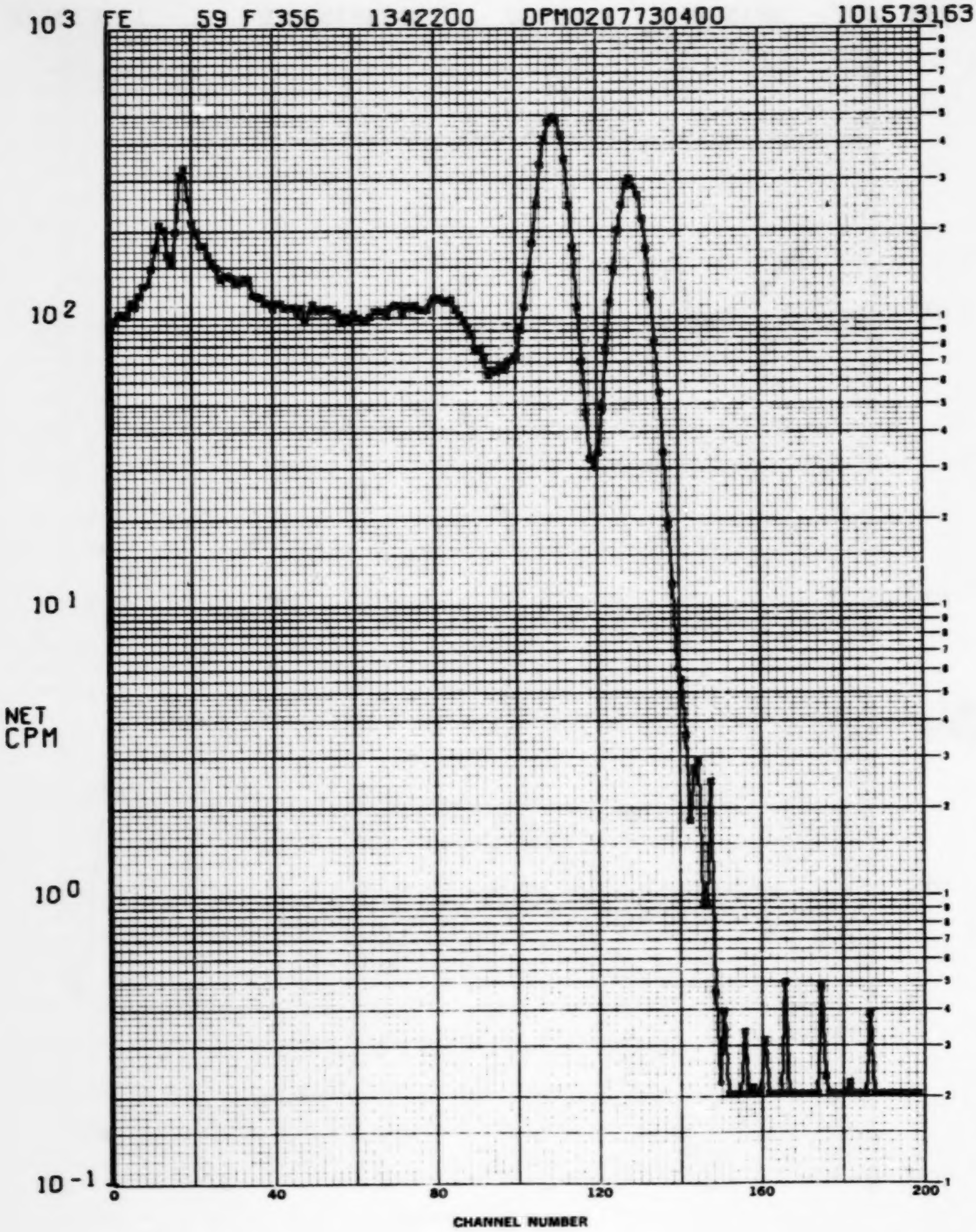

Figure E-12. Iron-59 spectrum calibrated at 10 keV per channel.

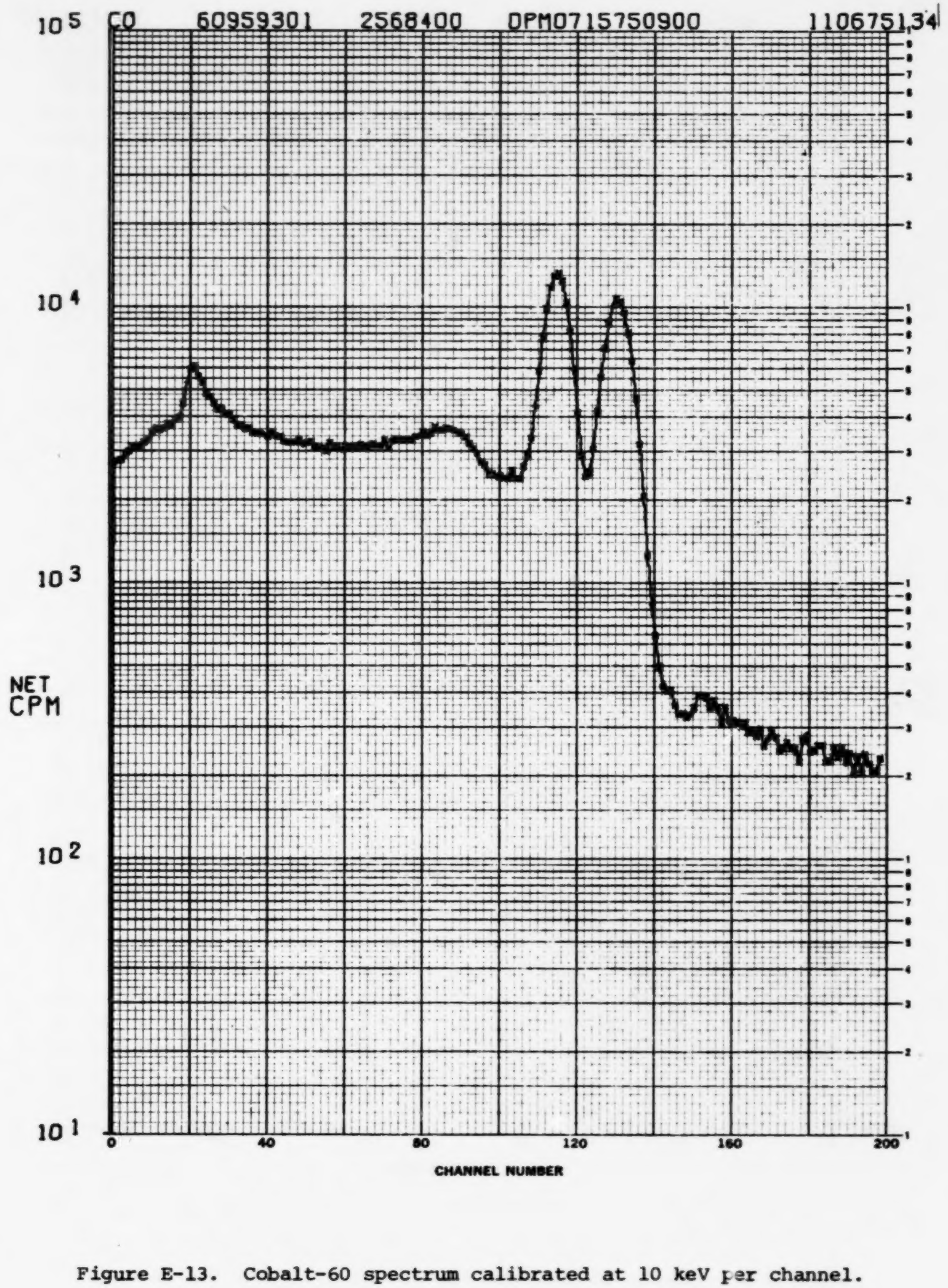

Figure E-13. Cobalt-60 spectrum calibrated at 10 keV per channel.

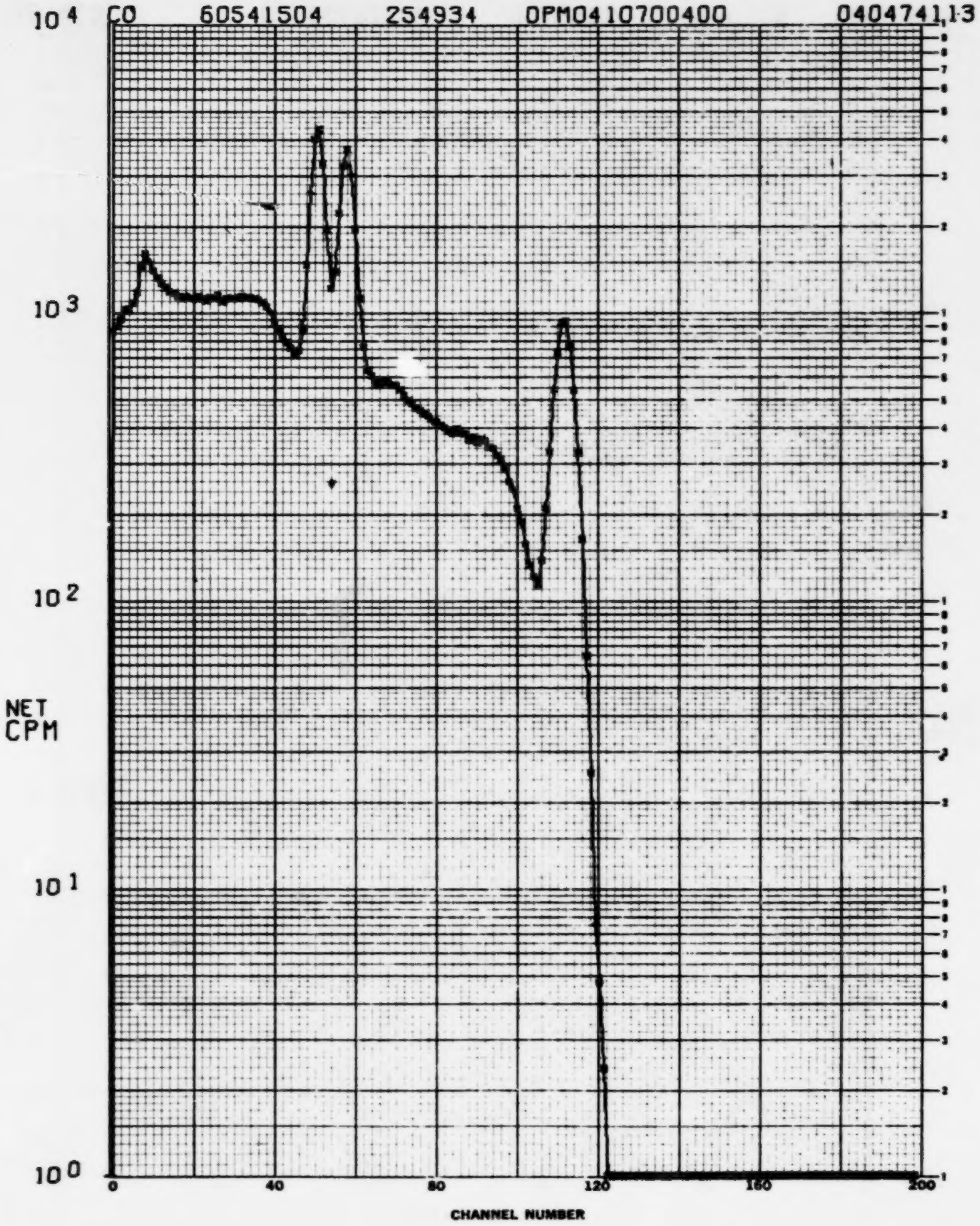

Figure E-14. Cobalt-60 spectrum calibrated at 20 keV per channel.*

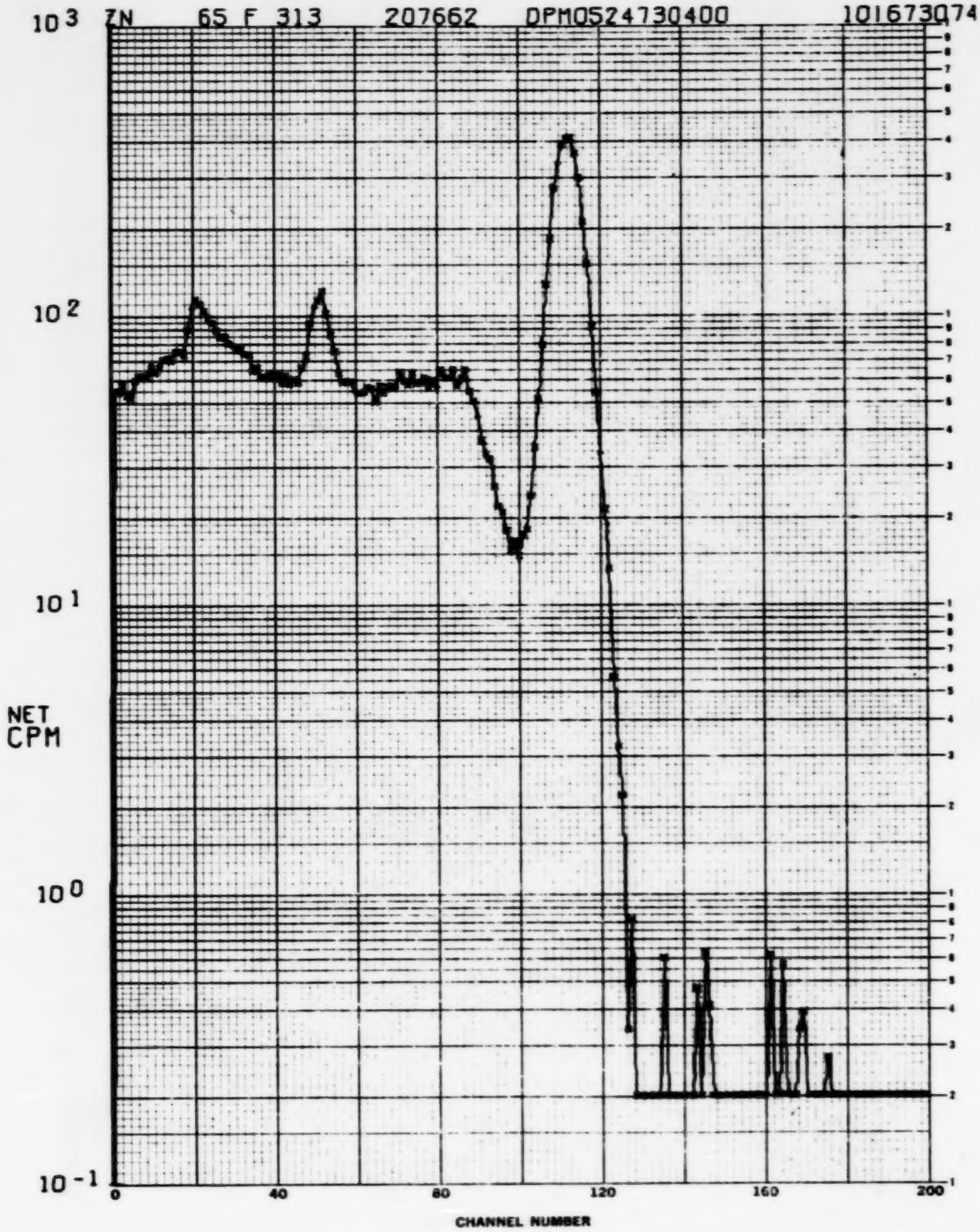

Figure E-15. Zinc-65 spectrum calibrated at 10 keV per channel.

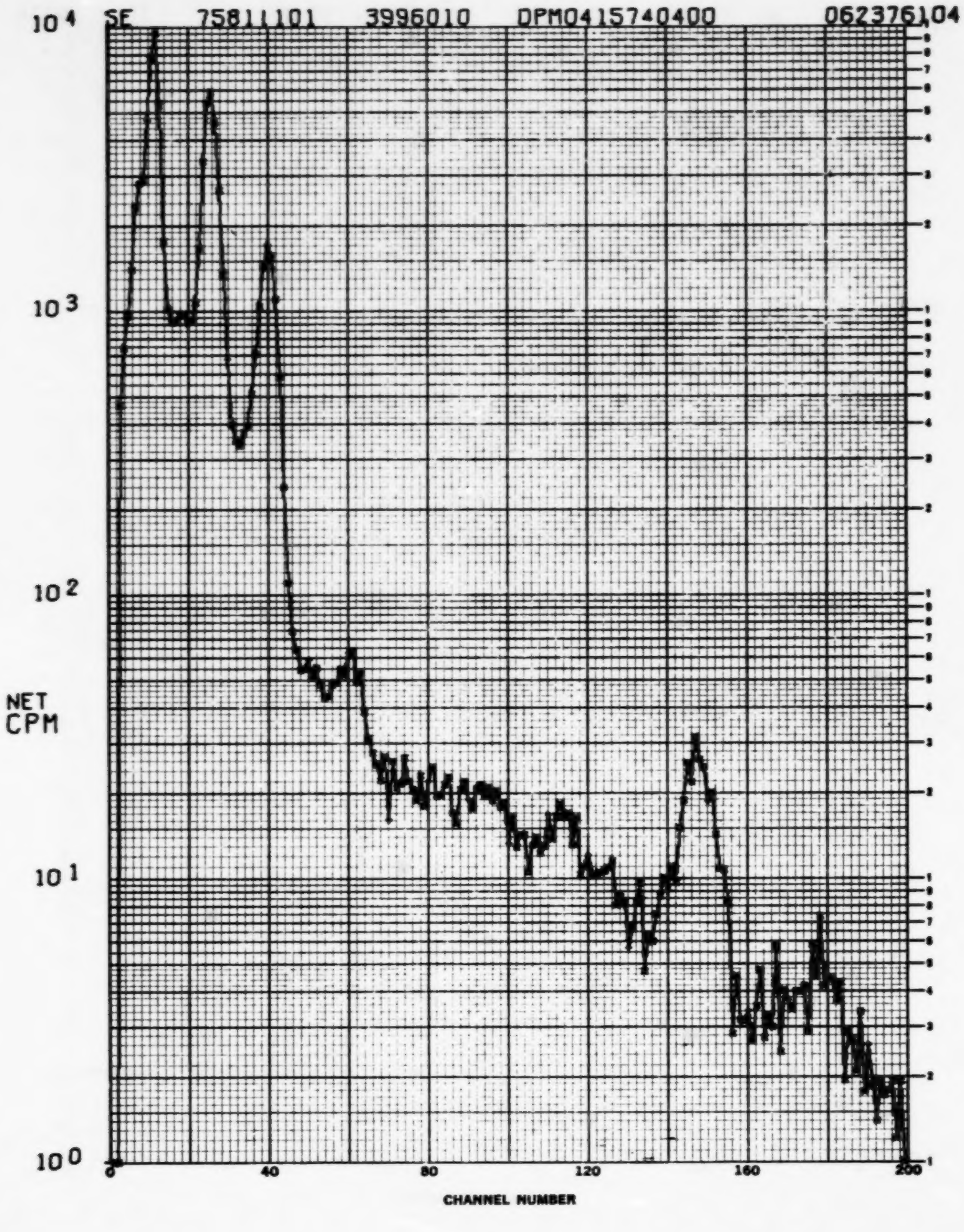

Figure E-16. Selenium-75 spectrum calibrated at 10 keV per channel.

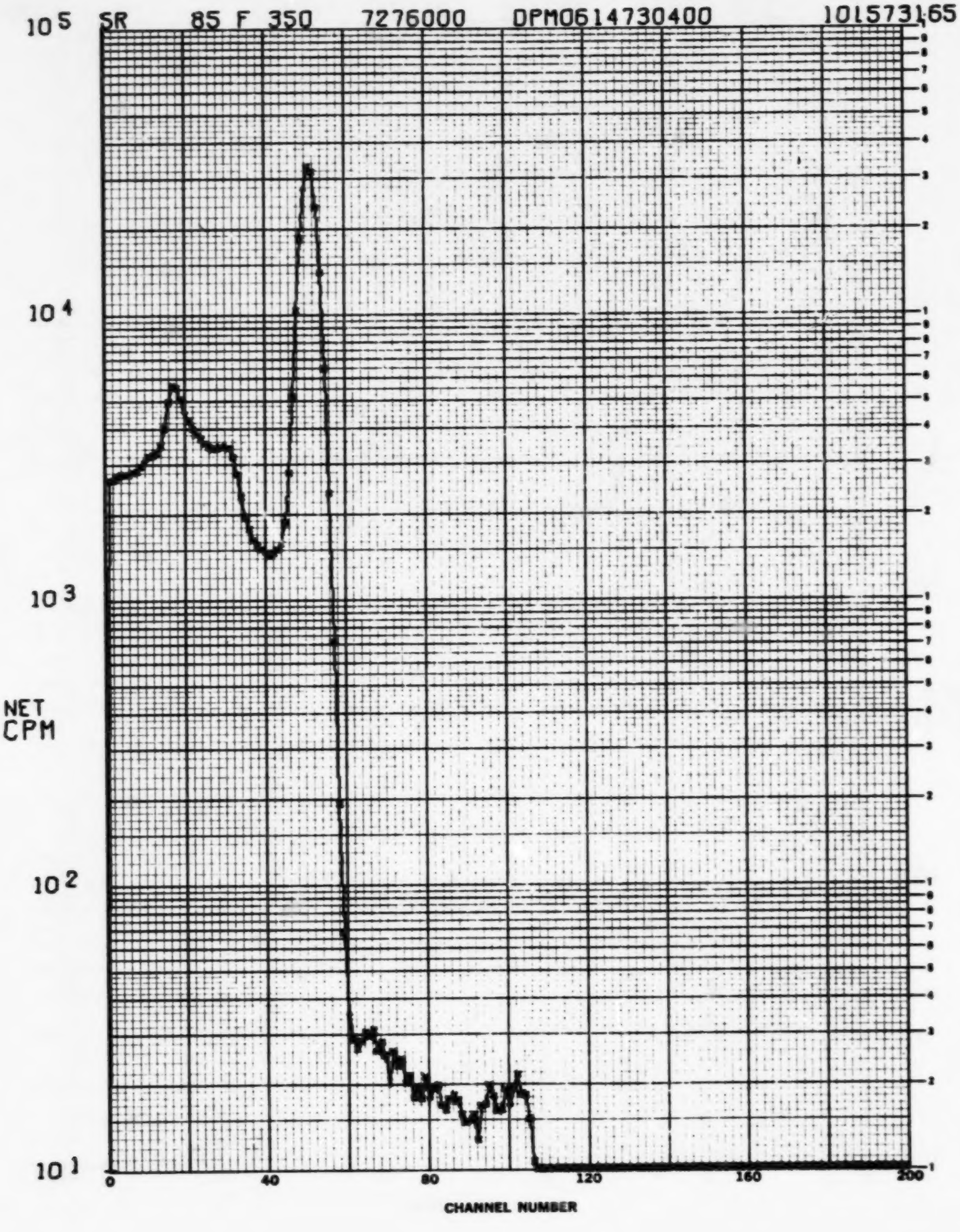

Figure E-17. Strontium-85 spectrum calibrated at 10 keV per channel.

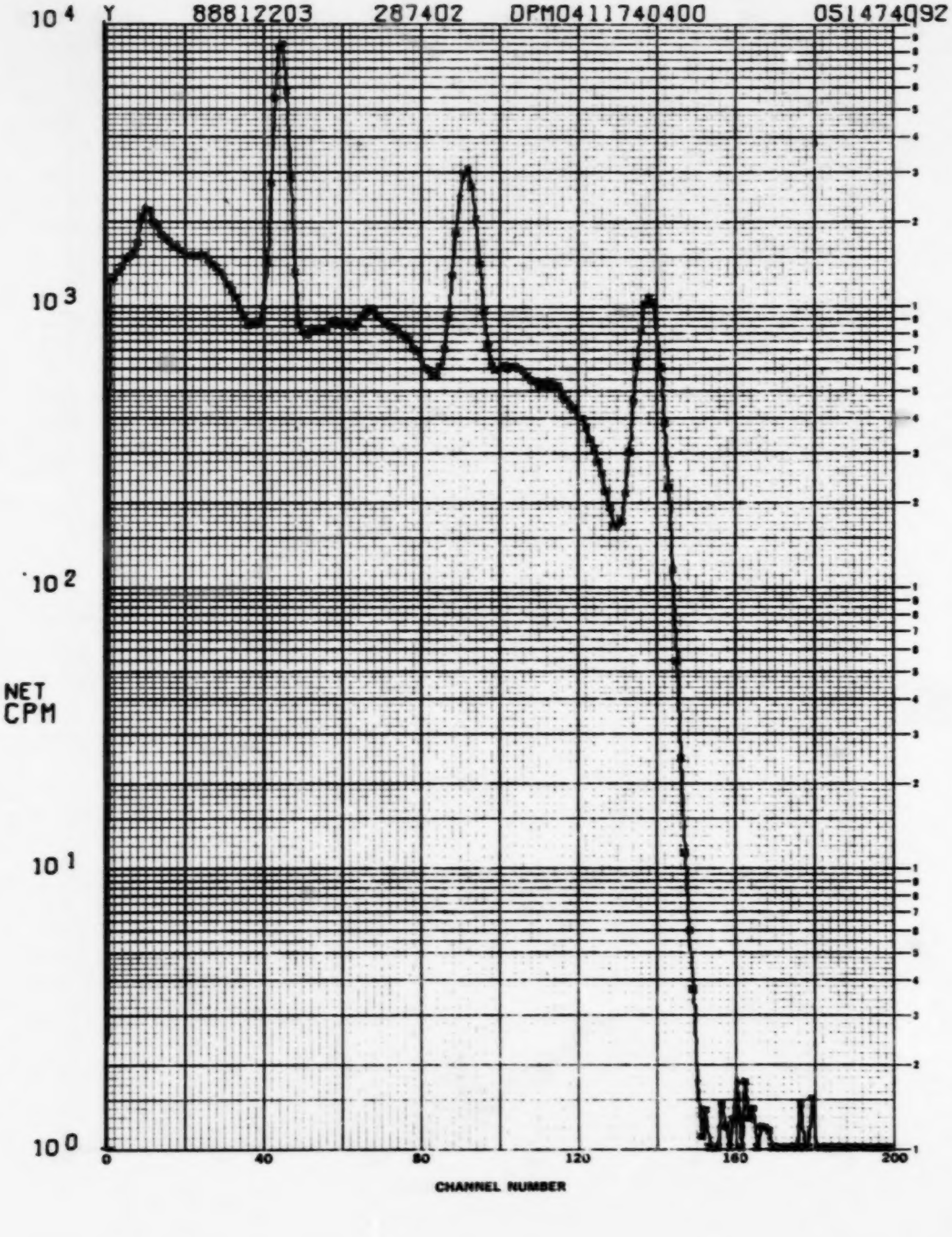

Figure E-18. Yttrium-88 spectrum calibrated at 20 keV per channel.*

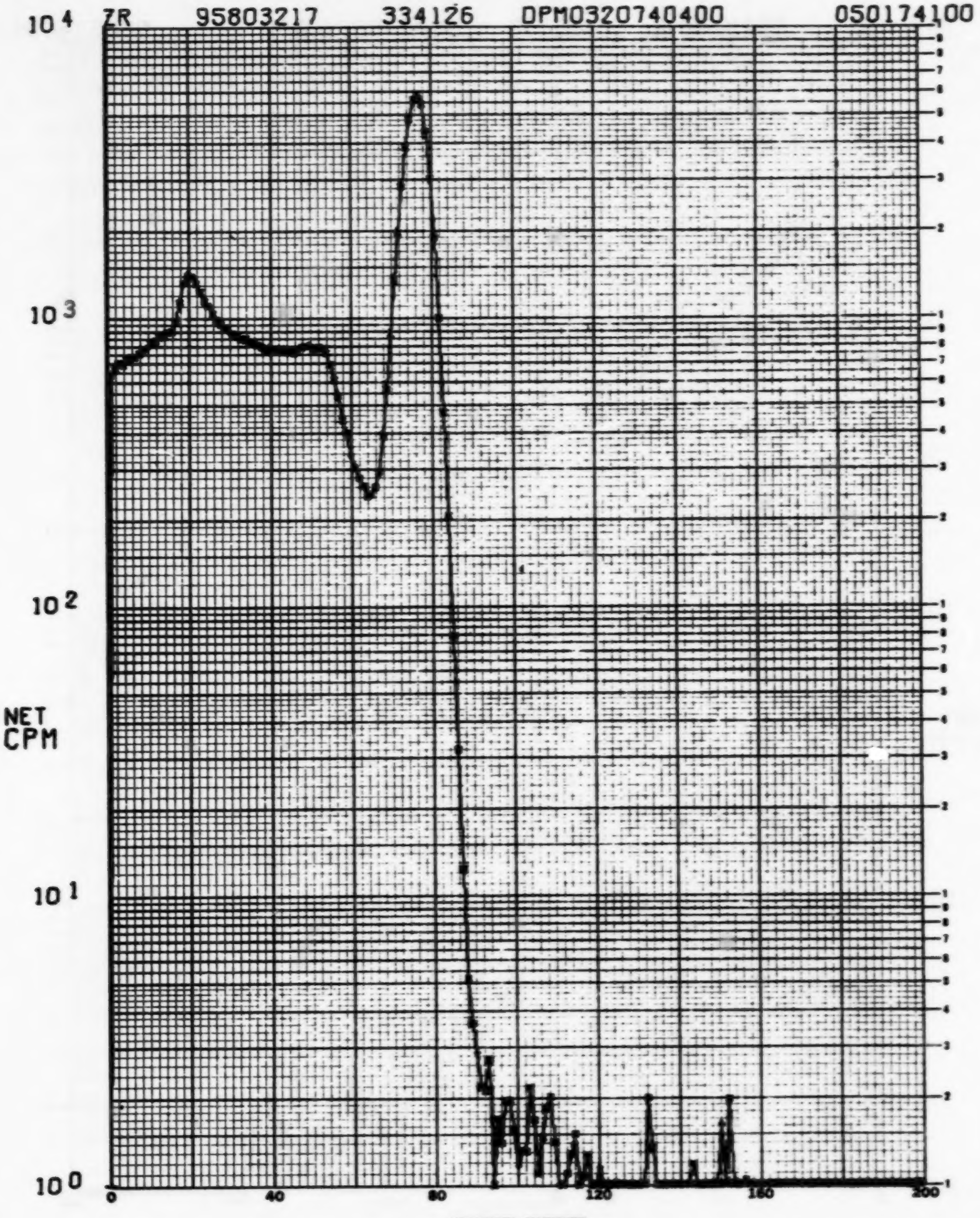

Figure E-19. Zirconium-95 spectrum calibrated at 10 keV per channel.

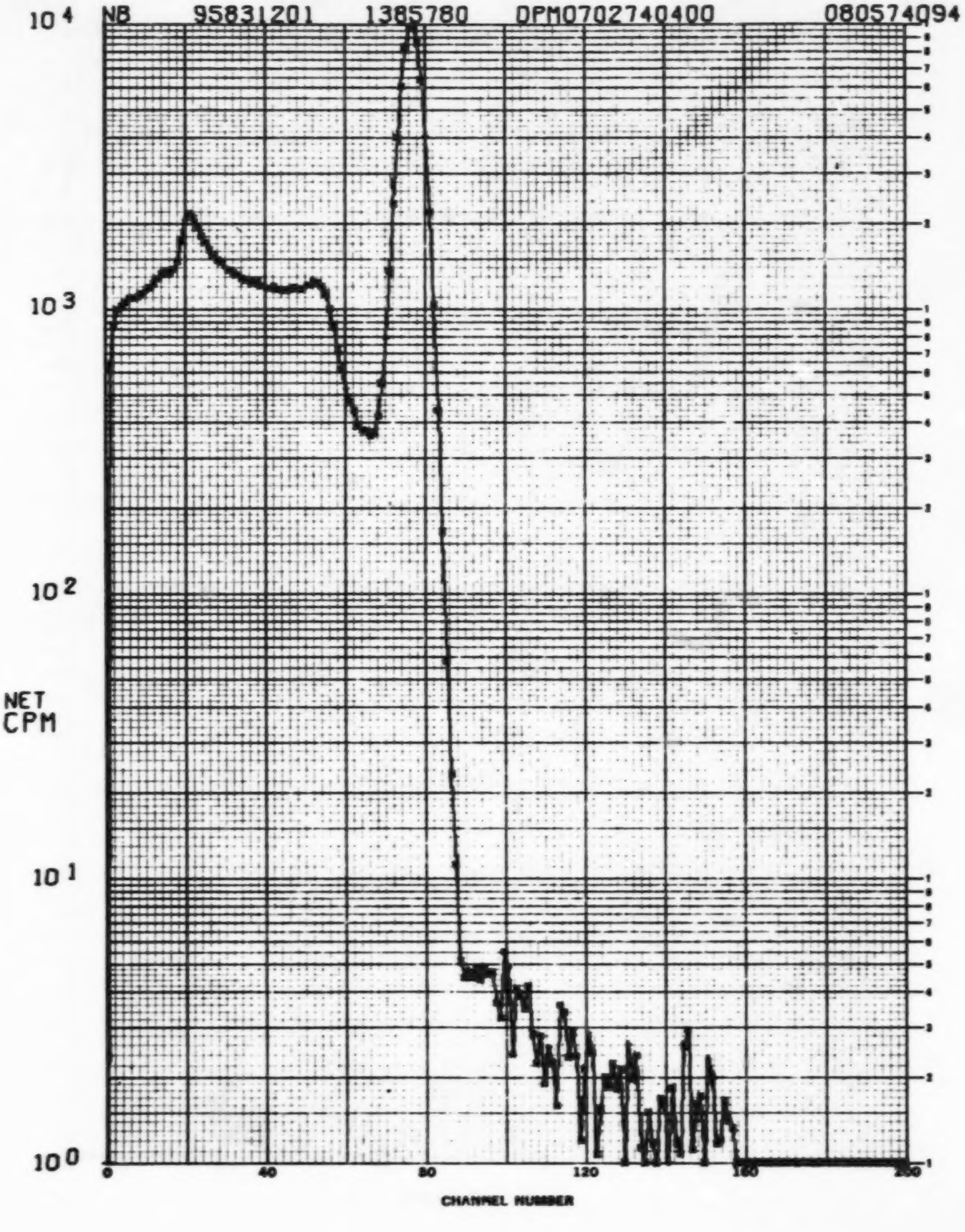

Figure E-20. Niobium-95 spectrum calibrated at 10 keV per channel.

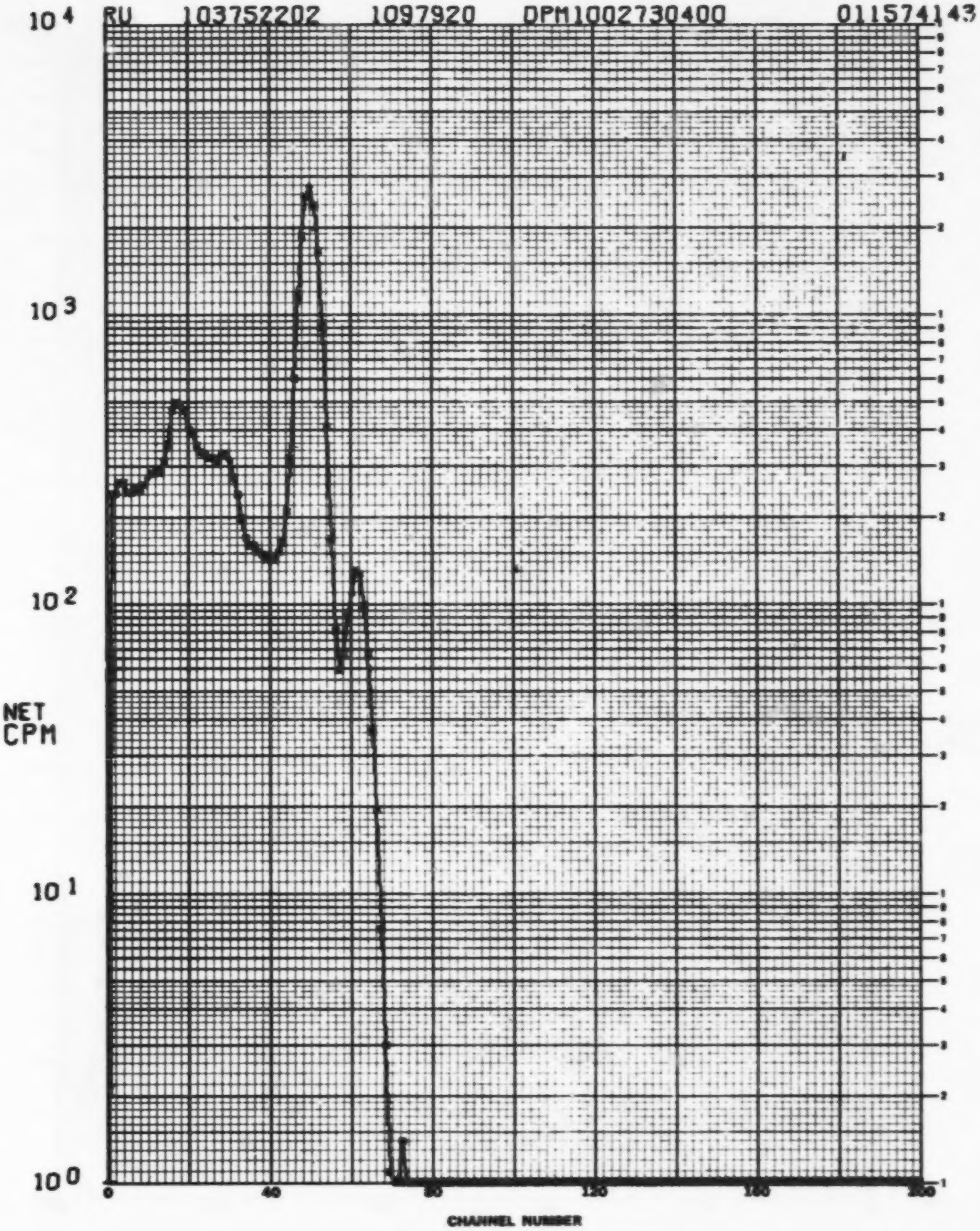

Figure E-21. Ruthenium-103 spectrum calibrated at 10 keV per channel.

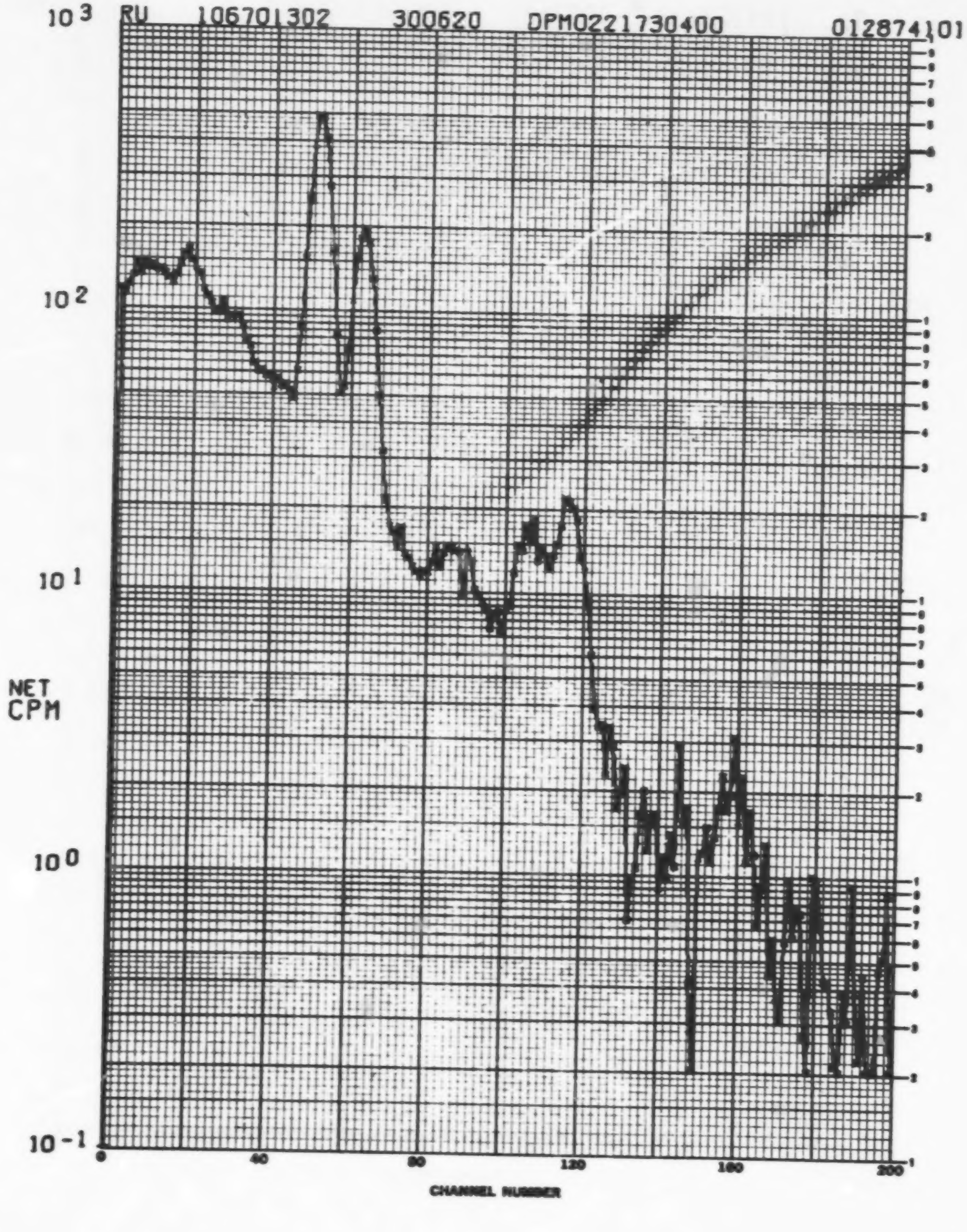

Figure E-22. Ruthenium-106 spectrum calibrated at 10 keV per channel.

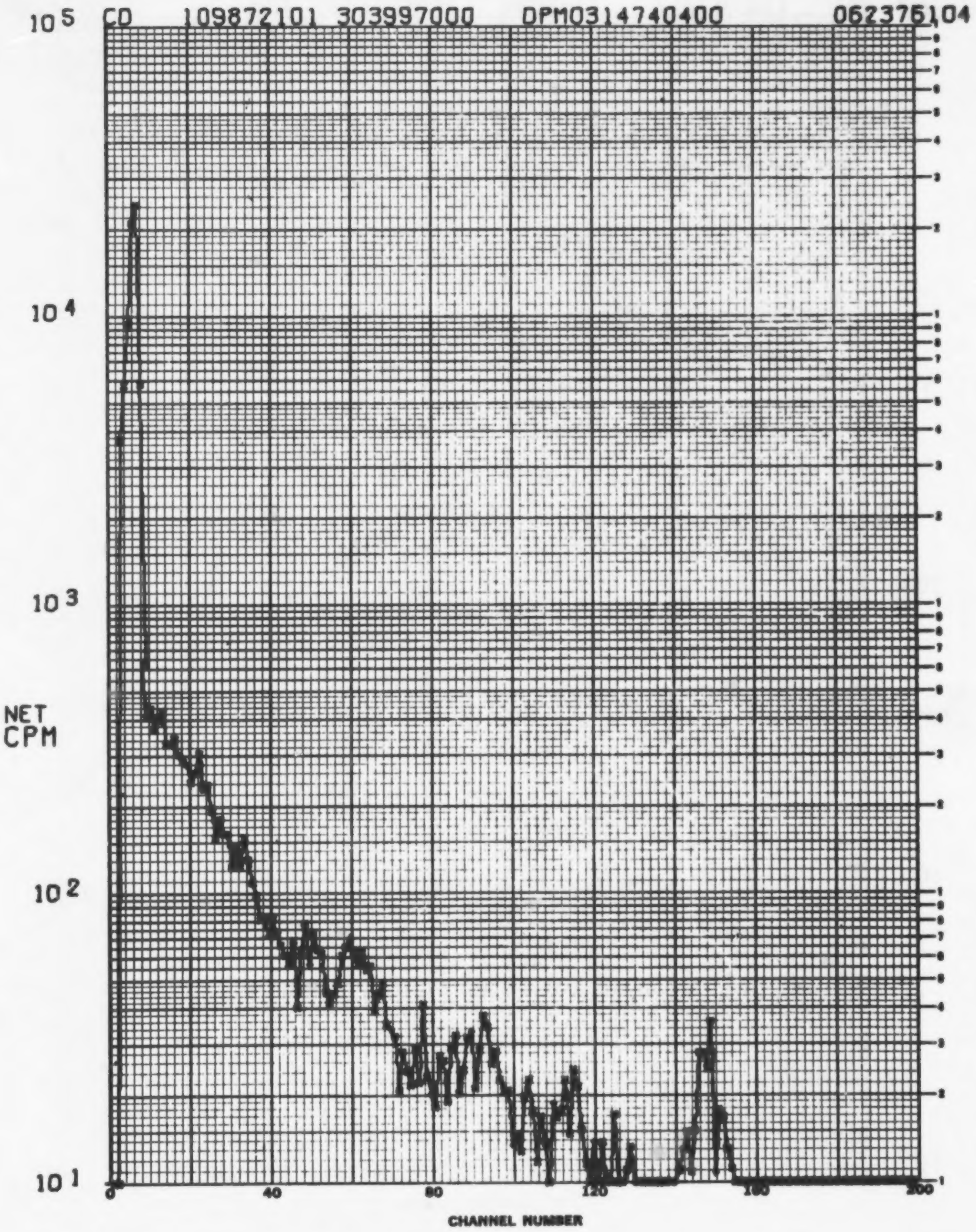

Figure E-23. Cadmium-109 spectrum calibrated at 10 keV per channel.

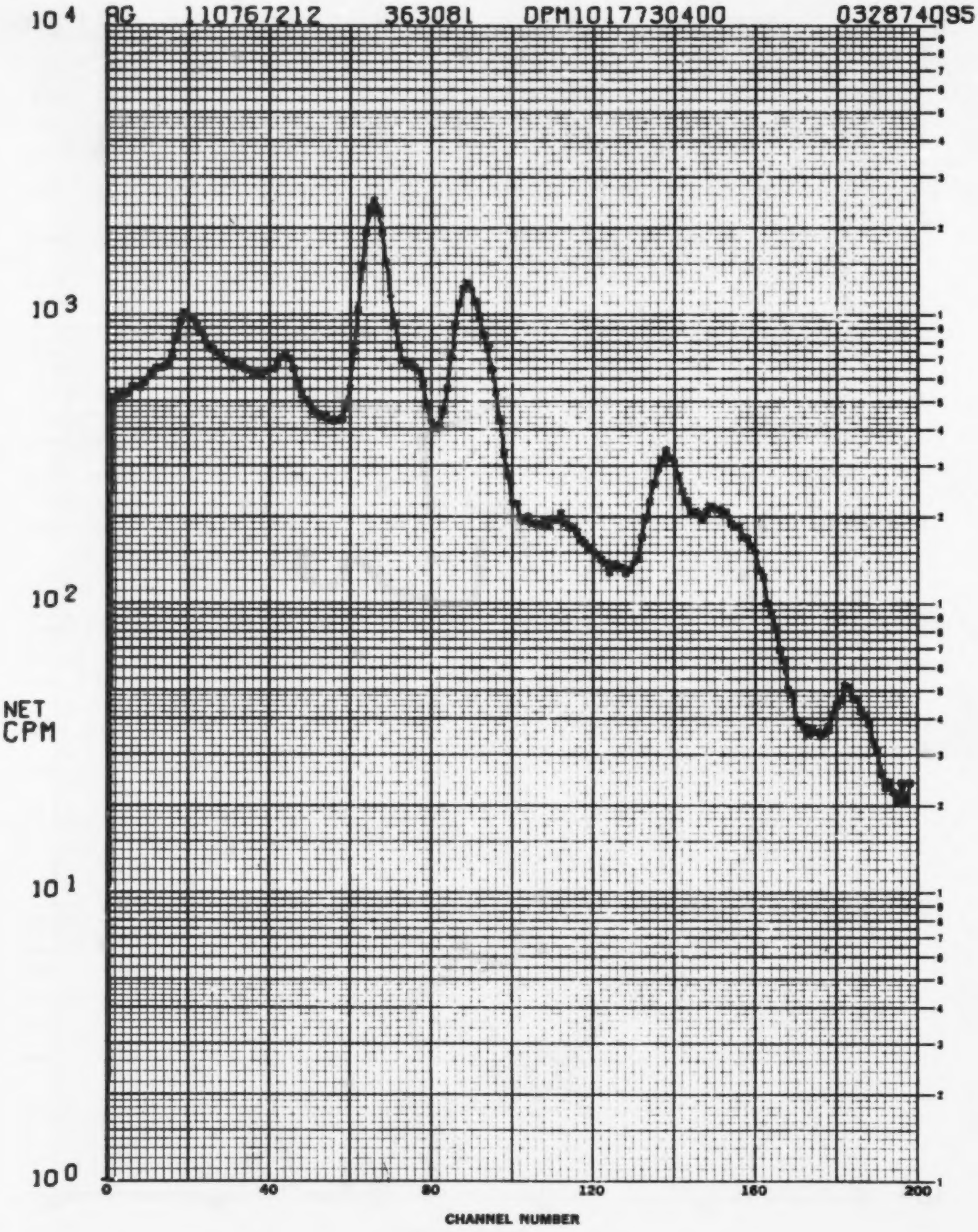

Figure E-24. Silver-110m spectrum calibrated at 10 keV per channel.

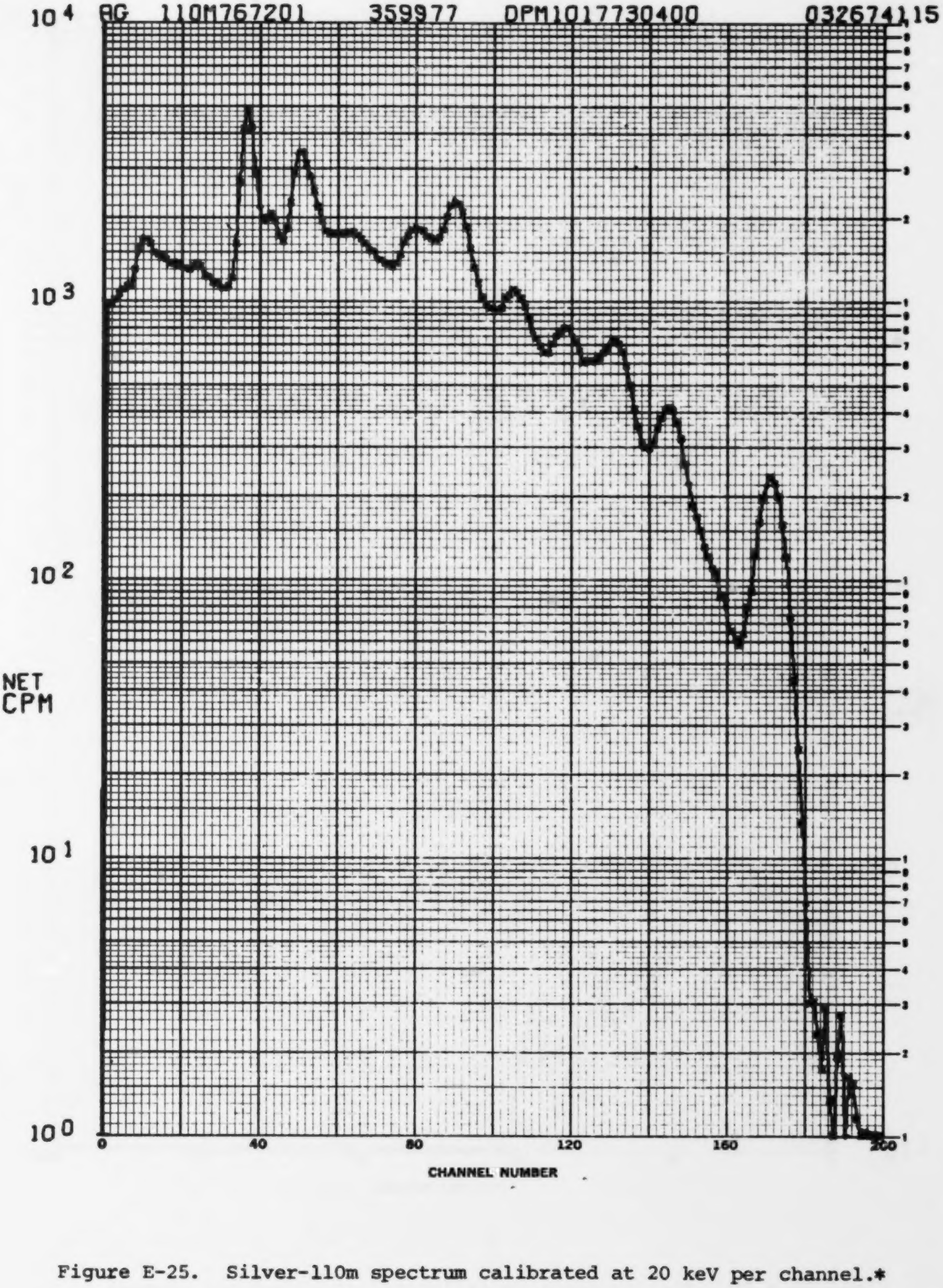

Figure E-25. Silver-110m spectrum calibrated at 20 keV per channel.*

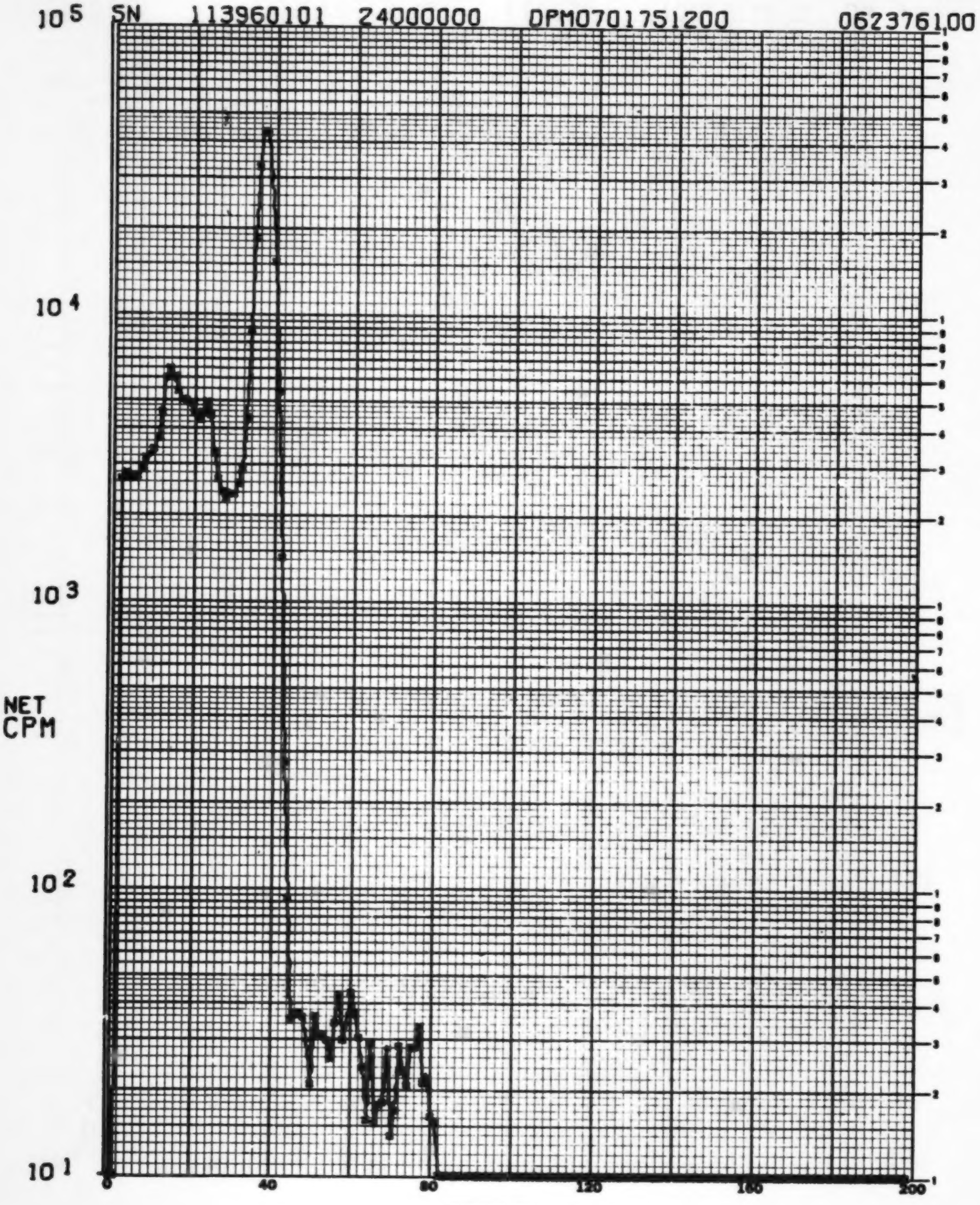

Figure E-26. Tin-113 spectrum calibrated at 10 keV per channel.

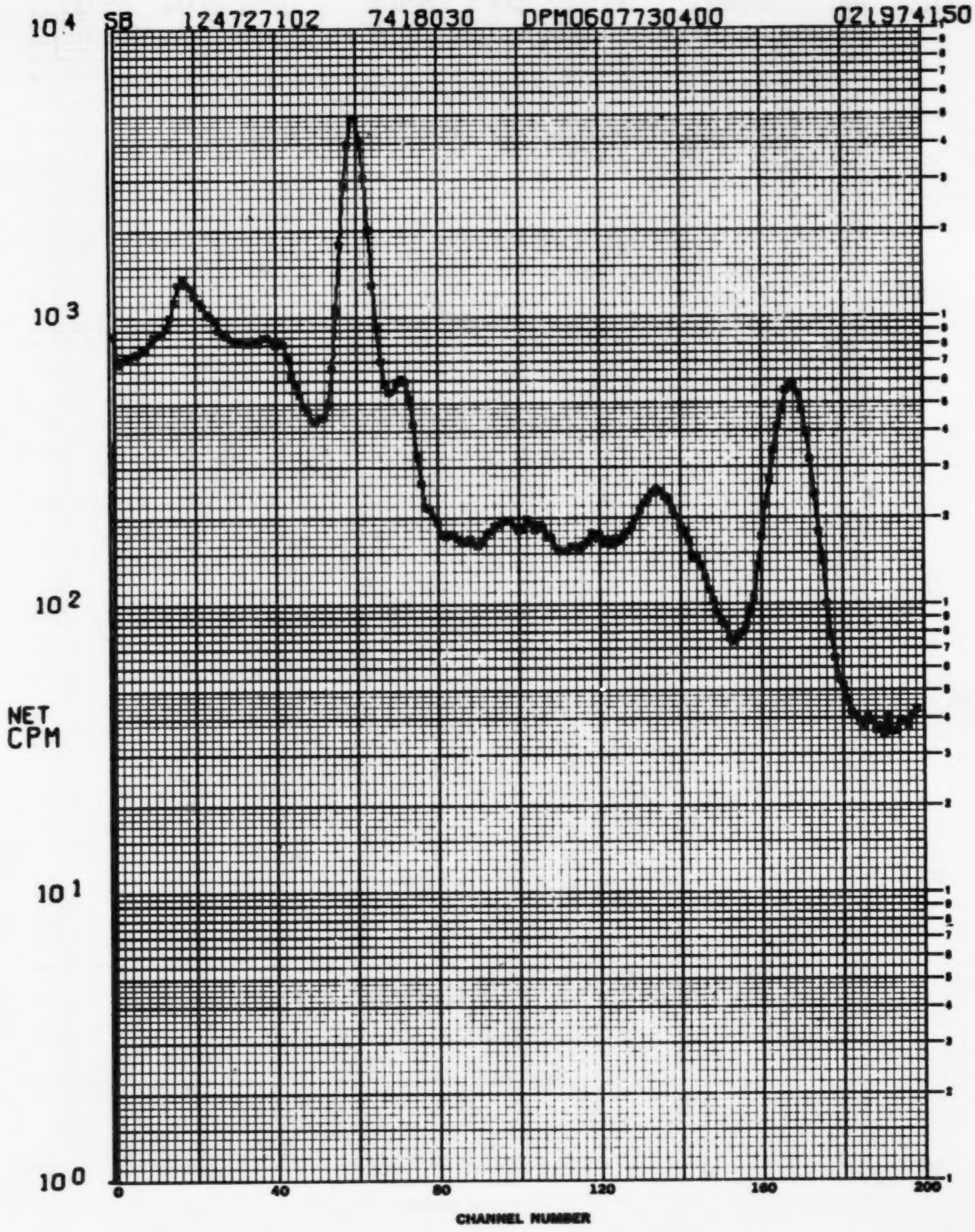

Figure E-27. Antimony-124 spectrum calibrated at 10 keV per channel.

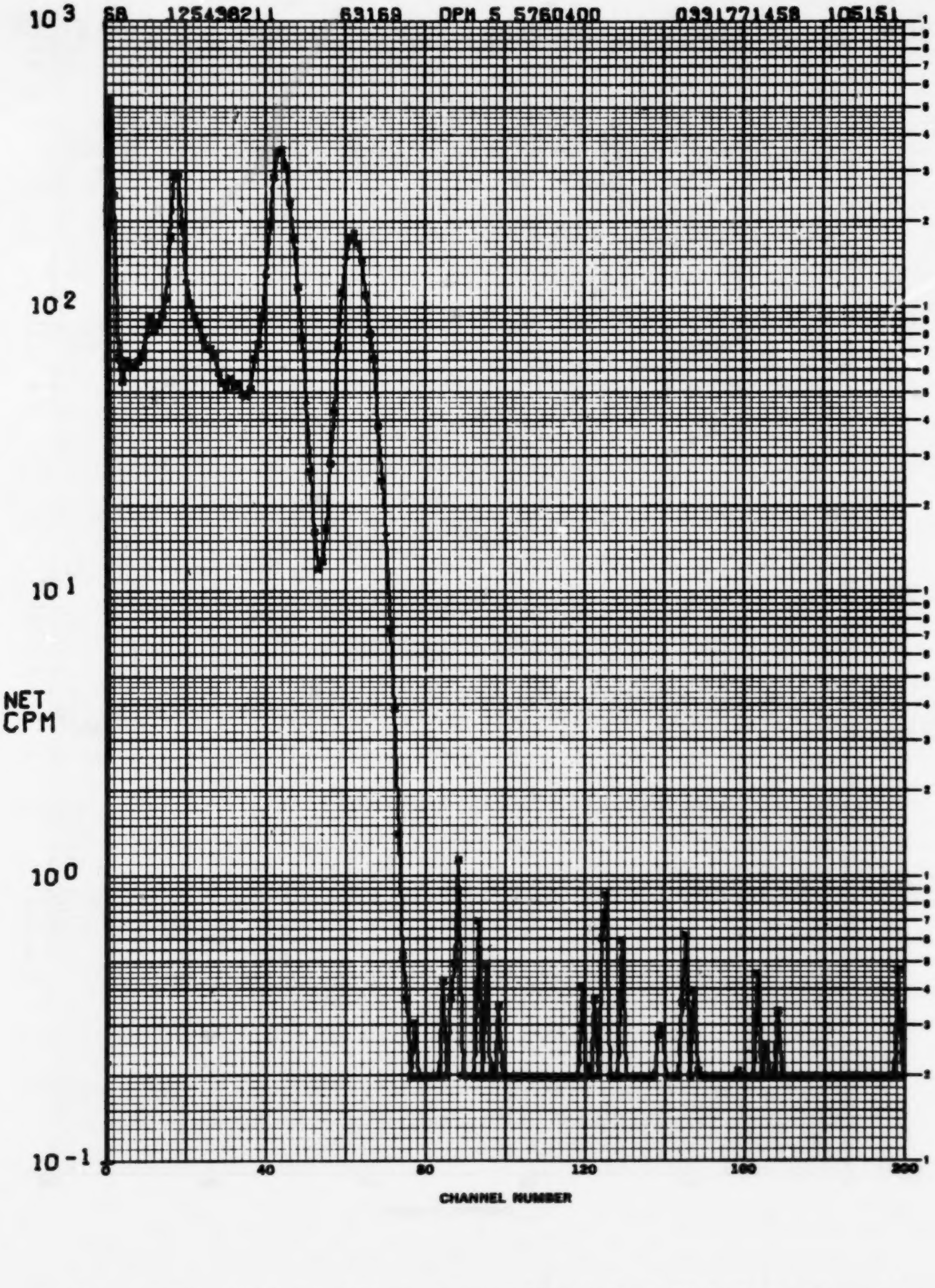

Figure E-28. Antimony-125 spectrum calibrated at 10 keV per channel.

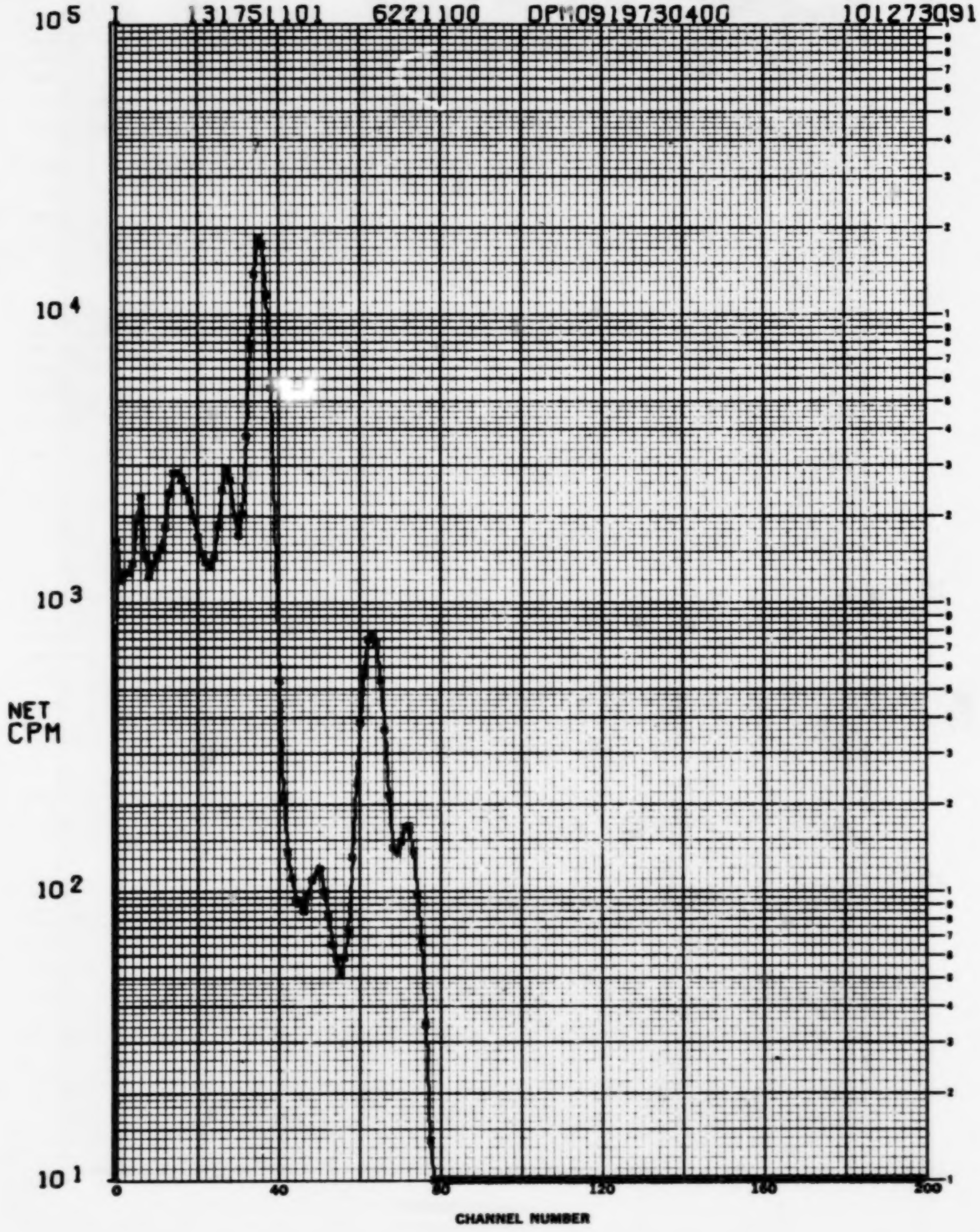

Figure E-29. Iodine-131 spectrum calibrated at 10 keV per channel.

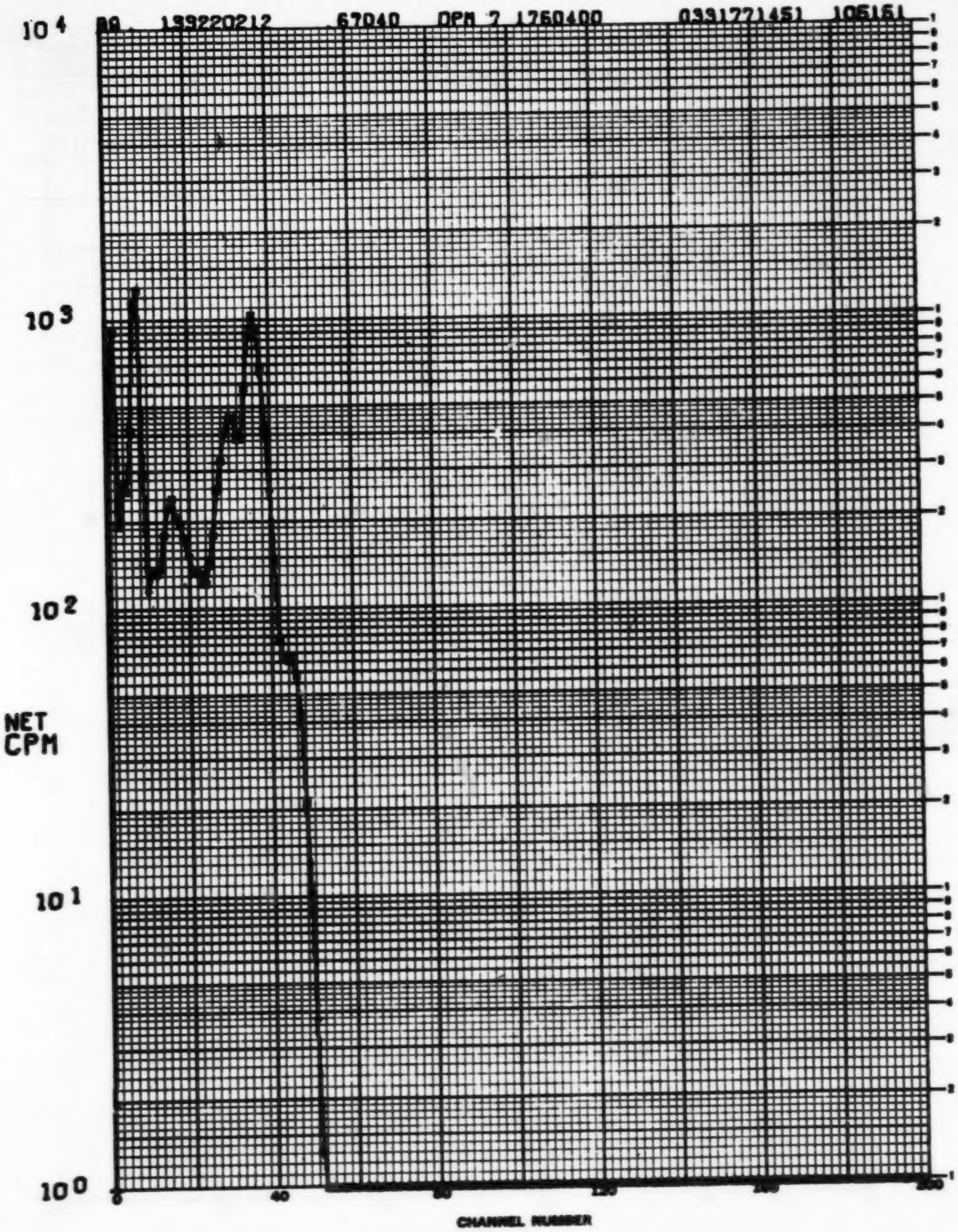

Figure E-30. Barium-133 spectrum calibrated at 10 keV per channel.

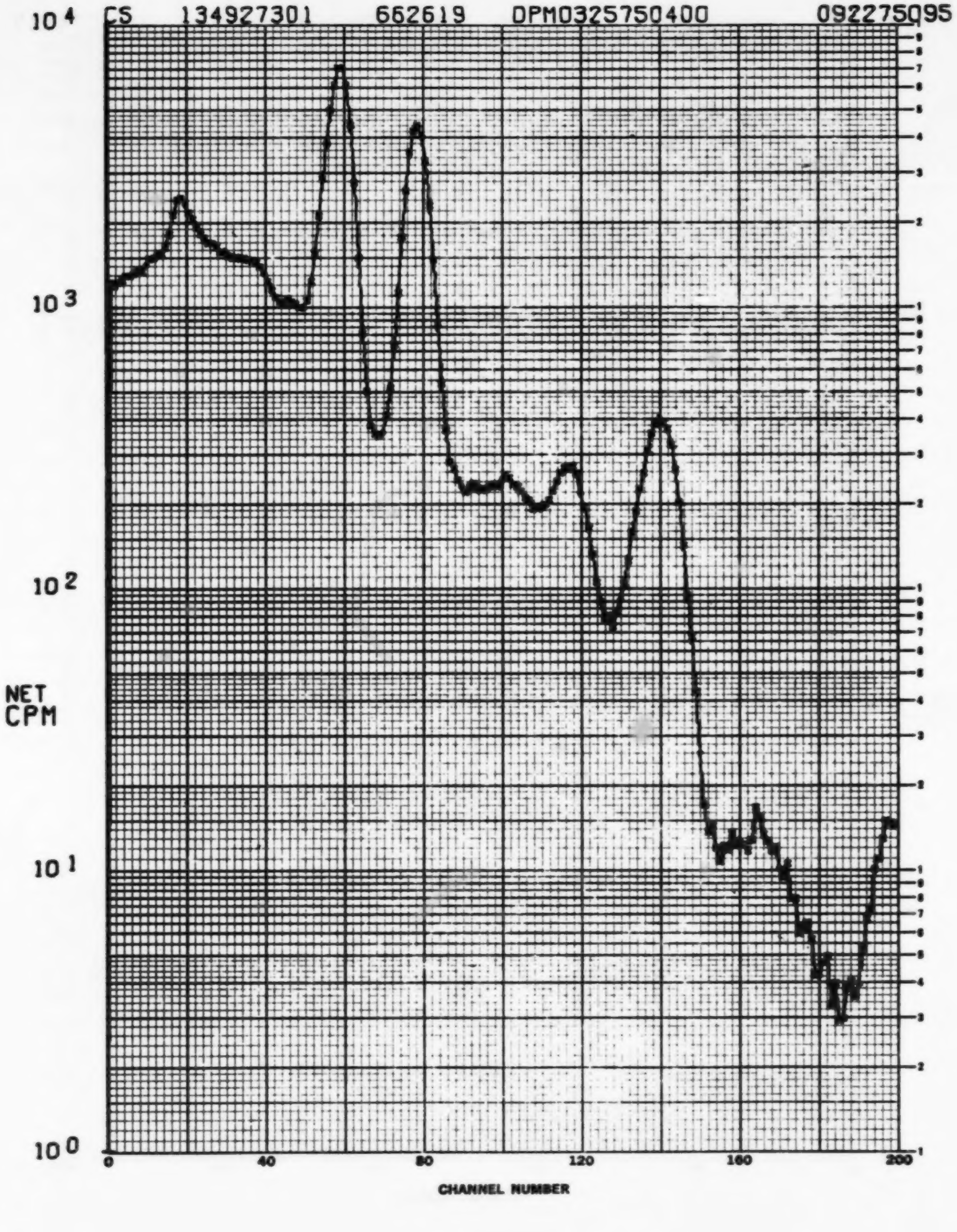

Figure E-31. Cesium-134 spectrum calibrated at 10 keV per channel.

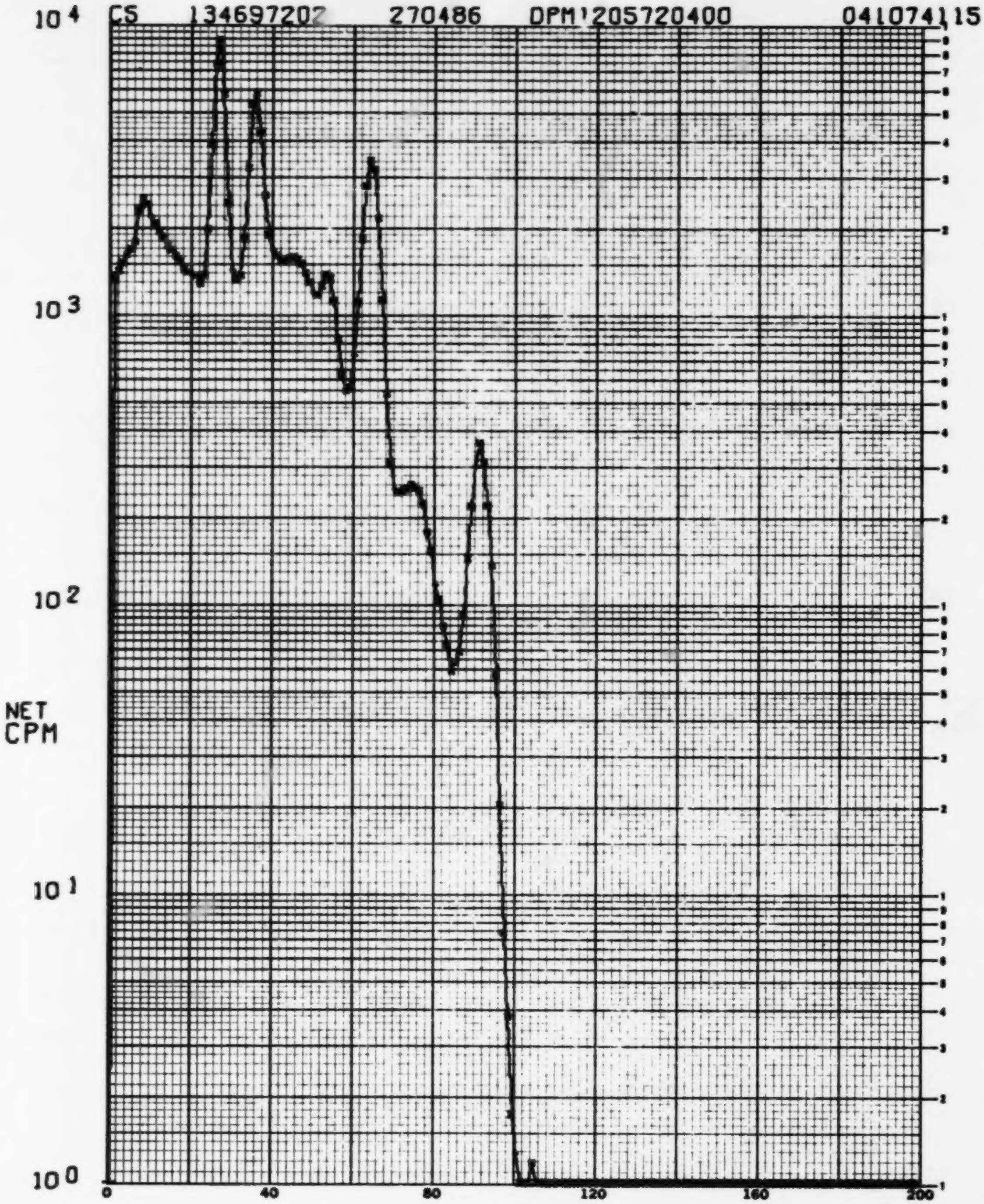

Figure E-32. Cesium-134 spectrum calibrated at 20 keV per channel.*

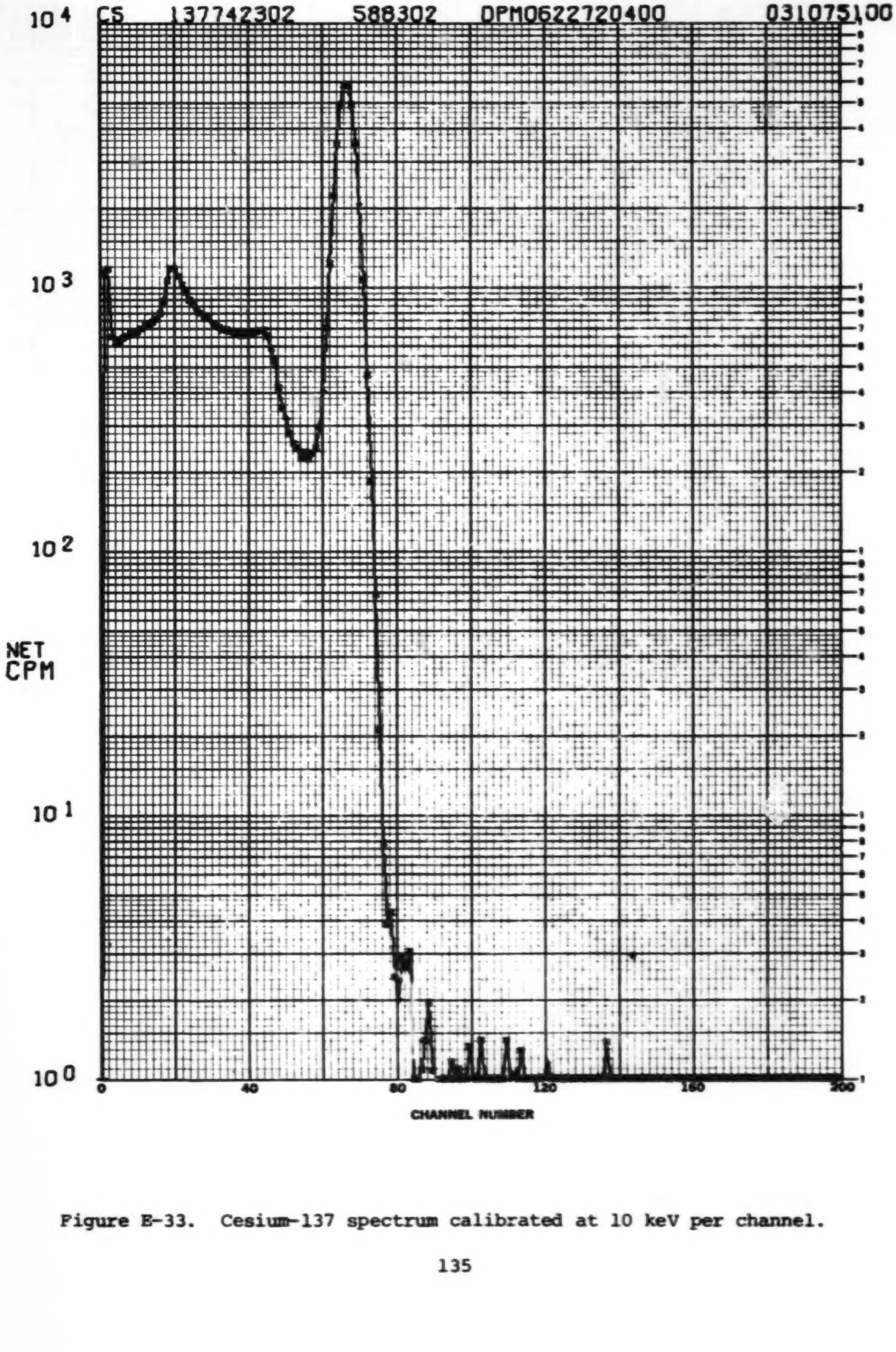

Figure E-33. Cesium-137 spectrum calibrated at 10 keV per channel.

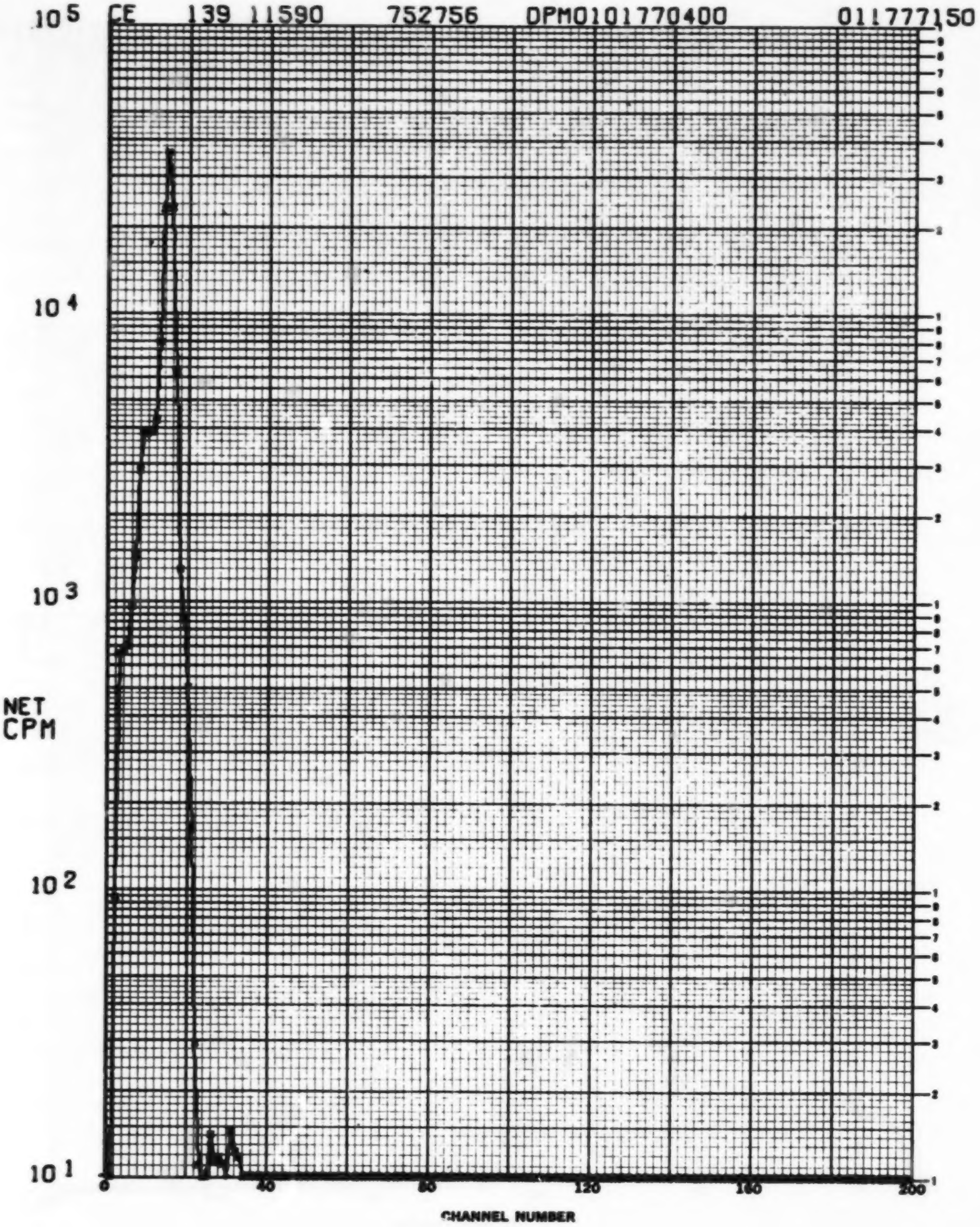

Figure E-34. Cerium-139 spectrum calibrated at 10 keV per channel.

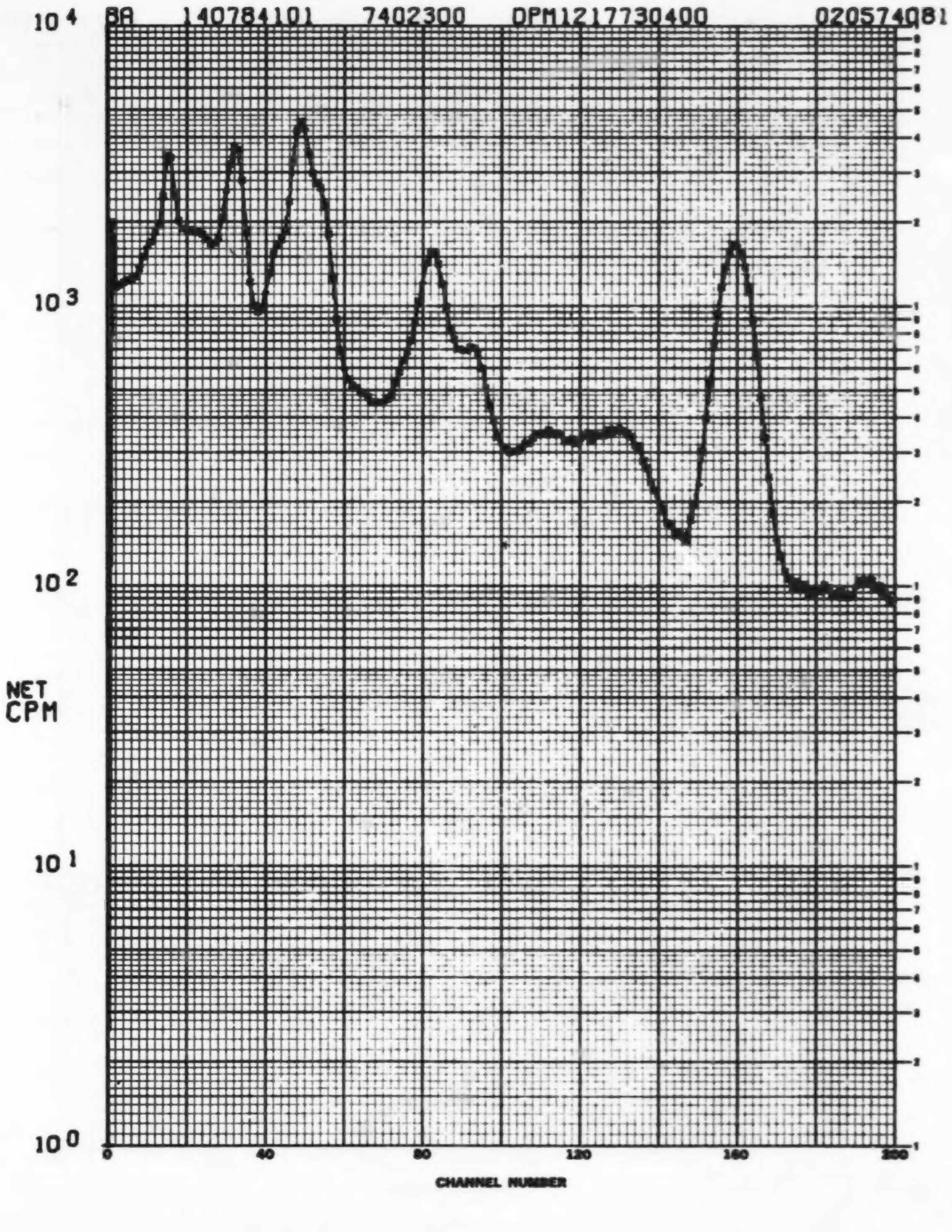

Figure E-35. Barium-140 spectrum calibrated at 10 keV per channel.

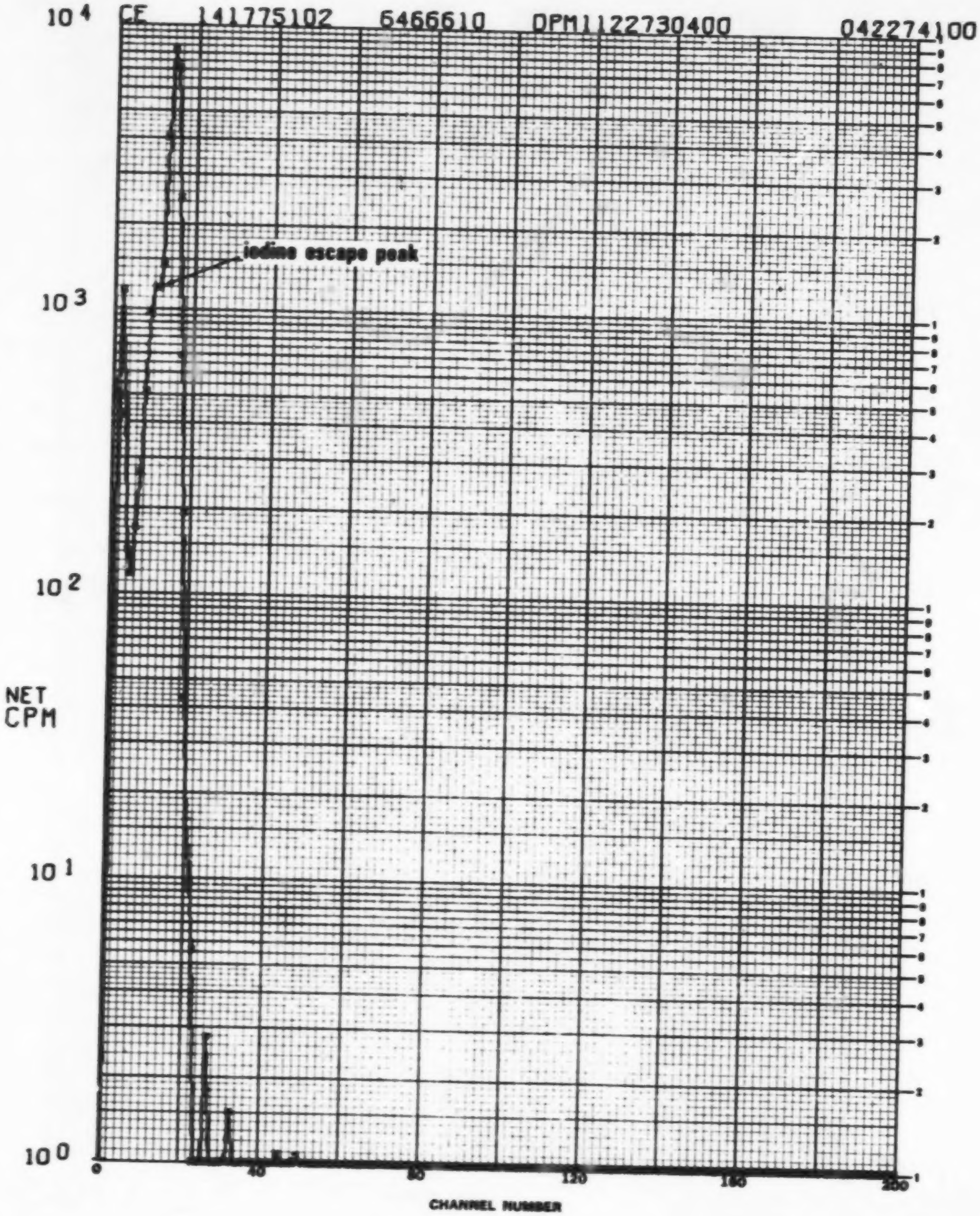

Figure E-36. Cerium-141 spectrum calibrated at 10 keV per channel.

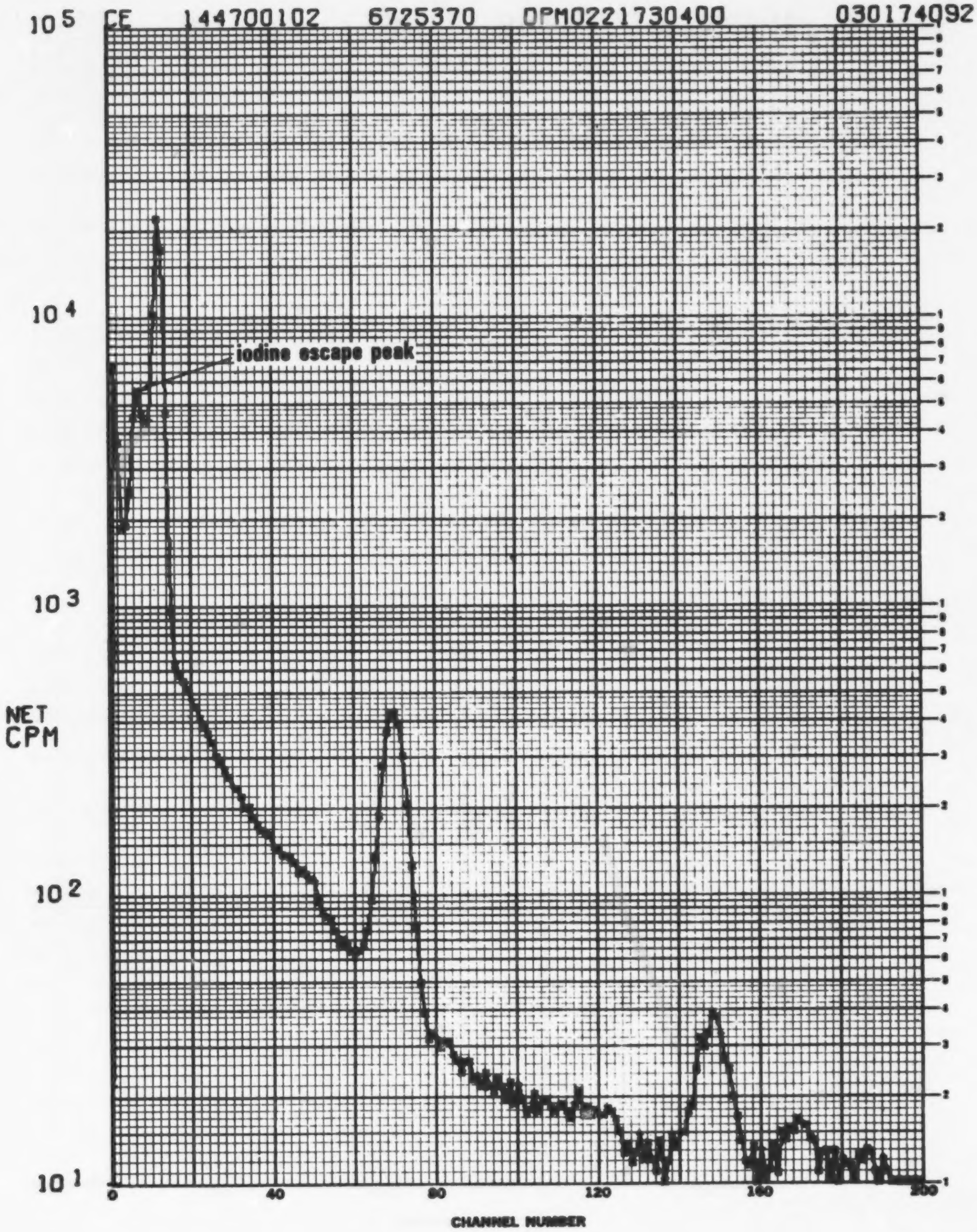

Figure E-37. Cerium-144 spectrum calibrated at 10 keV per channel.

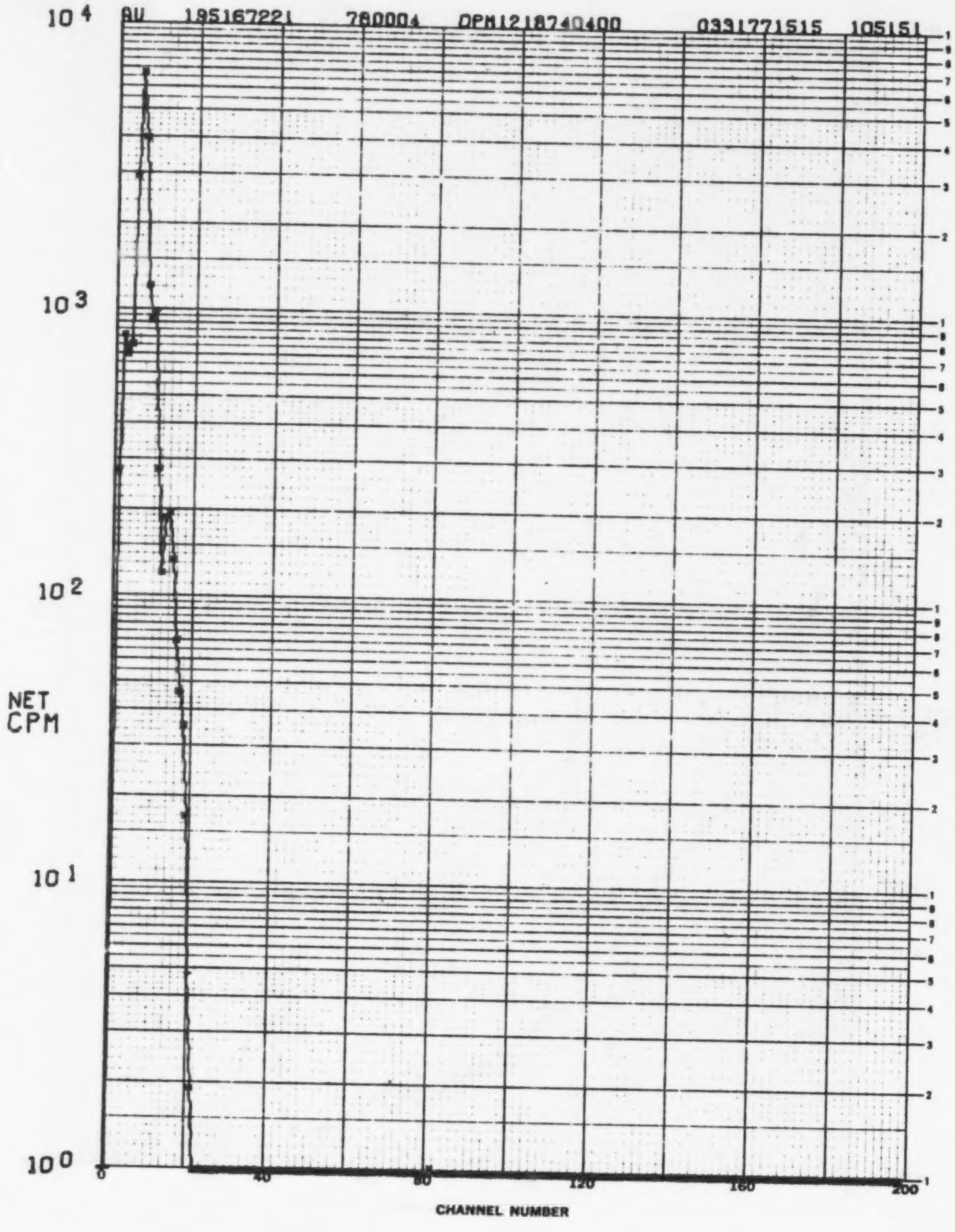

Figure E-38. Gold-195 spectrum calibrated at 10 keV per channel.

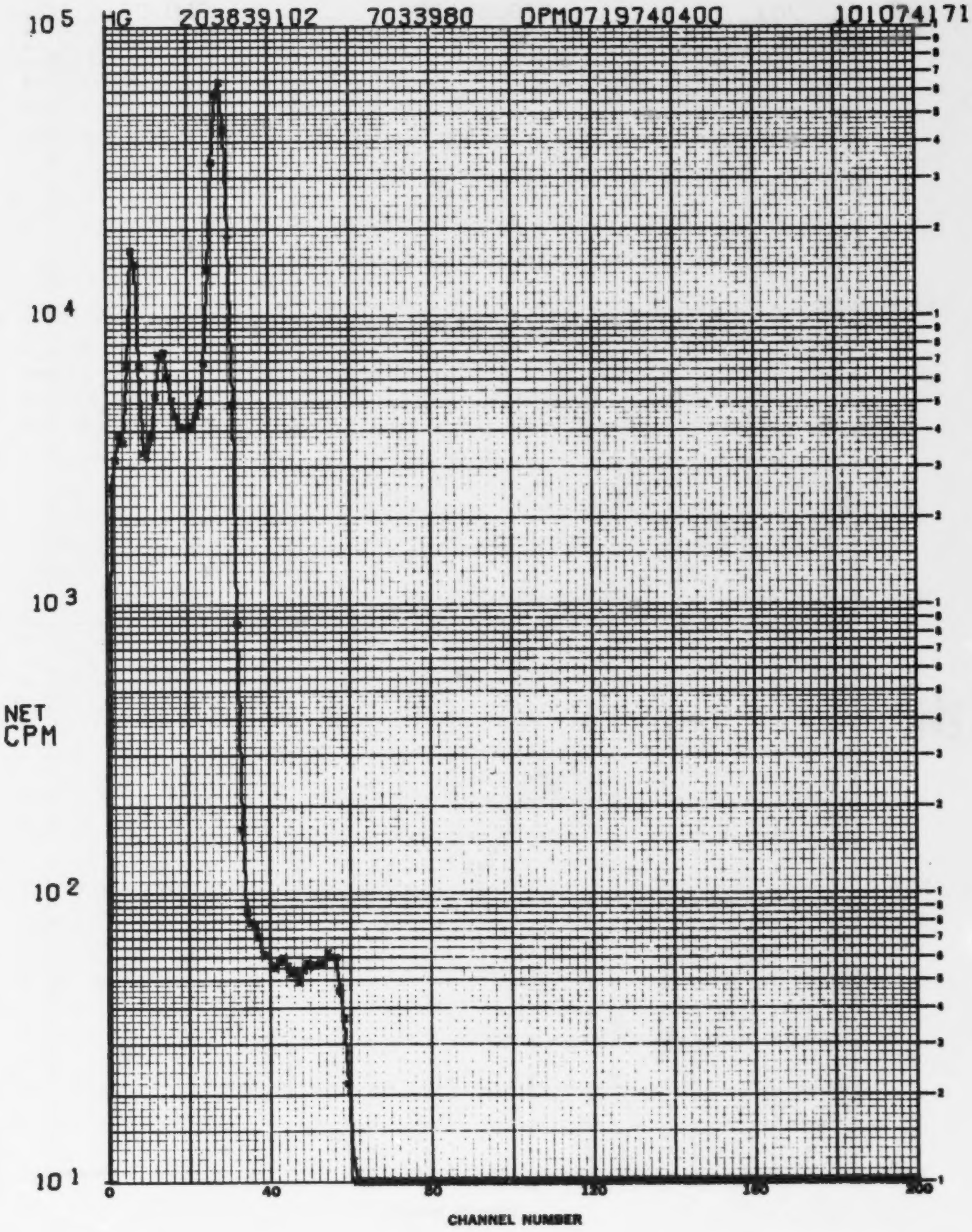

Figure E-39. Mercury-203 spectrum calibrated at 10 keV per channel.

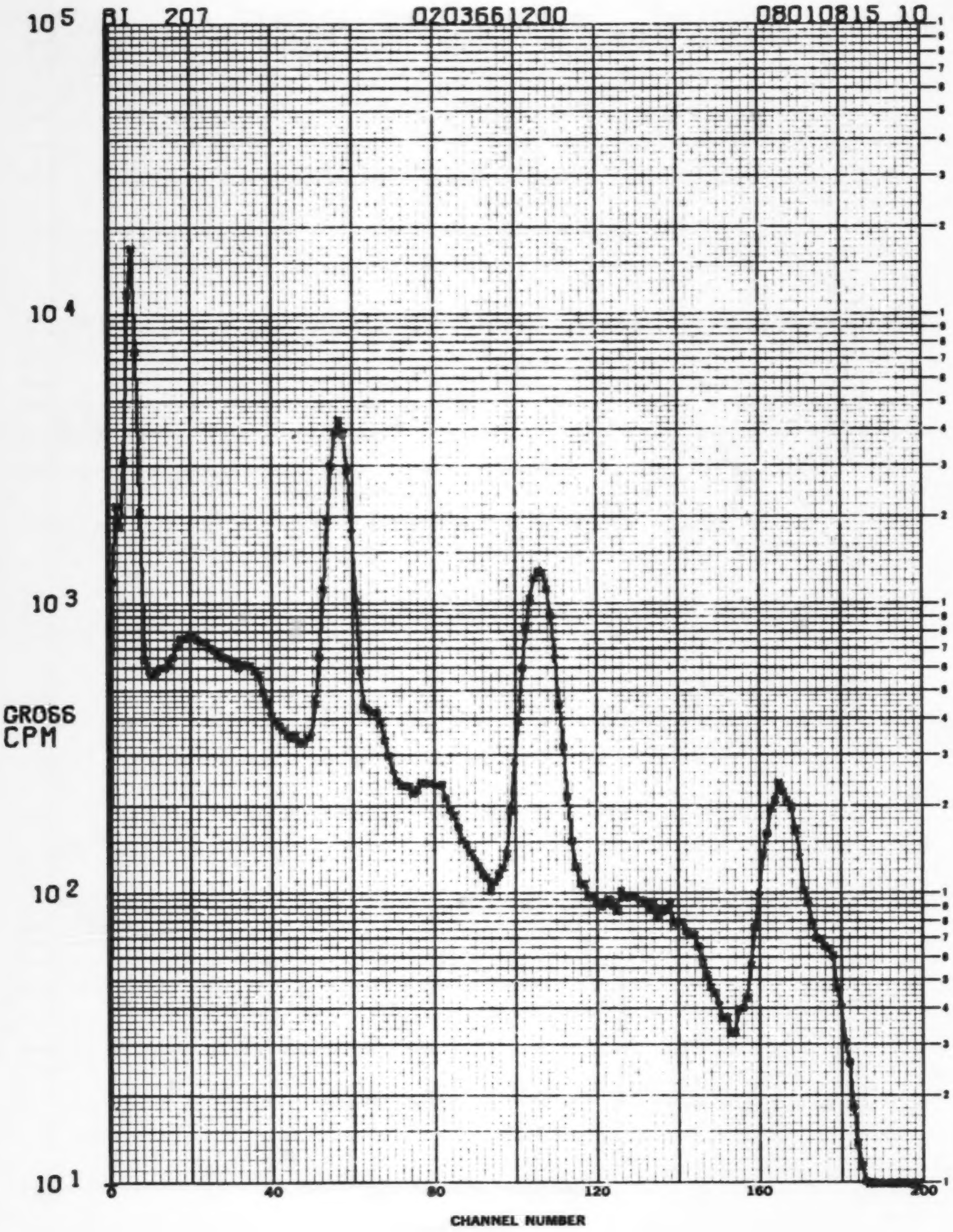

Figure E-40. Bismuth-207 spectrum calibrated at 10 keV per channel.

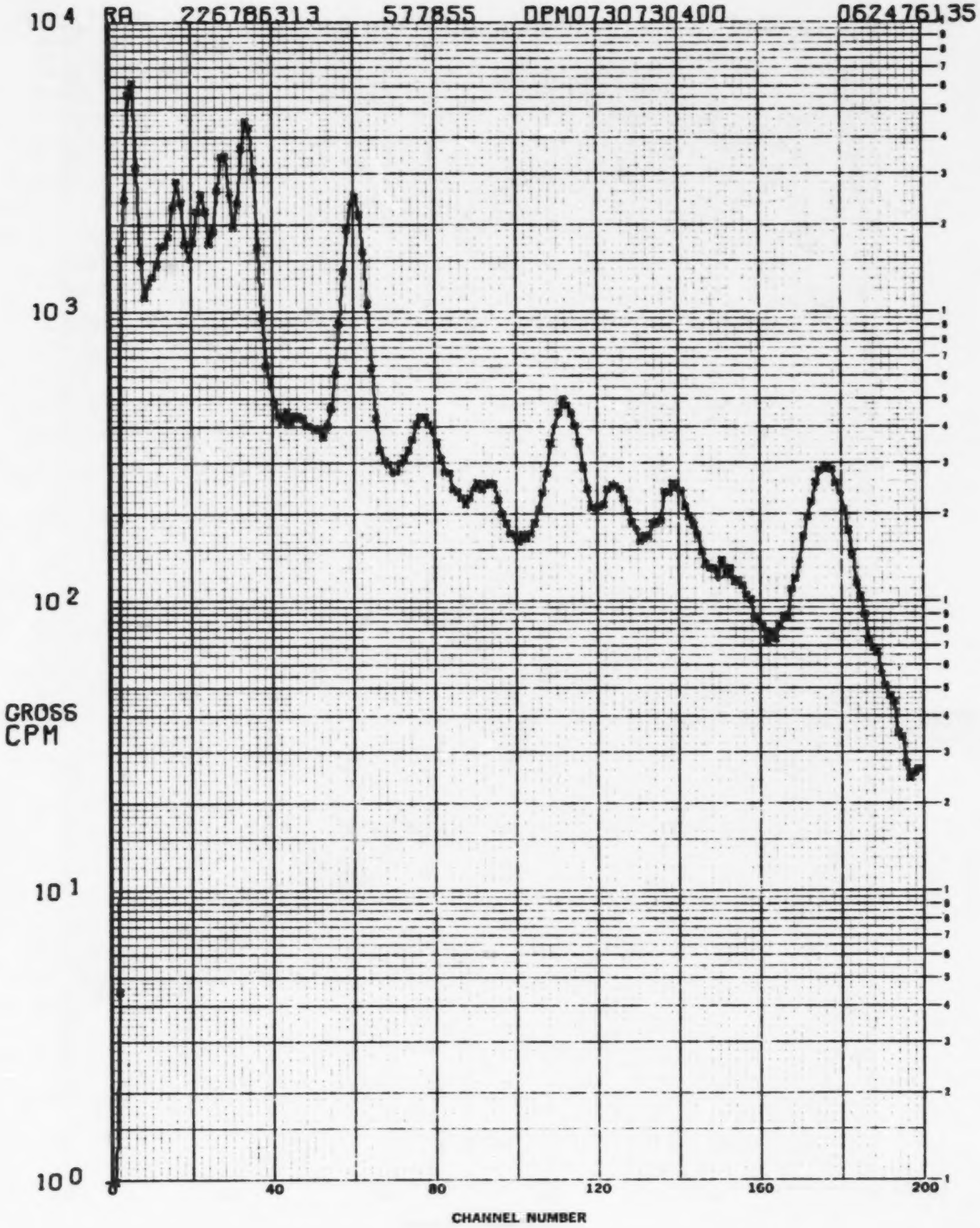

Figure E-41. Radium-226 spectrum calibrated at 10 keV per channel.

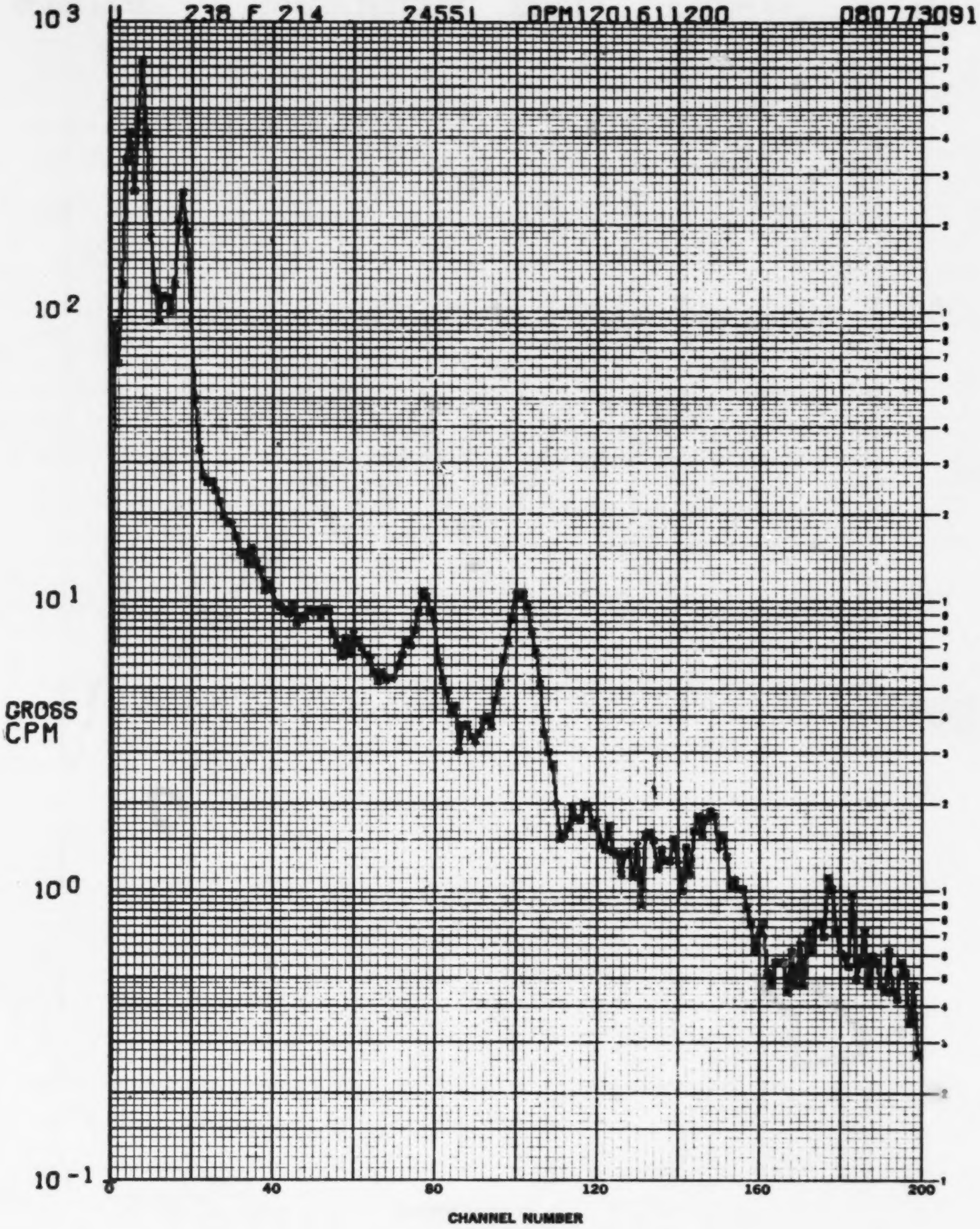

Figure E-42. Natural uranium spectrum calibrated at 10 keV per channel.

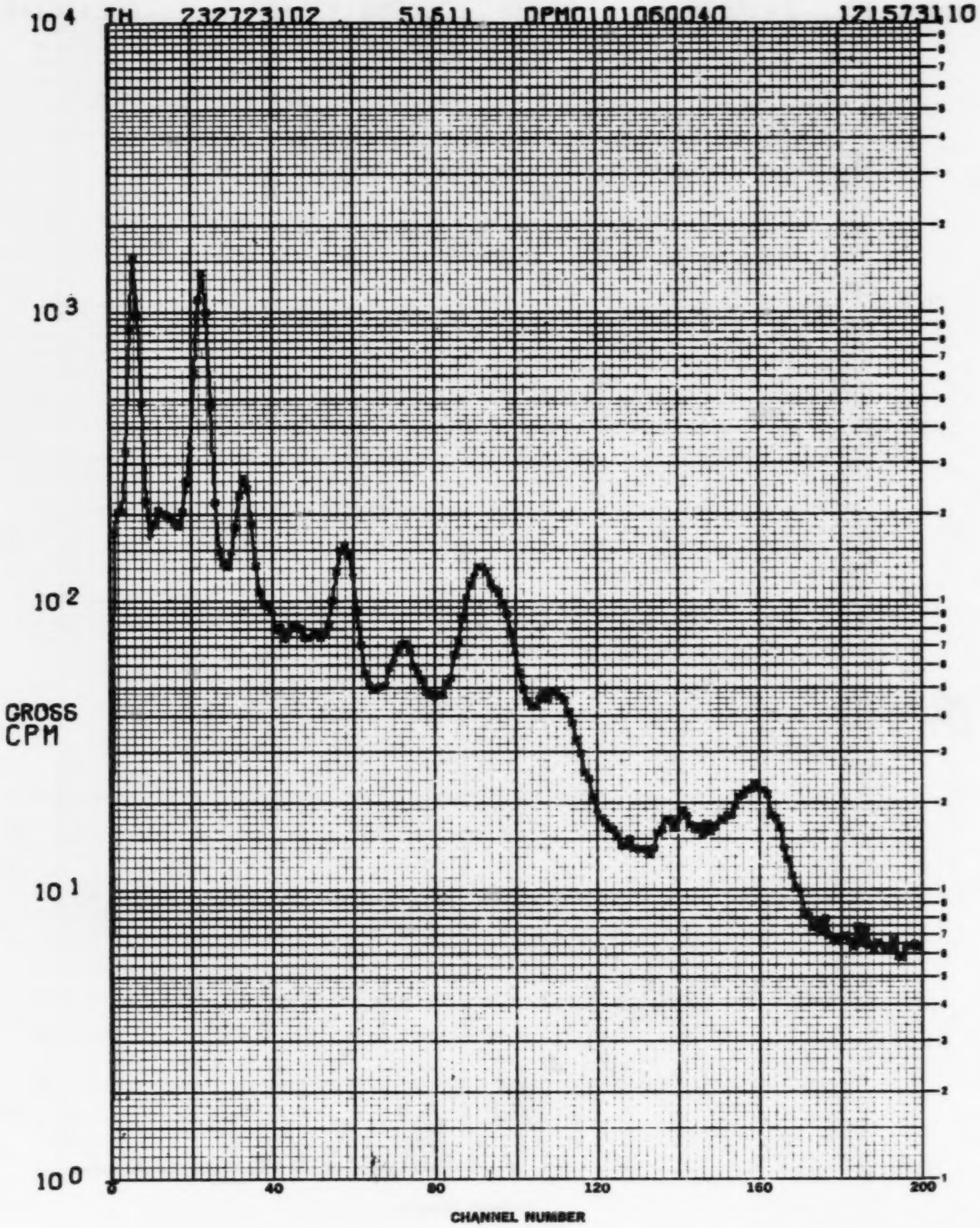

Figure E-43. Thorium-232 spectrum calibrated at 10 keV per channel.

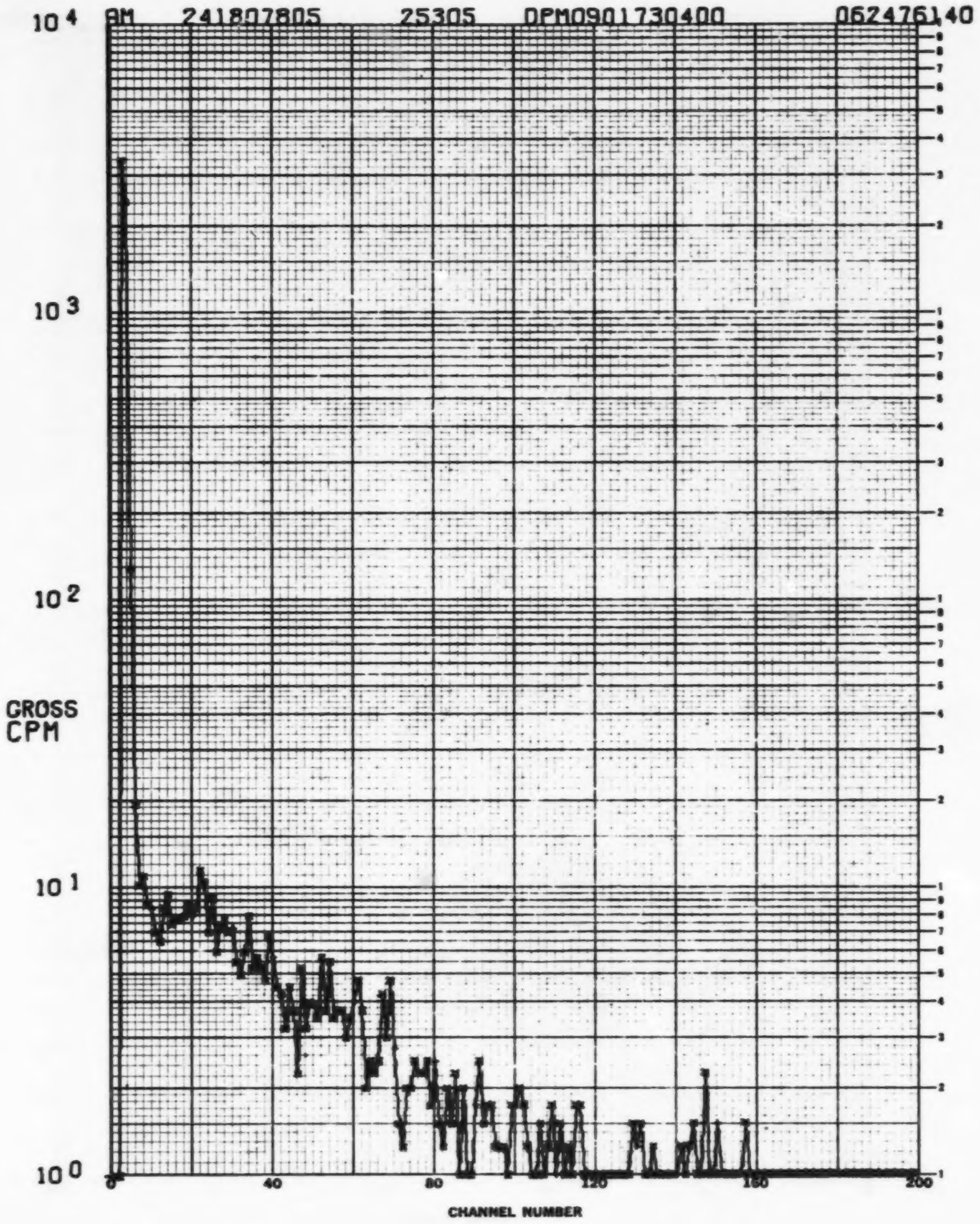

Figure E-44. Americium-241 spectrum calibrated at 10 keV per channel.

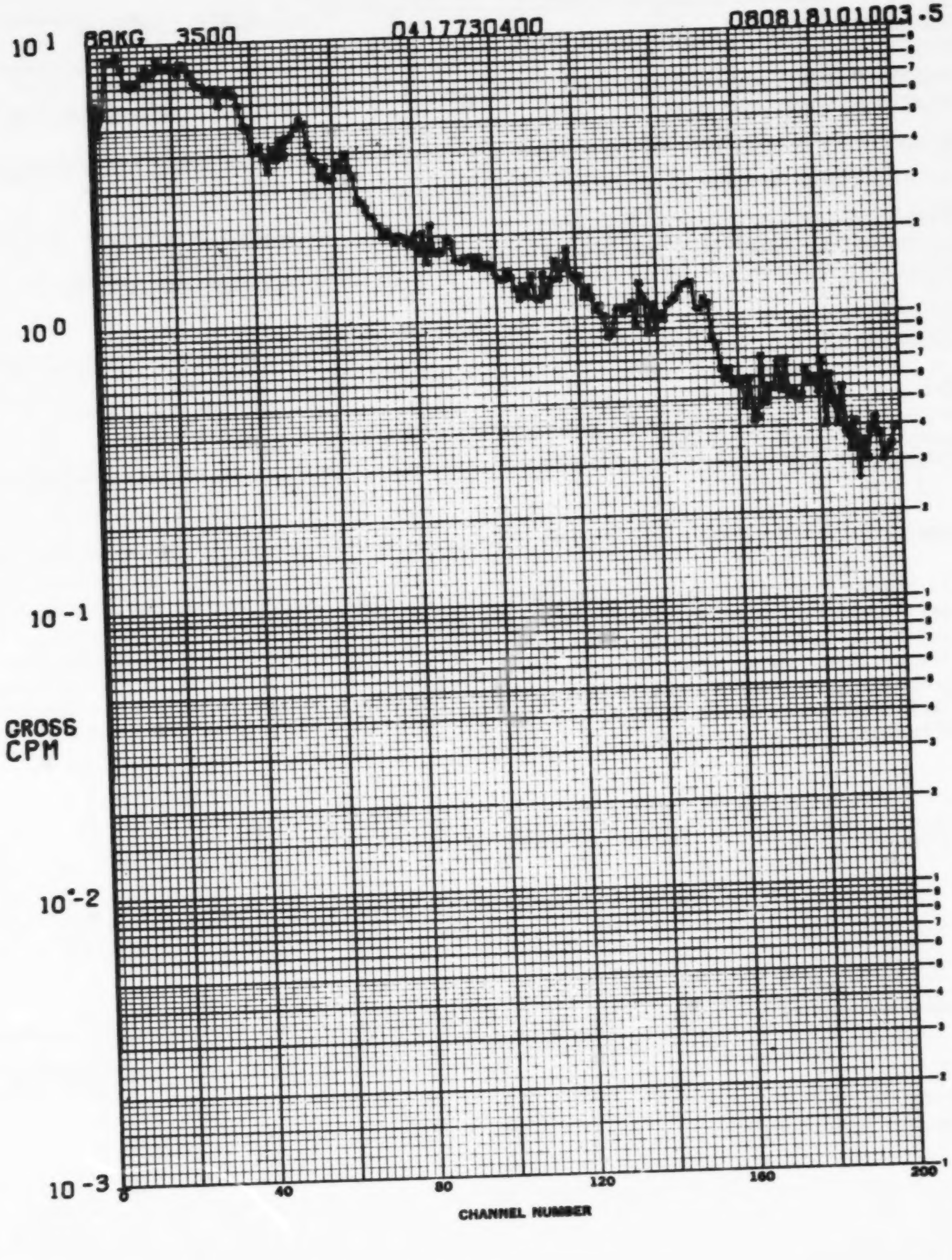

Figure E-45. Background spectrum calibrated at 10 keV per channel.

☆U. S. GOVERNMENT PRINTING OFFICE: 1978—785-327